Process and Equipment Development for

Textile Dyeing in Supercritical Carbon Dioxide

Martijn VAN DER KRAAN

Process and Equipment Development for

Textile Dyeing in Supercritical Carbon Dioxide

Proefschrift

ter verkrijging van de graad van doctor
aan de Technische Universiteit Delft,
op gezag van de Rector Magnificus prof. dr. ir. J.T. Fokkema,
voorzitter van het College van Promoties,
in het openbaar te verdedigen op maandag 12 september 2005 om 15:30 uur

door

Martijn VAN DER KRAAN
scheikundig ingenieur
geboren te Nieuwkoop.

Dit proefschrift is goedgekeurd door de promotor:
Prof. dr. G.J. Witkamp

Samenstelling promotiecommissie:

Rector Magnificus	Voorzitter
Prof. dr. G.J. Witkamp	Technische Universiteit Delft, promotor
Prof. dr. ir. J.T.F. Keurentjes	Technische Universiteit Eindhoven
Prof. dr. ir. A.B. de Haan	Universiteit Twente
Prof. dr. F. Recasens	Polytechnical University of Barcelona
Prof. ir. G.J. Harmsen	Technische Universiteit Delft
Prof. dr. J.A. Moulijn	Technische Universiteit Delft
Dr. ir. G.F. Woerlee	FeyeCon D&I B.V.

Dr. ir. G.F. Woerlee heeft als begeleider in belangrijke mate aan de totstandkoming van dit proefschrift bijgedragen.

Dit werk is financieel ondersteund door de ministeries van EZ, OCenW en VROM via het EET programma van SenterNovem, project EET K99101.

ISBN-10: 9090199128
ISBN-13: 9789090199122
Printed by Febodruk B.V., Enschede

Voor mijn ouders
en voor Uschi

Summary

Process and Equipment Development for Textile Dyeing in Supercritical Carbon Dioxide

The large-scale water pollution by the textile dyeing industry is a global environmental problem. The ever more stringent regulations on wastewater also make it an economical problem. In the last two decades therefore, research has been done on an environmentally benign technology, using supercritical carbon dioxide ($scCO_2$) as a dye solvent, rather than water.

The applicability of the technology is limited at this moment by two factors. Firstly, there is not enough knowledge on reactive and non-reactive dyeing. Secondly, because the process operates at conditions of typically 120ºC and 300 bar, high-pressure equipment is needed which results in high investment costs that stand in the way of industrial implementation. In this work, the supercritical dyeing process was investigated experimentally regarding both reactive and non-reactive dyeing and also new equipment was designed to minimize the equipment and process costs.

Silk, wool, nylon and polyester were dyed successfully in $scCO_2$ with two non-polar dyes containing vinylsulphone or dichlorotriazine reactive groups. It was found that the presence of a small amount of water increased the coloration of wool and nylon significantly and that silk only reacted with the dyes when water was added. This was the first time that silk was dyed successfully in $scCO_2$. Maximum color depths were observed when both the $scCO_2$ and the textiles were saturated with water.

To predict how much water is to be added to a supercritical dyeing vessel in order to obtain optimal coloration with reactive dyes, a thermodynamic model was developed. This model describes the equilibrium distribution of water over the supercritical and the textile phase, as a function of pressure, temperature, vessel

volume and textile mass. One part of the model is the calculation of the solubility of water in a supercritical fluid, which is done with a new equation, derived from statistical thermodynamics.

The non-reactive dyeing of polyester was investigated experimentally in a new 40-liter pressure vessel. The saturation coloration increased and the distribution coefficient decreased with temperature and $scCO_2$-density. The adsorption of the dye on the polyester was exothermic and followed Nernst adsorption. Since the values of the saturation colorations, the temperature dependence of the distribution coefficient and also the adsorption mechanism were the same as in aqueous dyeing, it was concluded that the disperse dyeing in $scCO_2$ behaved thermodynamically the same as in water.

Because no generally accepted procedure exists for the design of heat exchangers for supercritical fluids, this was investigated with computational fluid dynamics simulations. Heat transfer coefficients were determined for different temperatures, pressures and Reynolds numbers, for CO_2 flowing up or down through a vertical pipe.

The impairment and enhancement of heat transfer caused by the temperature-induced variation of physical properties was investigated, as well as the effect of buoyancy. It was determined when (i.e. for which process conditions) and how (i.e. with which Nusselt relation) these effects are to be taken into account in the calculation of heat transfer coefficients for the design of heat exchangers working at supercritical conditions.

A technical-scale, 100-litre dyeing machine was designed and built to test polyester beam dyeing in $scCO_2$ at 300 bar and 120ºC. A new type of pressure vessel was used, consisting of a steel liner with carbon fibers wound around to take up the radial forces and a yoke construction for the axial forces. This configuration lowers the investment cost but also the operating cost, because the amount of steam required to heat the vessel is lower than for a completely steel vessel. Furthermore, because the carbon fiber vessel requires less heating due to the low heat capacity of the carbon fibers, the process time is shortened. To circulate the CO_2 with the dissolved dye through the textile, a low-pressure centrifugal pump was designed for service in $scCO_2$ and placed inside the dyeing vessel.

Also a commercial-scale 1000-liter supercritical dyeing machine was designed, for treating 300 kg polyester while recycling all dye and 96% of the CO_2. An economical analysis showed that, although the purchase cost for a supercritical machine is higher (500 k€) than for an aqueous machine (100 k€), the operating cost is lower (0.35 instead of 0.99 € per kg polyester). This is caused by the higher rate of dyeing and by the simpler dye formulations that can be used in scCO_2. The overall result is a 50% lower process cost for the supercritical process.

This thesis contributes to the development of supercritical fluid dyeing technology in two ways. Firstly, knowledge was generated on reactive and non-reactive dyeing, two subjects that were insufficiently explored up to now. Secondly, new equipment was designed, lowering the investment and operating costs of the process. It was shown that the supercritical process is not only environmentally superior to aqueous dyeing, but also economically. The overall result of this thesis is a better understanding of textile dyeing in supercritical carbon dioxide and a lower threshold for the implementation in industry.

Martijn van der Kraan

Samenvatting

Proces- en apparaatontwikkeling voor textiel verven in superkritisch kooldioxide

De grootschalige watervervuiling door de textielindustrie is een wereldwijd milieuprobleem. De steeds strengere regelgeving betreffende afvalwater maken het tevens een economisch probleem. Daarom is in de laatste twee decennia door diverse wetenschappers onderzoek gedaan naar een milieuvriendelijke technologie waarbij superkritisch kooldioxide ($scCO_2$) wordt gebruikt als oplosmiddel voor kleurstof, in plaats van water.

De toepasbaarheid van de technologie wordt op dit moment beperkt door twee factoren. Ten eerste is er niet genoeg kennis van reactief en niet-reactief verven in $scCO_2$. Ten tweede, omdat het proces plaatsvindt bij condities van typisch 120ºC en 300 bar, zijn hoge-druk machines nodig, hetgeen resulteert in hoge investeringskosten die in de weg staan van industriële implementatie. In dit werk is het superkritische verfproces experimenteel onderzocht voor wat betreft reactief en niet-reactief verven en er is tevens nieuwe apparatuur ontwikkeld om de investerings- en proceskosten te minimaliseren.

Zijde, wol, nylon en polyester zijn met goed resultaat in $scCO_2$ geverfd met twee apolaire kleurstoffen met de reactieve groep vinylsulfon respectievelijk dichloortriazine. Er werd vastgesteld dat de aanwezigheid van een kleine hoeveelheid water de aankleuring van wol en nylon significant deed toenemen en dat zijde alleen reageerde met de kleurstof wanneer water werd toegevoegd. Dit was de eerste keer dat zijde in $scCO_2$ is geverfd met een goed resultaat. Maximale kleurdiepten werden gevonden wanneer zowel het $scCO_2$ als het textiel waren verzadigd met water.

Om te voorspellen hoeveel water moet worden toegevoegd aan een superkritisch verfvat om optimale aankleuring te verkrijgen, werd een thermodynamisch model

ontwikkeld. Dit model beschrijft de evenwichtsverdeling van water over de superkritische fase en de textielfase, als functie van druk, temperatuur, vatvolume en textielmassa. Een onderdeel van het model is de berekening van de oplosbaarheid van water in een superkritisch fluïdum, hetgeen werd uitgevoerd met een nieuwe vergelijking, afgeleid uit de statistische thermodynamica.

Het niet-reactief verven van polyester werd experimenteel onderzocht in een nieuw 40-liter drukvat. De verzadigingsaankleuring nam toe en de verdelingscoëfficiënt nam af met de temperatuur en dichtheid van de $scCO_2$. De adsorptie van kleurstof aan het polyester was exotherm en volgde Nernst adsorptie. Aangezien de waarden van de verzadigingsaankleuringen, de temperatuurafhankelijkheid van de verdelingscoëfficiënt en ook het adsorptiemechanisme hetzelfde waren als in waterverven, werd geconcludeerd dat dispers verven in $scCO_2$ hetzelfde thermodynamische gedrag vertoont als in water.

Omdat geen algemeen geaccepteerde procedure bestond voor het ontwerp van warmtewisselaars voor superkritische fluïda, werd dit onderzocht met “computational fluid dynamics” simulaties. Warmteoverdrachtscoëfficiënten werden bepaald voor verschillende temperaturen, drukken en Reynoldsgetallen, voor omhoog- en omlaagstromende CO_2 in een verticale pijp.

De verslechtering of verbetering van de warmteoverdracht, veroorzaakt door de temperatuurafhankelijke variatie van de fysische eigenschappen, werd onderzocht, evenals het effect van de zwaartekracht. Er werd vastgesteld wanneer (voor welke procescondities) en hoe (met welke Nusseltrelatie) deze effecten in rekening moeten worden gebracht bij de calculatie van warmteoverdrachtscoëfficiënten voor het ontwerp van warmtewisselaars werkend onder superkritische condities.

Een 100-liter verfmachine op technische schaal werd ontworpen en gebouwd om polyester boomverven te testen in $scCO_2$ bij 300 bar en 120ºC. Een nieuw type drukvat werd gebruikt, bestaande uit een stalen binnenvat omwikkeld met koolstofvezels om de radiale krachten op te vangen en met een jukconstructie voor de axiale krachten. Deze configuratie verlaagt de investeringskosten maar ook de operationele kosten, doordat de hoeveelheid energie om het vat te verwarmen lager is dan bij een volledig stalen vat. Om de CO_2 met de opgeloste kleurstof door het

textiel te circuleren, is een lage-druk centrifugaalpomp ontworpen voor gebruik in $scCO_2$, deze is binnen in het drukvat geplaatst.

Er is eveneens een 1000-liter superkritische verfmachine ontworpen, voor het verven van 300 kg polyester en het hergebruiken van alle kleurstof en 96% van de CO_2. Een economische analyse toonde aan dat, hoewel dat de aanschafkosten van een superkritisch machine hoger zijn (500 k€) dan van een waterverfmachine (100 k€), de operationele kosten lager zijn (0.35 in plaats van 0.99 € per kg polyester). Dit wordt veroorzaakt door de hogere snelheid van het verfproces en door de eenvoudigere kleurstofformuleringen die in $scCO_2$ gebruikt kunnen worden. Het overall resultaat is een 50% lagere proceskost voor het superkritische proces.

Dit proefschrift draagt bij tot de ontwikkeling van de superkritische verftechnologie op twee manieren. Ten eerste is er kennis gegenereerd op het gebied van reactief en niet-reactief verven, twee onderwerpen die tot nog toe onvoldoende waren onderzocht. Ten tweede is er nieuwe apparatuur ontworpen die de investerings- en operationele kosten hebben verlaagd. Er is aangetoond dat het superkritische proces niet alleen milieutechnisch superieur is aan waterverven, maar ook economisch. Het overall resultaat van dit proefschrift is een beter begrip van textiel verven in superkritisch kooldioxide en een lagere drempel voor de industriële implementatie.

Martijn van der Kraan

Contents

Chapter 1

Introduction

1.1. Environmental implications of textile dyeing

The importance of the textile processing industry is clearly illustrated by the world production in 2003, being 52 Mton. The two main fiber types are polyester (22 Mton) and cotton (20 Mton), the remainder is accounted for by wool, silk, nylon, viscose and some specialty fibers [1].

Virtually all of this textile is dyed, using worldwide 0.7 Mton of dye powder, with a total value of 19 billion € [2]. Approximately 5 to 10 % of the non-reactive dyes are lost with the wastewater, for reactive dyes this is even 50 %. The resulting pollution lies between 40 and 300 liter per kg textile [3], giving a total amount of 2 to 20 billion cubic meters of wastewater annually, which indicates the seriousness of this environmental problem.

Although other chemicals, such as salts and dispersing agents, are used in the dyeing process, the most problematic pollutant is the dye itself. Inherent to their purpose, dye molecules are designed to be resistant to degradation by light, water and many chemicals [4]. Therefore, treatment in municipal water purification facilities can not decolorize dye house effluents. Instead, the wastewater has to be treated at the site.

1.2. Solutions to the wastewater problem

Dye molecules can be decomposed in water by a range of chemical, physical and biological treatments [5]. The most widely used technique is the oxidative process, where hydrogen peroxide is added to the water and activated by ultra violet light to oxidize the dye molecules. An important draw-back of this technique is the

production of toxic sludge, which has to be disposed of or incinerated. All other techniques to purify the water are characterized by either a high process cost or a production of toxic waste. Since the treated water has to satisfy ever more stringent environmental regulations, the end-of-pipe solutions become increasingly expensive for the textile industry. It is therefore that a solution at the source of the problem, i.e. replacement of water as a dyeing solvent, is preferable.

In the sixties and seventies, this consideration has led to some research on the use of chlorinated hydrocarbons, mainly perchloroethylene, as dyeing media [6]. This so-called solvent dyeing has, however, a major disadvantage in the toxicity of the solvents. The technique has not been applied in industry and all research on the subject has been stopped.

A more promising alternative to water is the use of supercritical fluids. Such solvents have not yet been implemented in textile industry, but their use as dyeing medium has received considerable attention from researchers in the past two decades, as is illustrated by the 143 articles mentioned in the review by Bach et al. [7].

1.3. Supercritical fluids

When a solid is heated, the thermal motion of the molecules increases, the solid melts and a liquid and a vapor phase are formed. In figure 1.1 these three states of matter are graphically presented. When a vapor below its critical temperature is compressed, it condenses when the vapor-liquid equilibrium line is crossed. Above the critical temperature however, the thermal energy of the vapor molecules is so high, that condensation is no longer possible, no matter how much the pressure is increased. The vapor-liquid equilibrium line ends at the critical temperature. When a fluid is above its critical temperature and the corresponding critical pressure, it can not be regarded as a vapor or a liquid and it is referred to as a supercritical fluid.

The most widely used supercritical fluid is carbon dioxide, because it combines a relatively mild critical point with non-flammability, non-toxicity and a low price. Because of its green and safe character, it is the best supercritical solvent for textile

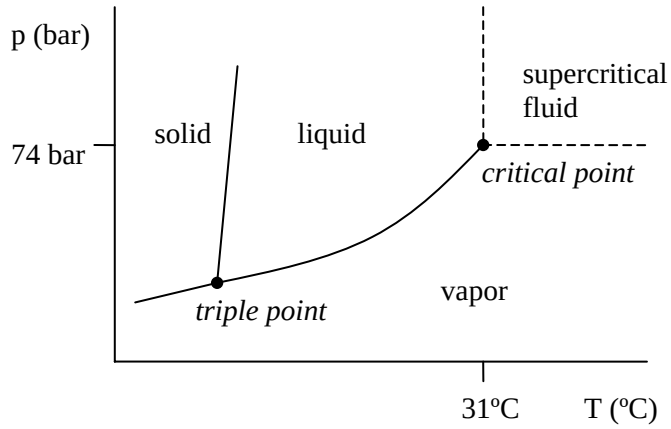

Figure 1.1. Phase diagram of carbon dioxide, phase behavior as a function of pressure (p) and temperature (T)

dyeing. The CO_2 is a waste product of combustion, fermentation and ammonia synthesis, so that no CO_2 has to be produced especially for dyeing.

To allow solubilization of low vapor pressure compounds such as the solid dyes, both the density and the temperature of CO_2 need to be sufficiently high, in the order of 600 kg/m^3 and 120ºC respectively. To obtain this set of conditions, the pressure needs to be around 300 bar, so that both the temperature and pressure are far above the critical point (31ºC, 74 bar).

The main advantage of using scCO_2 instead of water in a dyeing process, is the easy separation of the CO_2 and the unused dye that remains after the dyeing process. Depressurization leads to precipitation of the excess dye and gives clean, gaseous CO_2, so that both compounds can be recycled and no waste is generated. Furthermore, after the dyeing process, the textile does not need an energy-intensive drying step as it does in aqueous dyeing.

The above advantages are consequences of the high vapor pressure of CO_2, but also the physical properties that are characteristic of all supercritical fluids facilitate the dyeing process: The intense thermal motion of the molecules and the low viscosity

result in a high diffusivity in the fluid, facilitating the mass transport of the dye towards the fibers.

Additional advantages of $scCO_2$ exist for the case of polyester dyeing. Because $scCO_2$ is a non polar solvent, no dispersing agents are needed when non polar dyes are used. This means that simpler dye formulations can be used than in aqueous polyester dyeing where dispersing agent makes up around 50% of the dye powder. Another advantage specifically for polyester is that under supercritical conditions the CO_2-molecules penetrate and swell the polymer. This plasticizes the textile fibers and increases diffusion coefficients of dyes inside the polyester with one order of magnitude [9], relative to aqueous dyeing.

1.4. Textile dyeing in $scCO_2$ – state of the art

1.4.1. Process

In supercritical textile dyeing, the choice of dye depends on the dyeing mechanism which, in its turn, depends on the type of fiber that is to be dyed. For non polar textiles, such as polyester, non polar, non reactive dyes are dissolved into the supercritical phase, transported to the fiber and adsorbed to the surface. Finally, the dye molecules diffuse into the CO_2-swollen polymer matrix, where they are bound to the polyester molecules by physical attraction, mainly dispersion forces. Upon depressurization, the CO_2-molecules exit the shrinking fibers and the dye molecules are retained. This dyeing mechanism was suggested by Saus et al. [10] and subsequently confirmed by Tabata et al. [11]. Because these non polar dyes are also used in aqueous dyeing processes, where they are dispersed in the water, they are generally called disperse dyes.

The dyeing mechanism and therefore the type of dye is different for natural textiles. Since these are polar due to the presence of hydroxyl groups (cotton) or amino groups (wool, silk), they have no physical attraction towards disperse dyes. To bind a dye molecule to such a fiber, a chemical bond is needed to realize sufficient fastness, for which reason reactive dyes have to be used.

As is the case for polyester, for natural textiles the currently available dyes that are used in water can be used in $scCO_2$. However, these reactive dyes are polar and therefore not soluble in $scCO_2$. It has been shown by Jun et al. [12] that it is possible to dye natural fibers with these polar dyes in $scCO_2$ by using reverse micelles. This method is not suited for dyeing cotton/polyester blends since the latter fiber is not capable of forming chemical or physical bonds with the polar dyes. Another disadvantage is that the use of extra chemicals like dispersing agents complicates the process and therefore it is preferable to use new, non polar reactive dyes for natural fibers.

Non polar reactive dyes were used on cotton by Schmidt et al. [13] but the results were not satisfactory, and an unpractical long dyeing time of 4 hours was needed and during the process, corrosive byproducts were formed. Other researchers have tried to dye cotton in $scCO_2$ but did not succeed [7]. The successful development of a process for the dyeing of cotton in $scCO_2$ was carried out by Fernandez [14]. Since this falls beyond the scope of the present work, it will not be discussed further. Wool was dyed well in $scCO_2$ with non polar reactive dyes by Schmidt et al. [15], but silk has never been dyed to an acceptable depth [7].

Despite the research on disperse dyeing of non-polar fibers and the reactive dyeing of polar fibers, there is by far not enough knowledge in both fields, which currently limits the further development of supercritical fluid dyeing.

1.4.2. Equipment

It is generally accepted [16, 17] that a supercritical dyeing process should be operated as is shown in figure 1.2. During the dyeing, the CO_2 is circulated through a heat exchanger, a vessel where the dye is dissolved and through a vessel where the dye is delivered to the textile. When the desired coloration is attained, dye is still left in the CO_2, which is removed by passing the CO_2 through a pressure reducing valve into a separator vessel. In the separator, the CO_2 is gasified, so that the dye precipitates and the clean CO_2 can be recycled by pumping it back to the dyeing vessel.

Pilot plants such as drawn in figure 1.2 have been constructed [16, 17] but, up to now, no commercial-size machine has been built. This is caused by the high cost

associated with large-scale equipment operating around 300 bar. To facilitate commercialization, the price of large-scale pressure equipment has to be lowered. To do this, there are some important engineering issues to be faced.

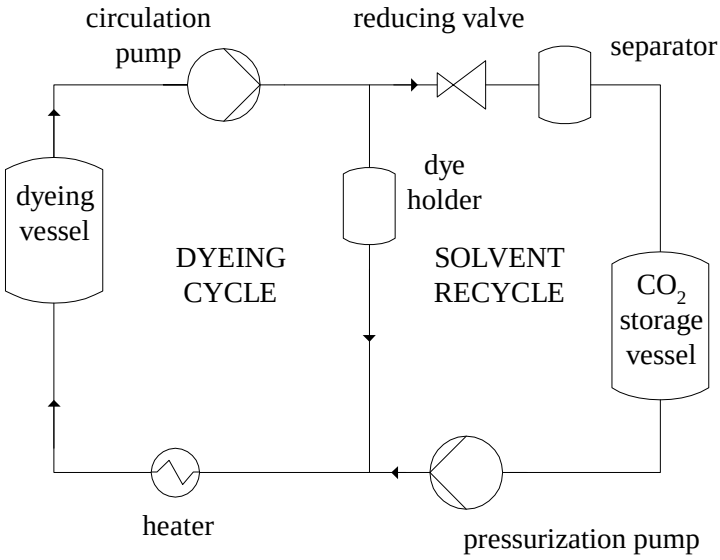

Figure 1.2. Simplified flow diagram of a process to dye textiles in supercritical CO_2.

The first issue concerns the pressure vessel containing the textile. Since industrial dye baths have volumes in the order of 1000 liters, the thick-walled supercritical dyeing vessels will consist of a large amount of steel compared to aqueous dyeing vessels. This does not only increase the investment costs, but also the operating costs because the vessel has to be heated to the dyeing temperature in each batch. Because more energy is needed for the heating, a larger heat exchanger or a longer process time is required, which increases either the investment or the operating cost even more.

The second engineering issue is the circulation of $scCO_2$ through the dyeing vessel. Centrifugal pumps for static pressures of around 300 bar are expensive and weigh heavily on the equipment cost [16].

A further complication encountered when designing a supercritical dyeing machine, concerns heat transfer. Literature gives no clear indications on how to

calculate heat transfer coefficients for the design of a heat exchanger for high-pressure CO_2.

The above three problems have not been solved up to now, which hinders the implementation of supercritical fluid dyeing in industry.

1.5. Aim and contents of this thesis

This work treats the above discussed limiting aspects on both the process (non-reactive and reactive dyeing) and on the equipment (pressure vessel, circulation pump and heat transfer).

The aim of this thesis is:
To develop and apply the knowledge required to solve the process and equipment technology issues that are currently limiting the further development and implementation of the supercritical textile dyeing technology.

As was discussed above, the dyeing of natural fibers in $scCO_2$ is a research area where only a start has been made. Therefore, in chapter 2 experiments are discussed with new, reactive, non polar dyes on several textile types.

Since it was found in chapter 2 that the presence of a small amount of water in the $scCO_2$ increases the coloration in reactive dyeing, a model was developed which is described in chapter 3, to predict how much water is to be added to a supercritical dyeing vessel to obtain optimum coloration.

In chapter 4, the dyeing of polyester is discussed, experiments in a 40-liter pressure vessel are described and the influence of temperature and CO_2-density on the coloration and distribution coefficient in $scCO_2$ is investigated quantitatively.

Chapter 5 describes computational fluid dynamics simulations of heat transfer to near- and supercritical CO_2, to clarify how a supercritical fluid heat exchanger can be designed.

In chapter 6, the process and equipment design of a 100-liter beam dyeing machine for supercritical polyester dyeing is treated. A new type of pressure vessel and centrifugal pump are described, both equipment items are meant to decrease the process cost significantly.

A short description of a commercial-scale 1000-liter beam dyeing machine is given in chapter 7, together with an economical comparison of the supercritical and the conventional aqueous process.

In the epilogue, recommendations are made for further research and the future of the technology of textile dyeing in supercritical carbon dioxide is discussed.

References

1. E.M. Aizenshtein, World Chemical Fiber and Thread Production in 2003, *Fibre Chem*. **36** (6), 467 (2004).
2. H.S. Rai, M.S. Bhattacharyya, J. Singh, T.K. Bansal, P. Vats, and U.C. Banerjee, Removal of Dyes from the Effluent of Textile and Dyestuff Manufacturing Industry: A Review of Emerging Techniques with Reference to Biological Treatment, *Crit. Rev. Env. Sci. Tec*. **35**, 219 (2005).
3. U. Rott, Multiple Use of Water in Industry – The Textile Industry Case, *J. Env. Sci. Health, part A – Tox*. **A38** (8), 1629 (2003).
4. H. Zollinger, Color Chemistry, Synthesis, Properties of Organic Dyes and Pigments, 2nd ed., VCH Publishers, New York, 92 (1987).
5. T. Robinson, G. McMullan, R. Marchant, and P. Nigam, Remediation of Dyes in Textile Effluent: A Critical Review on Current Treatment Technologies with a Proposed Alternative, *Bior. Technol*. **77**, 247 (2001).
6. R.B. Love, *Rev. Prog. Color*. **6**, 18 (1975).
7. E. Bach, E Cleve, and E. Schollmeyer, Past, Present and Future of Supercritical Fluid Dyeing Technology – An Overview, *Rev. Prog. Color*. **32**, 88 (2002).
8. G. Brunner, Topics in Physical Chemistry 4: Gas Extraction, Steinkopf, Darmstadt (1994).

9. S. Sicardi, L. Manna and M. Banchero, Comparison of Dye Diffusion in Poly(ethylene terephtalate) Films in the Presence of a Supercritical or Aqueous Solvent, *Ind. Eng. Chem. Res.* **39**, 4707 (2000).
10. W. Saus, D. Knittel and E. Schollmeyer, Dyeing of Textiles in Supercritical Carbon Dioxide, *Text. Res. J.* **63**, 135 (1993).
11. I. Tabata, J. Lyu, S. Cho, T. Tominaga, and T. Hori, Relationship Between the Solubility of Disperse Dyes and the Equilibrium Dye Adsorption in Supercritical Fluid Dyeing, *Color. Technol.* **117**, 346 (2001).
12. J.H. Jun, K. Sawada and M. Ueda, Application of Perfluoropolyether Reverse Micelles in Supercritical CO_2 on Dyeing Process, *Dyes and Pigments* **61**, 17 (2004).
13. A. Schmidt, E. Bach and E. Schollmeyer, in: E. Reverchon (Ed.), Proc. 6^{th} Conf. Supercrit. Fluids Appl., Maiori, Italy, 557 (2001).
14. M.V. Fernandez Cid, Cotton Dyeing in Supercritical Carbon Dioxide, Delft University of Technology, Dissertation, Delft (2005).
15. A. Schmidt, E. Bach and E. Schollmeyer, The Dyeing of Natural Fibers with Reactive Disperse Dyes in Supercritical Carbon dioxide, *Dyes and Pigments* **56** (1), 27 (2003).
16. W.A. Hendrix, Progress in Supercritical CO_2 Dyeing, *J. Ind. Text.* **31** (1), 43 (2001).
17. E. Bach, E. Cleve, E. Schollmeyer, M. Bork P. and Koerner, Experience with the Uhde CO_2-Dyeing Plant on Technical Scale. Part 1: Optimization Steps of the Pilot Plant and First Dyeing Results, *Melliand Int.* **3**, 192 (1998).

Chapter 2

Dyeing of Natural and Synthetic Textiles in Supercritical Carbon Dioxide with Disperse Reactive Dyes

Abstract

Polyester, nylon, silk and wool were dyed with disperse reactive dyes in supercritical carbon dioxide ($scCO_2$). The dyes were substituted with either vinylsulphone or dichlorotriazine reactive groups. Since earlier research showed that water, distributed over the $scCO_2$ and the textile, increased the coloration, experiments were done with the vinylsulphone dye with varying amounts of water in the dyeing vessel, to investigate if there is an optimum water concentration. The amounts were such, that no liquid water was present. The maximum coloration was obtained when both the $scCO_2$ and the textiles were saturated with water. At the saturation point, deep colors were obtained with the vinylsulphone dye for polyester, nylon, silk and wool, with fixation percentages between 70 and 92% when the dyeing time was 2 hours. The positive effect of water was due to its ability to swell fibers or due to an effect of water on the reactivity of the dye-fiber system. Also the dichlorotriazine dye showed more coloration when the $scCO_2$ was moist. With this dye, experiments were conducted in water-saturated $scCO_2$, varying the pressure from 225 to 278 bar and the temperature from 100 to 116ºC. The coloration of polyester increased with pressure, the results for silk and wool were not sensitive to pressure. Increasing the temperature had no influence on the dyeing of polyester, silk and wool. The fixations on polyester, silk and wool, being between 71 and 97%, were also independent of pressure and temperature.

Contents submitted to the Journal of Supercritical Fluids

2.1. Introduction

In current industrial textile dyeing processes, large amounts of wastewater are produced. This is an environmental burden and, due to the ever more stringent regulations on water pollution, also an economical problem. The use of $scCO_2$ as dyeing medium solves this problem: the CO_2 and the residual dye remaining in the dye bath after the process can easily be separated so both can be recycled. Additional advantages are the high diffusivity and low viscosity of $scCO_2$, which make the dyeing process faster than in water. The low surface tension allows the $scCO_2$ to penetrate small pores easier than water. Furthermore, after dyeing no energy-demanding drying step is needed. These considerations have led to a considerable research effort on $scCO_2$ dyeing in the last two decades, as was reviewed by Bach et al. [1].

Textiles can be classified into synthetics (e.g. polyester and nylon) and natural textiles. The latter category can be divided into proteins (e.g. silk and wool) and cellulosics (e.g. cotton). In this work, polyester, nylon, silk and wool are investigated. Cotton is also under investigation in our laboratory but will not be discussed in this work.

When dyeing in scCO2, non-polar dyes are used to enable dissolution. Polyester (polyethylene terephtalate or PET) is also non-polar and during the dyeing process, the dye molecules can diffuse into the polymer matrix, where they are physically bonded. Because of its non-polarity, polyester can be dyed in $scCO_2$ with non-reactive, so-called disperse dyes. Nylon is non-polar as well, although slightly more polar than PET, and it can also be dyed with disperse dyes. Since the nylon molecules have amino end-groups, it is also possible to use dyes that are able to react with these nucleophiles, forming a covalent bond, as was shown by Liao et al. [4]. Silk and wool are polar and therefore have no affinity for the non-polar dye molecules. It is only possible to dye these textiles in $scCO_2$ when the dyes are reactive towards the amino groups in the protein fibers of silk and wool. These non-polar reactive dyes are generally called disperse reactive.

In the disperse dyeing of synthetic textiles, the CO_2 penetrates and swells the fibers, thereby facilitating the diffusion of dye molecules through the polymer. Upon depressurization, the CO_2 molecules exit the shrinking fiber and the dye is

retained in the textile. The mechanism of PET dyeing in $scCO_2$ has been discussed extensively, e.g. by Saus et al. [2] and Tabata et al. [3].

In reactive dyeing, four steps can be distinguished in the process, each of which is potentially rate determining:

1. Transport of dye to the fibers. The dye powder is dissolved in the $scCO_2$ and transported towards the textile. The solubility of the dye determines the transport rate of dye towards the textile.
2. Diffusion of dye into the fibers. Natural fibers are porous and their accessibility needs to be sufficient to allow diffusion of dye molecules into the pores.
3. Adsorption of dye to the textile. Before a dye molecule can react with a fiber, it needs to be adsorbed to its surface. The affinity or substantivity of the dye for the textile determines whether or not this step takes place.
4. Reaction of the dye with the textile. The dye has to form a covalent bond with the amino groups of the proteins.

Two different dyes are used in this work:

1. Vinylsulphone dye. This dye is chosen because the vinylsulphone group is able to react with protein fibers in an aqueous dyeing process, according to Heyna et al. [5]. Fig. 2.1.A gives the reaction of the dye with a textile amino group.
2. Dichlorotriazine dye. Although the dichlorotriazine group was originally developed and patented by Rattee et al. [6] for cotton dyeing in alkaline water by reaction of the dye with the hydroxyl groups of cotton, it is investigated here if it is also able to react with amino groups of silk and wool in $scCO_2$. Fig. 2.1.B shows the reaction of a dichlorotriazine dye with a textile amino group.

It is known from Schmidt et al. [7] that a vinylsulphone dye is able to react with the functional amino groups of nylon and wool in $scCO_2$ but they found no coloration of silk. Schmidt et al. [8] also found that a dichlorotriazine dye was unable to dye silk; they did not report on dyeing of wool with a dichlorotriazine dye. However, these publications describe dyeing in dry CO_2, while the patent by Veugelers et al. [9] claims that the addition of water enhances coloration when natural fibers are dyed with reactive dyes in $scCO_2$.

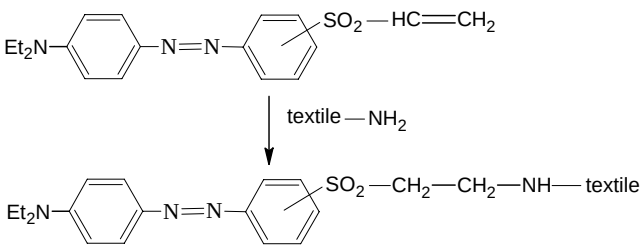

A. Vinylsulphone reaction

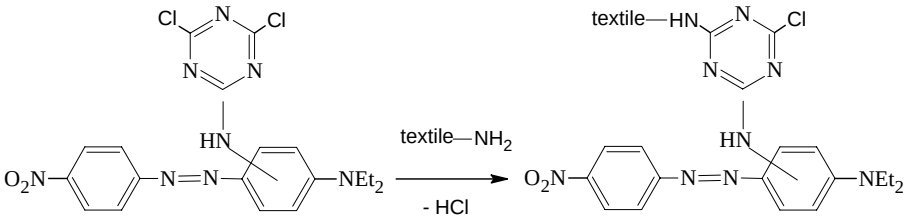

B. Dichlorotriazine reaction

Fig. 2.1. Reaction of vinylsulphone (A) and dichlorotriazine (B) dyes with textile amino sites

It is not yet known why water has this positive effect on the process. One possible explanation is that it acts as a modifier, enhancing the solubility of the dye. It could also be that water works as a swelling agent for the polar, natural textiles. As explained by Kraessig [10], the macromolecules of a natural fiber are kept together by intermolecular hydrogen bonds. Water breaks up these interactions and allows the chain molecules to increase their distance, thereby swelling the textile fiber. Dye molecules can then penetrate more easily into the fibrous structure. It is expected that nylon, silk and wool are susceptible to this effect of water and polyester is not. The third possible effect of water on the supercritical dyeing process is that it somehow participates in the reaction between the dye and the fiber. There are, however, no reports on this last possibility.

The aim of the present work is to investigate whether a vinylsulphone and a dichlorotriazine dye are suitable for protein textiles in moist scCO_2. For the vinylsulphone dye, it is determined how much water should be added to the process

to obtain maximum coloration. Experiments are done with different dyeing times, to get an indication of the rate of the process. With the dichlorotriazine dye, the influence of water addition is also investigated. Furthermore, the effects of pressure and temperature on the coloration of different textiles in moist $scCO_2$ are investigated with the dichlorotriazine dye. Finally, by dyeing polyester and nylon in the same batch as silk and wool it is checked if also blends of synthetics and natural textiles can be dyed in $scCO_2$ with both dyes.

2.2. Experimental section

2.2.1 Materials

The orange vinylsulphone dye and the purple dichlorotriazine dye, shown in Fig.1A and 1B were designed for use in $scCO_2$ and synthesized by a well-known dye manufacturer. Both powders were used as received. The textiles were all dyed as pieces of cloth. The polyester (polyethylene terephtalate; 120 g/m^2) and the nylon (polyamide 6.6; 150 g/m^2) were knitted and free of spinning oils. The wool (62 g/m^2) and the silk (120 g/m^2) were woven. Polyester was received from Ames Europe, the other textiles were from the Center for Test Materials (Netherlands). The carbon dioxide (99.97 %) was purchased from HoekLoos. The acetone that was used in the extractions was technical grade from Chemproha. Demineralised water was used, in the extractions and in the dyeing vessel.

2.2.2. Equipment and procedure

A 4-litre stainless steel autoclave from Uhde Hochdrucktechnik (Germany) was used as pressure vessel (Fig. 2.2). The temperature of the dyeing process was determined by setting the temperature of an oil heater and pumping the oil through the jacket of the dyeing vessel for 2 hours prior to each experiment. After this preheating step, dye powder (0.2 ± 0.01 g) was placed at the bottom of the vessel, between two stainless steel filter plates with a pore size of 10 μm, to prevent entrainment of undissolved dye particles. A piece of cotton (20 ± 0.2 g) was folded around small pieces of polyester, nylon, silk and wool (each 0.2 ± 0.02 g). The textile was placed in the dyeing vessel in such a way, that the CO_2 was forced to flow through the layers of textile.

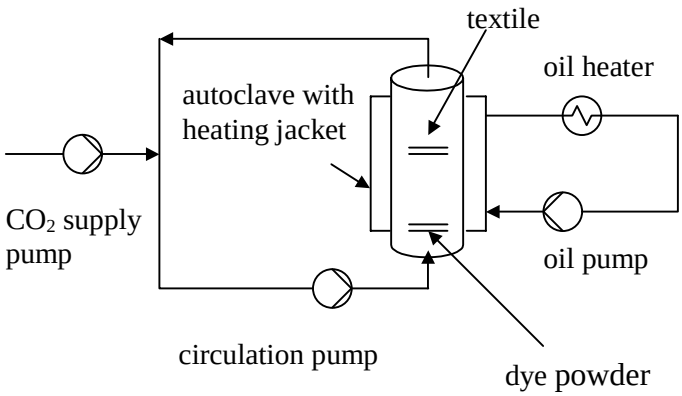

Fig. 2.2. Experimental set-up for textile dyeing in $scCO_2$

In the experiments in moist $scCO_2$, the cotton was wetted with the desired amount of water prior to placing it in the vessel. The system was then pressurized with an air-driven plunger pump, from Williams Instrument Company. The CO_2 was pumped around for 2, 4 or 6 hours, at a flow rate of 0.10 ± 0.02 m^3/hr, with a centrifugal pump with magnetic coupling from Autoclave Engineers. The flow direction was upwards through the vessel: first through the dye and then through the textiles. Temperature and pressure increased slowly in the first hour but were constant afterwards (± 1ºC and ± 2 bar). The stable values in the second hour are the reaction conditions that are mentioned in the presentation of the results below. In the experiments of 2 and 4 hours, there was dye powder left between the filter plates. The amount was different for each experiment and varied from 0.3 to 0.1 g. In the 6 hour experiments, no remaining dye was found.

2.2.4 Color analysis

The dyed pieces of polyester, nylon, silk and wool were analyzed by measuring the reflectance curve between 350 and 750 nm with a portable spectrophotometer from Avantes. The minimum of the curve (R_{min}) was used to determine the ratio of light absorption (K) and scatter (S) via the Kubelka-Munk function [10]:

$$(K/S)_{dyed} = \frac{(1 - R_{min})^2}{2R_{min}} \quad (1)$$

The ratio K/S is used as a measure of coloration in textile industry and also in this paper. After this analysis, each sample was stripped of unfixed dye by Soxhlet extraction with a 50 weight% solution of acetone in water for 30 min. The K/S-value of the extracted textile $(K/S)_{extr}$ was determined and used to calculate the percentage of dye molecules that was fixed to the textile (F):

$$F = (K/S)_{extr} / (K/S)_{dyed} * 100\ \% \qquad (2)$$

2.3. Results and discussion

2.3.1 Vinylsulphone dye

The influence of water addition was investigated in a series of 5 experiments. Different amounts of water were added and the equilibrium distribution of water was calculated with a model that is presented elsewhere (Van der Kraan et al. [11]). This calculation was done neglecting the water-uptake of silk, wool, polyester and nylon, since the mass of cotton in the vessel is 97% of the total mass of textiles. The model allows calculation of the relative humidity RH of the $scCO_2$ from pressure, temperature, vessel volume, textile mass and amount of water added to the vessel. For the 5 experiments done in the vinylsulphone series, the relative humidities were: 4, 25, 51, 73 and 97 %. Earlier experiments at our laboratory have shown that the presence of liquid water in the dyeing vessel led to staining of the textile. Therefore, in this work, RH < 100% in all experiments. The amounts of water that were absorbed by the textile from the air, prior to the experiment, were measured gravimetrically and taken into account in the calculation of RH. Therefore, when no water was added to the dyeing vessel, a relative humidity of 4% was obtained. Although the results (Fig. 2.3) are given as a function of the relative humidity RH of the $scCO_2$, it could just as well be the relative humidity of the textile that plays a role in the dyeing process. However, since a rise in CO_2 humidity also means a rise in the humidity of the textile, it effectively makes no difference which humidity is treated as the independent variable.

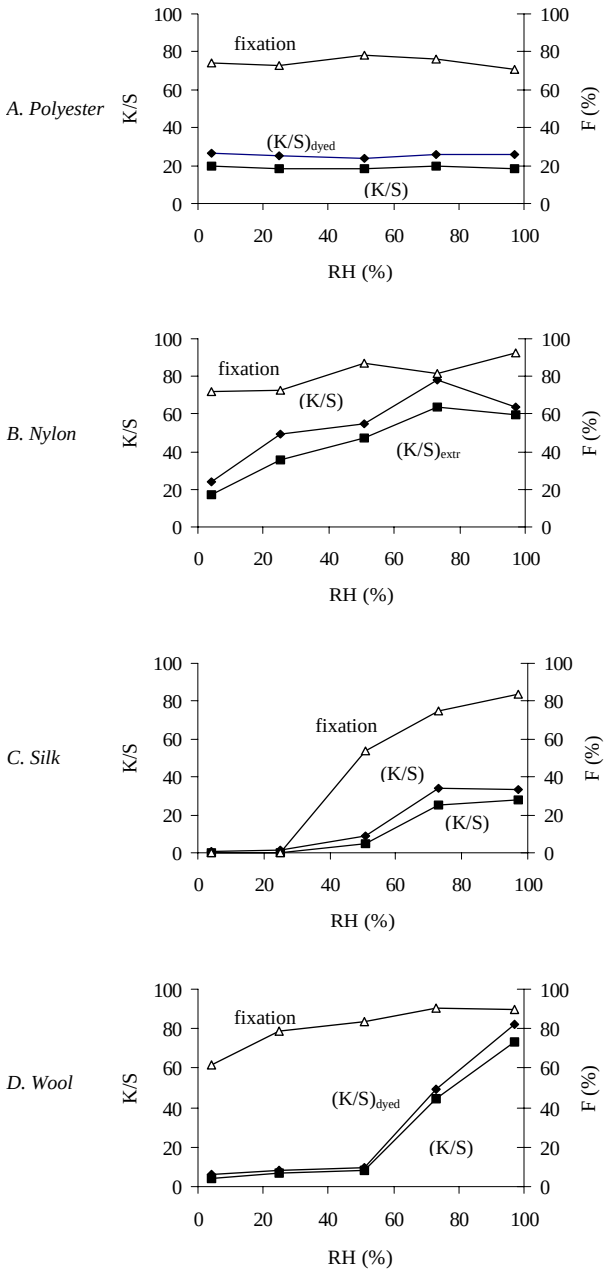

Fig. 2.3. Influence of relative CO_2-humidity (RH) on the coloration (K/S) and fixation (F) of textiles dyed in scCO_2 with a vinulsulphone dye during 2 hours at 230 bar and 112ºC, for polyester (A), nylon (B), silk (C) and wool (D)

The 5 experiments in this series were all done with the vinylsulphone dye, in 2 hours dyeing at a pressure of 230 bar and a temperature of 112ºC. The coloration and fixation of polyester were independent of humidity. A dark orange color was obtained before ($(K/S)_{dyed}$ = 25.5 ± 1.5) and after Soxhlet extraction ($(K/S)_{extr}$ = 19.5 ± 1.5), the fixation percentage was 75 ± 5 %. Nylon was also dyed well. Fig. 2.3.B shows an increase of coloration with humidity, but also in dry CO_2 nylon could be colored deeply (K/S = 20). The fixation percentages showed a slight increase with humidity. The results for silk show that no coloration was obtained without water addition, as was found by Schmidt et al. [7]. However, Fig. 2.3.C shows that, as the humidity increased, so did the coloration and the fixation of silk. Wool gave light colors in dry $scCO_2$ but, as can be seen in Fig. 2.3.D, a higher coloration and fixation were obtained when water was added.

For these amino containing textiles, the experiments gave maximum colorations when the textile and the scCO2 were nearly saturated (RH = 97%). To investigate the influence of dyeing time, the experiments were repeated at the same pressure and temperature but with 4 and 6 hours dyeing time, with relative $scCO_2$ humidity RH = 97%. It was found that the polyester coloration before and after extraction increased between 2 and 4 hours from $(K/S)_{extr}$ = 19.5 to 49 (Fig. 2.4.A). Between 4 and 6 hours, the coloration did not increase any further for polyester. This indicates that the polyester was saturated with dye molecules after 4 hours. Also the fixation (84 ± 1.5) does not change significantly between 4 and 6 hours.

Although silk is colored well by both dyes in moist $scCO_2$, it remains white when dyeing in dry $scCO_2$, despite the fact that dye is dissolved in the $scCO_2$, as is indicated by the dark coloration of polyester in dry $scCO_2$. It can be stated from this that the positive effect of water on the coloration of the amino containing textiles is not due to an action of water as a solubility enhancer. Because water is a polar component, it can also not enhance the substantivity between the dye and the fiber. An increase in fixation with water content, as observed with the amino containing textiles, indicates that water plays a role in the reaction between the dye and the fiber. Whether or not the accessibility of the fibers is enhanced by the

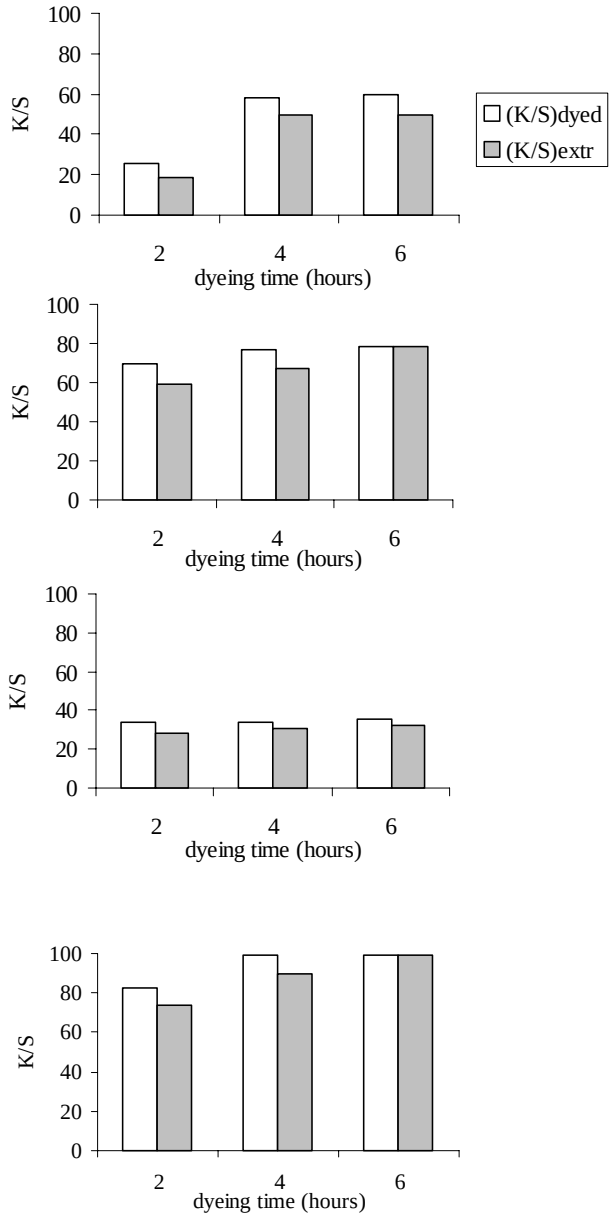

Fig. 2.4. Coloration of textiles with a vinylsulphone dye in $scCO_2$ at 230 bar, 112ºC and different CO_2-humidities (RH) as a function of time, for polyester (A), nylon (B), silk (C) and wool (D)

swelling effect of water, does not follow from the results, but can also not be ruled out.

For the amino containing textiles, the results given in Fig. 4B-D show that coloration after extraction increased with time up to 6 hours; after 4 hours nylon, silk and wool were not yet saturated with dye. Fig. 2.4.B-D also reveal that, as the dyeing time of the amino containing textiles progressed, the fixation increased. This reflects the dyeing mechanism described above: First the dye adsorbs to the textile surface and, after that, it reacts with the amino sites.

2.3.2 Dichlorotriazine dye

Firstly, two experiments were done with the dichlorotriazine dye: one in dry $scCO_2$ (RH = 4%) and one in moist, almost saturated $scCO_2$ (RH = 97%). As can be seen in table 2.1, the results correspond qualitatively with those of the vinylsulphone experiments for all textiles: The coloration before and after extraction and the fixation of polyester were independent of water addition. The coloration after extraction of silk was negligible in dry $scCO_2$ but increased with relative $scCO_2$-humidity, the fixation on silk increased with water addition. Wool could be colored lightly in dry $scCO_2$ and darker in moist $scCO_2$, the fixation on wool increased when water was added. As was the case for the vinylsulphone dye, for the dichlorotriazine dye it follows that the reactivity is increased by water addition. Whether or not the accessibility of the fibers is also increased does not follow from the results.

Table 2.1. Influence of relative $scCO_2$-humidity RH on the coloration before ($(K/S)_{dyed}$) and after ($(K/S)_{extr}$) Soxhlet extraction and the calculated fixations F of textiles dyed with dichlorotriazine dye in $scCO_2$ at 250 bar and 100ºC for 2 hours

Textile	$(K/S)_{dyed}$		$(K/S)_{extr}$		F (%)	
	RH = 4%	RH = 97%	RH = 4%	RH = 97%	RH = 4%	RH = 97%
Polyester	10.1	10.3	10.1	10.1	100	98
Silk	0.44	4.24	0.25	3.22	57	76
Wool	4.26	5.79	2.47	4.05	58	70

With the dichlorotriazine dye, the influence of pressure and temperature on the coloration and fixation of polyester, silk and wool was investigated. In all of these

experiments, the relative humidity of the $scCO_2$ was 97%. For the calculation of the amounts of water in the textile and the $scCO_2$, i.e. to calculate how much water had to be added, the same procedure as above was followed, taking only the mass of the cotton into account. Because the distribution of water between cotton and $scCO_2$ depends on temperature and pressure, different amounts of water were added in each experiment, varying from 22 g at (225 bar, 100ºC) to 30 g water at (250 bar, 116ºC), to reach the same CO_2-humidity of 97%.

In table 2.2 the results are given for varying pressures (from 225 to 278 bar) at 100ºC and 2 hours dyeing time. The colorations $(K/S)_{dyed}$ and $(K/S)_{extr}$ of polyester were good and increased with pressure at constant temperature, as was reported by Chang et al. [12] for disperse non-reactive dyes. The increase of dye uptake with pressure is caused by enhanced dye solubility and by increased swelling of the polyester. Although less than polyester, silk and wool were dyed well and the $(K/S)_{dyed}$ and $(K/S)_{extr}$ varied within the experimental error range, i.e. the colorations were independent of pressure. This is clear from Fig. 2.5, which gives a graphical representation of the influence of pressure on the coloration after extraction. Table 2.2 shows that the fixations on polyester, silk and wool are independent of pressure.

Table 2.2. Influence of pressure on the coloration before ($(K/S)_{dyed}$) and after ($(K/S)_{extr}$) Soxhlet extraction and the calculated fixations F of textiles dyed with dichlorotriazine dye in $scCO_2$ at 100ºC for 2 hours

P	polyester			silk			wool		
bar	$(K/S)_{dyed}$	$(K/S)_{extr}$	F %	$(K/S)_{dyed}$	$(K/S)_{extr}$	F %	$(K/S)_{dyed}$	$(K/S)_{extr}$	F %
225	6.83	5.95	87	3.91	3.57	91	3.29	2.65	81
235	8.83	8.73	99	4.60	4.32	94	4.71	3.52	75
250	10.4	10.1	97	4.73	4.05	86	4.40	3.22	73
260	10.7	9.82	92	4.66	4.31	92	4.05	3.20	79
265	11.5	11.2	97	4.02	3.60	90	4.68	4.00	85
275	11.5	10.9	95	4.60	4.05	88	3.73	2.94	79

Table 2.3 shows that, when temperature was varied from 100 to 116ºC at constant pressure (250 bar), the colorations of polyester, silk and wool before and after extraction showed no significant changes. This is also clear from Fig. 2.6, where the colorations after extraction are presented graphically. The fixation percentages of polyester, silk and wool showed no dependency on temperature. Although the K/S-values for polyester were much higher in all the dichlorotriazine experiments, the K/S-values for silk and wool, being between 3 and 4, also corresponded with a dark purple color.

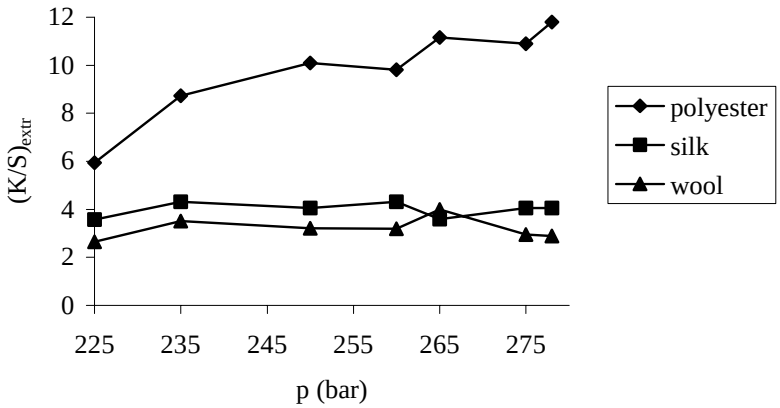

Fig. 2.5. Influence of pressure on the coloration $(K/S)_{extr}$ of polyester, silk and wool dyed for 2 hours at 100ºC with dichlorotriazine dye in $scCO_2$ with relative humidity RH = 97%.

Table 2.3. Influence of temperature on the coloration before ($(K/S)_{dyed}$) and after ($(K/S)_{extr}$) Soxhlet extraction and the calculated fixations F of textiles dyed with dichlorotriazine dye in $scCO_2$ at 250 bar for 2 hours

T	polyester			silk			wool		
ºC	$(K/S)_{dyed}$	$(K/S)_{extr}$	F %	$(K/S)_{dyed}$	$(K/S)_{extr}$	F %	$(K/S)_{dyed}$	$(K/S)_{extr}$	F %
100	10.4	10.1	97	4.66	4.05	87	4.19	3.22	89
105	11.2	11.0	98	4.29	3.98	93	4.00	3.53	88
111	10.9	10.9	100	4.26	3.85	90	4.40	3.64	83
116	11.8	11.5	97	5.31	4.80	90	4.46	4.05	91

Pressure and temperature are the two parameters that determine the solubility of dye in $scCO_2$. Therefore, the negligible influence of both parameters on the coloration of the amino containing textiles suggests that the solubility is not the rate determining factor in the process. However, since it is not known how strong the solubility varies with pressure and temperature, this cannot be stated with certainty. Research is needed on the influence of pressure and temperature on the solubility of this particular compound in $scCO_2$.

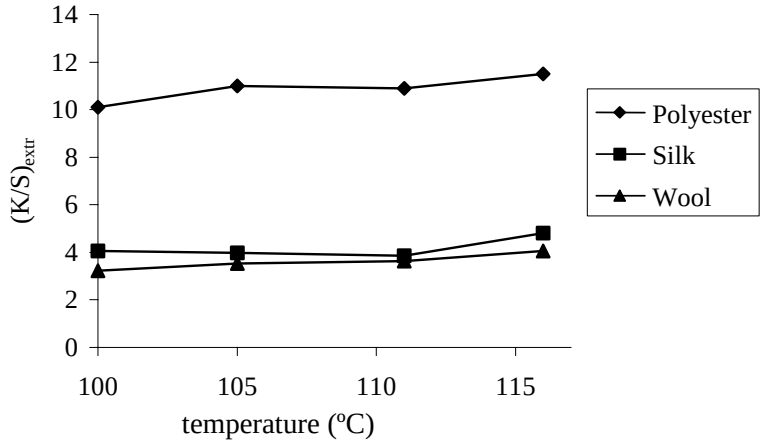

Fig. 2.6. Influence of temperature on the coloration $(K/S)_{extr}$ of polyester, silk and wool dyed for 2 hours at 250 bar with dichlorotriazine dye in $scCO_2$ with a relative humidity of 97%

The observation that temperature has negligible influence on coloration also suggests that the reaction rate is not rate determining. However, since no information is available on the kinetics of this reaction in $scCO_2$, this cannot be positively concluded. Additional research is needed on the kinetics of the dye-fiber reaction.

2.4. Conclusions

Disperse dyes containing a reactive vinylsulphone or a dichlorotriazine group, are suitable for dyeing textiles containing polyester, nylon, silk, wool or blends of these fibers in supercritical carbon dioxide. The dye uptake by polyester is

independent of water addition. For the amino-containing textiles, the coloration increases with the concentration of water in the $scCO_2$ and the textiles. Experiments with the vinylsulphone dye show that maximum coloration of nylon, silk and wool is obtained when both the $scCO_2$ and the textiles are saturated with water. The fixation percentage of vinylsulphone dye on polyester was 75% and independent of pressure. Fixations on nylon, silk and wool increased with relative humidity of the $scCO_2$. In saturated $scCO_2$, values are reached in 2 hours of 94, 85 and 90%, respectively. When dyeing with the dichlorotriazine dye in $scCO_2$ saturated with water, the fixations of polyester, silk and wool are 93, 88 and 79%.

When the dyeing time is varied for the vinylsulphone dye, the coloration of the amino containing textiles increases as expected. Also the fixation grows in time, indicating that more and more of the dye molecules present in the textile are covalently bonded to the amino sites.

The positive effect of water on the dyeing process is caused either by water facilitating the chemical reaction between the dye and the fiber, or by water acting as a swelling agent for the textiles. Whatever the reason for this phenomenon, it is concluded that water should be added in supercritical dyeing of nylon, silk and wool with disperse dyes containing vinylsulphone or dichlorotriazine reactive groups.

The experimental results on the dichlorotriazine dye suggest that the solubility and the reactivity can be ruled out as the rate-determining step of the dyeing process. However, for this conclusion to be made with certainty, more research is needed on solubility and reaction kinetics.

References

1. E. Bach, E. Cleve and E. Schollmeyer, Past, Present and Future of Supercritical Fluid Dyeing Technology – an Overview, *Rev. Prog. Color.* **32**, 88 (2002).
2. W. Saus, D. Knittel and E. Schollmeyer, Dyeing of Textiles in Supercritical Carbon Dioxide, *Text. Res. J.* **63** (3), 135 (1993).

3. I. Tabata, J. Lyu, S. Cho, T. Tominaga and T. Hori, Relationship between the Solubility of Disperse Dyes and the Equilibrium Dye Adsorption in Supercritical Fluid Dyeing, *Color. Technol.* 117, 346 (2001).
4. S.K. Liao, Y.C. Ho, P.S. Chang, Dyeing of Nylon 66 with a Disperse-Reactive Dye using Supercritical Carbon Dioxide as the Dyeing Medium, *J. Soc. Dyers and Color.* **116**, 403 (2000).
5. J. Heyna, W. Schumacher and Hoe, German P 925,902 (1949).
6. I.D. Rattee, W.E. Stephen and ICI, BP 772,030 774,925 871,930 (1954).
7. A. Schmidt, E. Bach and E. Schollmeyer, Use of Fiber Reactive Groups in Supercritical Carbon Dioxide, *Melliand Textilberichte* **83** (9), 648 (2002).
8. A. Schmidt, E. Bach and E. Schollmeyer, The Dyeing of Natural Fibers with Reactive Disperse Dyes in Supercritical Carbon Dioxide, *Dyes and Pigments* **56** (1), 27 (2003).
9. W.J.T. Veugelers, H. Gooijer, J.W. Gerritsen and G.F. Woerlee, European Patent EP 1 126 072 A2, 2001.
10. R. McDonald (Ed.), Colour Physics for Industry, 2nd ed., Society of Dyers and Colourists, Bradford (1995).
11. M. van der Kraan, M.V. Fernandez Cid, G.F. Woerlee, W.J.T. Veugelers, C.J. Peters and G.J. Witkamp, Equilibrium Distribution of Water in the Two-Phase System Supercritical Carbon Dioxide-Textile, *J. Supercrit. Fluids*, submitted for publication.
12. K.-H. Chang, H.-K. Bae and J.-J. Shim, Dyeing of PET Textile Fibers and Films in Supercritical Carbon Dioxide, *Korean J. Chem. Eng.* **13** (3), 310 (1996).

Chapter 3

Equilibrium Distribution of Water in the Two-phase System Supercritical Carbon Dioxide - Textile

Abstract

When natural fibers are dyed in supercritical carbon dioxide, the addition of a small amount of water increases coloration. For a process design it is important to know how much water has to be added to obtain a desired humidity of both textile and carbon dioxide. In this work a thermodynamic model is proposed to calculate the distribution of water over the textile phase and the supercritical phase as a function of pressure and temperature. The phase equilibrium is described with Raoult's law for non-ideal fluids. The absorbed water in the textile is a condensed phase and is modeled here as a non-ideal liquid, using the NRTL-equation. The non-ideality of the supercritical phase is described by a solubility enhancement factor, a new equation derived from statistical thermodynamics. Although the model is applied to cotton, viscose, silk and wool, it can be used for all water absorbing textiles.

Contents submitted to the Journal of Supercritical Fluids

Symbols

A	Antoine constant	[MPa]
b, b_1, b_2, b_{12}	Van der Waals volume	[m^3/mole]
B	Antoine constant	[K]
c_{12}, c_{21}	NRTL-parameters	[J/mole]
C	Antoine constant	[K]
g	NRTL-parameter	[-]
G_{12}, G_{21}	NRTL-parameters	[-]
h	Planck's constant	[Js]
k	Boltzmann's constant	[J/K]
L	relative $scCO_2$-humidity	[-]
m	particle mass	[kg]
m_{CO2}	mass of $scCO_2$	[kg]
m_{H2O}^{CO2}	mass of water in $scCO_2$	[kg]
m_{H2O}^{text}	mass of water in textile	[kg]
m_{H2O}	total mass of water in dyeing vessel	[kg]
m_{text}	mass of textile	[kg]
M_{H2O}, M_{CO2}	molar mass of water and carbon dioxide	[g/mole]
n	number of particles	[-]
N_i^{α}	molar concentration of component i in phase α	[mole/m^3]
N_A	Avogadro's number	[$mole^{-1}$]
p	pressure	[MPa]
p_{H2O}^{sat}	water vapor pressure	[MPa]
$q_{r,v}$	rotational and vibrational part of partition function	[-]
r	distance	[m]
R	universal gas constant	[J/(moleK)]
T	temperature	[K]
U	potential energy	[J]
V	volume	[m^3]
V_m	molar volume	[m^3/mole]
V_{ex}	excluded volume	[m^3]
x	regain	[kg water/kg dry textile]
x_{max}	regain in saturated textile	[kg water/kg dry textile]
y	mass fraction of water in the supercritical phase	[-]

Y	mole fraction of water in $scCO_2$	[-]
y^{sat}	water mass fraction in saturated $scCO_2$	[-]
Z	partition function	[-]
α_{max}	constant	[-]
β	= 1/(kT)	[J^{-1}]
γ_{H2O}	activity coefficient of water in textile	[-]
Γ	enhancement factor in terms of density	[-]
ε	Lennard-Jones parameter	[J]
θ_{H2O}	water content of textile, relative to saturation	[-]
θ_{text}	textile fraction in wet textile	[-]
κ	constant	[Km^3/kg]
λ	constant	[K]
μ	chemical potential	[J/mole]
ρ	density	[kg/m^3]
ρ_{CO2}	density of $scCO_2$	[kg/m^3]
ρ_{text}	density of textile	[kg/m^3]
ρ_{CO2}^{max}	maximum density of CO_2	[kg/m^3]
ρ_{H2O}^{sat}	water vapor density at vapor pressure	[kg/m^3]
σ, σ_1, σ_2, σ_{12}	Lennard-Jones parameter	[m]
τ_{12}, τ_{21}	NRTL-parameters	[-]
Φ	non-ideality factor in terms of pressure	[-]

3.1. Introduction

Using supercritical carbon dioxide ($scCO_2$) as a solvent for dyeing textiles has been the subject of several researchers in the last few years, as was reviewed by Bach et al. [1]. Typical dyeing conditions are 373 K and 30 MPa. Veugelers et al. [2] and Van der Kraan [3] reported that in reactive dyeing of natural textiles the addition of a small amount of water to the dyeing vessel increased the uptake of dye.

The positive effect of water can be attributed to one or more of the following three causes. Firstly, water can act as a modifier, increasing the solubility of dye in

$scCO_2$. Secondly, water can participate in the reaction of dye with the textile reactive sites. This option has not yet been investigated. Thirdly, water can have an influence on the structure of the textile. Natural textiles consist of proteins (e.g. silk and wool) or cellulose (e.g. cotton). These molecules contain amine or hydroxyl groups that are capable of forming intermolecular hydrogen bonds that keep the protein or cellulose chains and, therefore, the whole textile structure together. When water is added to the textile, it breaks up the hydrogen bonds between the chains, forms its own hydrogen bonds with the amine or hydroxyl groups and takes position between the chains. This means that the chains are driven apart and that the textile volume increases, i.e. water acts as a swelling agent (Nevell [4]). The swollen structure of the textile allows dye molecules to penetrate the textile and, therefore, has a positive effect on a dyeing process.

For a process design, it is important to be able to calculate the desired amount of water in a specific dyeing batch. When the cause of coloration improvement by water addition is the enhancement of dye solubility, the water content of the $scCO_2$ is the factor to be calculated. When coloration is improved by participation of water in the reaction or by the swelling effect, the humidity of the textile is the factor of interest. A model is needed to calculate the water content of both the textile and the $scCO_2$.

In a dyeing vessel, the water is distributed over the textile and the supercritical phase. In this work a thermodynamic equilibrium distribution is modeled, taking into account the non-ideal behavior of water in textile and in $scCO_2$. To quantify the interactions water-textile and water-$scCO_2$, equations are derived that are fitted to experimental data from literature. The resulting thermodynamic model enables calculation of how much water has to be added to a supercritical dyeing process to obtain a desired water content in the textile and in the $scCO_2$. An example is given showing how to apply the model in the case that the humidity of the textile is the factor to be calculated. The case that the humidity of the $scCO_2$ is to be calculated is an analogous procedure. The model is developed for cotton, silk, wool and viscose but can also be used for other water absorbing textiles.

3.2. Thermodynamic model

3.2.1. Equilibrium water distribution

A dyeing vessel is considered containing textile, $scCO_2$ and water. All water is dissolved in either the textile or the $scCO_2$; no liquid water is present. The textile is modeled here as a homogeneous phase with n_{tot} sites available for water adsorption, of which n_{H2O} are occupied by adsorbed water molecules. Since the water molecules that are adsorbed to the textile sites are in fact a condensed phase, they are modeled here as a non-ideal liquid. When the mole fraction of water in the textile is defined as $\theta_{H2O} = n_{H2O}/n_{tot}$, the equilibrium distribution of water over the textile and the $scCO_2$ can be described by Raoult's law for non-ideal fluids (Smith and Van Ness [5]):

$$\theta_{H2O}\gamma_{H2O}p^{sat}_{H2O} = Y\Phi p \qquad (1)$$

where γ_{H2O} is the activity coefficient of water in the textile, p^{sat}_{H2O} is the vapor pressure of pure water, Y is the mole fraction of water in the $scCO_2$, p is the pressure inside the dyeing vessel and Φ is the factor describing the non-ideality of the supercritical phase. Φ is a function of the fugacity coefficient of water in $scCO_2$ and of the Poynting factor and therefore a complex function of pressure and temperature [5].

In this study, it is convenient to write Eq. (1) in terms of mass and mass density instead of moles and pressure:

$$\theta_{H2O}\gamma_{H2O}\Gamma\rho^{sat}_{H2O} = y\rho \qquad (2)$$

where ρ^{sat}_{H2O} is the mass density of pure water at the vapor pressure, ρ is the mass density of the supercritical phase, y is the mass fraction of water in the supercritical phase and Γ is the factor describing the non-ideality of the supercritical phase. The advantage of using mass densities instead of pressures is that Γ is a simple function of density and temperature (see Eq. (19)). Eq. (2) is the basis upon which the thermodynamic model is constructed.

The first term in Eq. (2), θ_{H2O}, is defined in Eq. (1) as a mole fraction but is equal to the following mass fraction:

$$\theta_{H2O} = \frac{x}{x_{max}} \tag{3}$$

where x is the regain, a term used in textile industry to indicate textile humidity. Its maximum value x_{max} is the regain in saturated $scCO_2$. The regain is defined as the mass of water in the wet textile m_{H2O}^{text} relative to mass of dry textile m_{text}:

$$x = \frac{m_{H2O}^{text}}{m_{text}} \tag{4}$$

Inspection of Eq. (3) and Eq. (4) reveals that θ_{H2O} is the same in terms of mass as in terms of moles.

If the total mass of water distributed over the textile and the $scCO_2$ is m_{H2O} and the mass of water in the $scCO_2$ is m_{H2O}^{CO2}, then the water mass balance is:

$$m_{H2O} = m_{H2O}^{text} + m_{H2O}^{CO2} \tag{5}$$

with the amount of water dissolved in the $scCO_2$ given by:

$$m_{H2O}^{CO2} = y\left(m_{H2O}^{CO2} + m_{CO2}\right) \tag{6}$$

where y is the mass fraction of water in the supercritical phase and m_{CO2} denotes the mass of $scCO_2$ in the dyeing vessel, calculated from the volume of the vessel, the density's of water and textile (ρ_{CO2} and ρ_{text}) and the mass of (dry) textile m_{text}:

$$m_{CO2} = \rho_{CO2}\left(V - \frac{m_{text}}{\rho_{text}}\right) \tag{7}$$

The values for the textile density ρ_{text}, taken from Morton and Hearle [6], are given in table 3.1. The density ρ_{CO2} needed in Eq. (7) is taken from the IUPAC tables (Angus et al. [7]). The density ρ_{CO2} is also used for ρ in Eq. (2) because the solubility of water in $scCO_2$ is small and therefore it is assumed that it has negligible influence on the CO_2-density: according to Evelein et al. [8], the value of y at typical dyeing conditions of 30 MPa and 373 K is $y^{sat} = 10^{-2}$.

Table 3.1. Density ρ_{text} of dry cotton, silk, wool and viscose rayon from Morton and Hearle [6]

Textile material	ρ_{text} (kg/m^3)
cotton	1550
silk	1340
wool	1300
viscose rayon	1520

The terms in Eq. (2) and Eq. (3) that remain to be discussed represent the thermodynamics of the water-textile mixture (activity coefficient γ_{H2O} and maximum regain x_{max}) and the thermodynamics of the water-$scCO_2$ mixture (non-ideality factor Γ).

3.2.2. Thermodynamics of the system water-textile

maximum regain x_{max}

The maximum regain x_{max} is defined as the humidity of a textile that is in equilibrium with air that is saturated with water. In such a situation the chemical potential of the adsorbed water is equal to the chemical potential of water in saturated air which, in its turn, is equal to the chemical potential of liquid water. When not air but high-pressure CO_2 is regarded, the situation remains the same: the chemical potential of the adsorbed water is the same as in liquid water. Since the latter is independent of pressure and the surrounding medium, it can be stated that the chemical potential of adsorbed water is the same in air as in $scCO_2$, at the same temperature. Because the chemical potential depends on the water content of the textile, also the maximum regain x_{max} is the same in air as in $scCO_2$. In this work, experimental data measured in air are used to fit an equation for x_{max} that is to be used in supercritical dyeing.

Wiegerink [9] observed that in humid air at atmospheric pressure the logarithm of the regain x in silk, wool, cotton and viscose is inversely proportional to temperature for a given relative air humidity. In the case of saturated air the water regain is at its maximum x_{max} :

$$x_{max} = \alpha_{max} \exp\frac{\lambda}{T} \tag{8}$$

where α_{max} and λ are constants and T is temperature in K. Below the saturation point of the textile, Eq. (8) is valid for calculating x, with a different pre-exponential factor (α) but with the same λ [9]. Therefore, the ratio x/x_{max} (= θ_{H2O}) is independent of temperature.

Eq. (8) can be used for supercritical dyeing with parameters determined by fitting the equation to data from Wiegerink who measured the regains of cotton, silk, wool and viscose as a function of relative air humidity for several temperatures. Taking from Wiegerink [9] data points (T, x_{max}) allows calculation of the parameters α_{max} and λ for a textile material (table 3.2). For a given temperature, the value of x_{max} can now be calculated from Eq. (8).

Table 2: Empirical parameters of Eq. (8), calculated from Wiegerink [9]

Textile material	$\alpha_{max}/10^{-2}$	λ (K)
mercerized cotton	0.97	1031
degummed silk	2.27	711
clothing wool	3.57	625
viscose rayon	4.33	594

activity coefficient

The activity coefficient γ_{H2O} in Eq. (2) follows from the NRTL equation (Prausnitz et al., [10]):

$$\ln\gamma_{H2O} = \theta_{text}^2\left[\tau_{21}\left(\frac{G_{21}}{\theta_{H2O}+\theta_{text}G_{21}}\right)^2 + \tau_{12}\frac{G_{12}}{(\theta_{text}+\theta_{H2O}G_{12})^2}\right] \tag{9}$$

where $\theta_{text} \equiv 1-\theta_{H2O}$. The four parameters τ_{12}, τ_{21}, G_{12} and G_{21} are determined by three independent parameters c_{12}, c_{21} and g:

$$\tau_{12} = \frac{c_{12}}{RT} \qquad \tau_{21} = \frac{c_{21}}{RT} \tag{10}$$

$$G_{12} = \exp(-g\tau_{12}) \qquad G_{21} = \exp(-g\tau_{21}) \tag{11}$$

It has been shown earlier that the chemical potential of water in textile is the same in air as in $scCO_2$. Therefore, also the activity coefficient is independent of the surrounding medium. The NRTL-equation can be used for $scCO_2$ when it is fitted to Wiegerink's data [9] measured in air. This is done by defining a relative $scCO_2$-humidity L as:

$$L = \frac{y\rho_{CO2}}{\Gamma\rho_{H2O}^{sat}} \tag{12}$$

and combining Eq. (2), (3) and (12) to obtain:

$$\theta_{H2O}\gamma_{H2O} = \frac{x}{x_{max}}\gamma_{H2O} = L \tag{13}$$

Taking points (L,x) from Wiegerink [9] for a certain temperature, calculating x_{max} from Eq. (8) and using Eq. (13), allows calculation of points (θ_{H2O},γ_{H2O}) that are used to fit the NRTL-equation, i.e. to determine the parameters G_{12}, G_{21}, τ_{12} and τ_{21}. Fig. 3.1 shows that temperature has a negligible influence on the activity coefficient of water in cotton, silk, wool and viscose, from 347 to 377 K.

The observed independence of the activity coefficient on temperature is not seen in the formal NRTL-equation (see Prausnitz et al. [10]), in which temperature-dependent mass- or mole fractions are used instead of normalized mass fractions θ_{H2O} and θ_{text} that are temperature-independent. The temperature-dependence introduced by Eq. (10) is concluded to be negligible between 347 and 377. In the practice of textile dyeing the temperature-independence has the advantage that for

each textile type one set of NRTL-parameters can be used for all dyeing temperatures between 347 and 377 K.

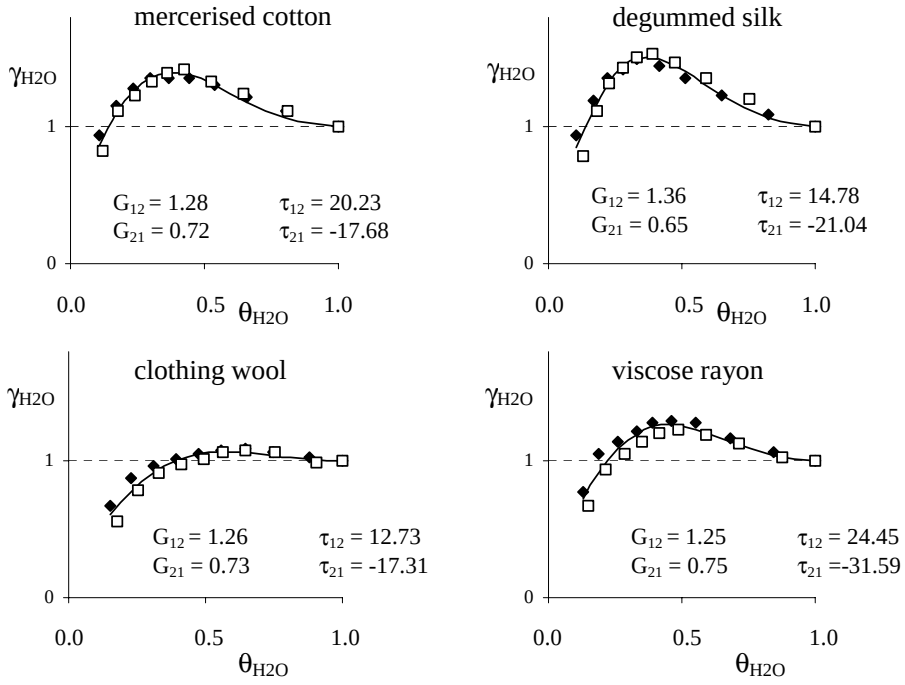

Fig. 3.1. Activity coefficient of water in textile (γ_{H2O}) as a function of relative textile humidity (θ_{H2O}), for 377 K (♦) and 347 K (□) and the NRTL-equation (—) with the fitted parameters G_{12}, G_{21}, τ_{12} and τ_{21}

3.2.3. Thermodynamics of the system water-supercritical CO_2

For calculation of the water mass concentration ρ_{H2O}^{sat} in Eq. (2), the Antoine equation is the starting point:

$$p_{H2O}^{sat} = A \exp\left(\frac{B}{T - C}\right) \tag{14}$$

with temperature T expressed in K and the constants taken from Poling et al. [11]: A = $1.32 \cdot 10^4$ MPa, B = -3884 K and C = 43.0 K. Eq. (14) is combined with the ideal gas law:

$$p_{H2O}^{sat} = \frac{\rho_{H2O}^{sat}}{1000 M_{H2O}} RT \tag{15}$$

where M_{H2O} is the molar mass of water, R is the universal gas constant and the factor 1000 is introduced to match the units. This allows elimination of vapor pressure to obtain ρ_{H2O}^{sat}, the density of pure gaseous water at the vapor pressure:

$$\rho_{H2O}^{sat} = \frac{1000 A M_{H2O}}{RT} \exp\left(\frac{B}{T - C}\right) \tag{16}$$

Eqs. (14) to (16) describe the behavior of ideal gases. For a supercritical phase, the factor Γ in Eq. (2) corrects for the non-ideality in the fluid. Eq. (2) can be rewritten as:

$$\Gamma = \frac{y \rho_{CO2}}{\theta_{H2O} \gamma_{H2O} \rho_{H2O}^{sat}} \tag{17}$$

The behavior of the supercritical phase is independent of the properties of the condensed phase, or: Γ is independent of θ_{2O} and γ_{H2O}. Furthermore, Γ is independent of y because, as was shown above, the solubility of water in $scCO_2$ is low. From these considerations it follows that Γ is the same below and at saturation; for Γ one can substitute in Eq. (2) the value calculated with:

$$\Gamma = \frac{y^{sat} \rho_{CO2}}{\rho_{H2O}^{sat}} \tag{18}$$

Inspection of Eq. (18) reveals that Γ is the water concentration in $scCO_2$ ($= y\rho_{CO2}$) relative to the water concentration in the absence of $scCO_2$ ($= \rho_{H2O}^{sat}$), i.e. Γ describes the extra solubility of water in the gas (or supercritical) phase that is

caused by non ideal behavior, or by the interaction of water molecules with CO_2-molecules. Therefore, Γ is called here the solubility enhancement factor.

The following expression, derived in appendix A, is used to calculate the enhancement factor:

$$\Gamma = \frac{y^{sat}\rho_{CO2}}{\rho_{H2O}^{sat}} = \left(1 - \frac{\rho_{CO2}}{\rho_{CO2}^{max}}\right)\exp\left(\frac{\kappa\rho_{CO2}}{T} - \frac{b_1}{M_{CO2}}\frac{\rho_{CO2}^{max}\rho_{CO2}}{\rho_{CO2}^{max} - \rho_{CO2}}\right) \tag{19}$$

where ρ_{CO2}^{max} = 1560 kg/m^3 is the maximum (solid state) density of CO_2 (Perry and Green [12]), M_{CO2} = 44.0 g/mole is the molar mass of CO_2. As is shown in appendix A, b_1 represents the molar excluded volume and can be taken as the Van der Waals volume b_1 = 0.0305 liter/mole (Lide [13]). In Eq. (19), κ is the only parameter that is to be determined by fitting the equation to literature data. Evelein et al. [8] give water solubilities in scCO2 as a function of pressure for several temperatures. These data are used to determine κ = 2.08 K·m^3/kg and to construct the fitted curves shown in Fig. 3.2. The solubilities predicted by Eq. (19) are in good agreement with the data from literature, especially at typical dyeing conditions of 373 K and 30 MPa. This proves that the approximations introduced in the derivation of Eq. (19), in appendix A, are justified, at least for the system H_2O-CO_2.

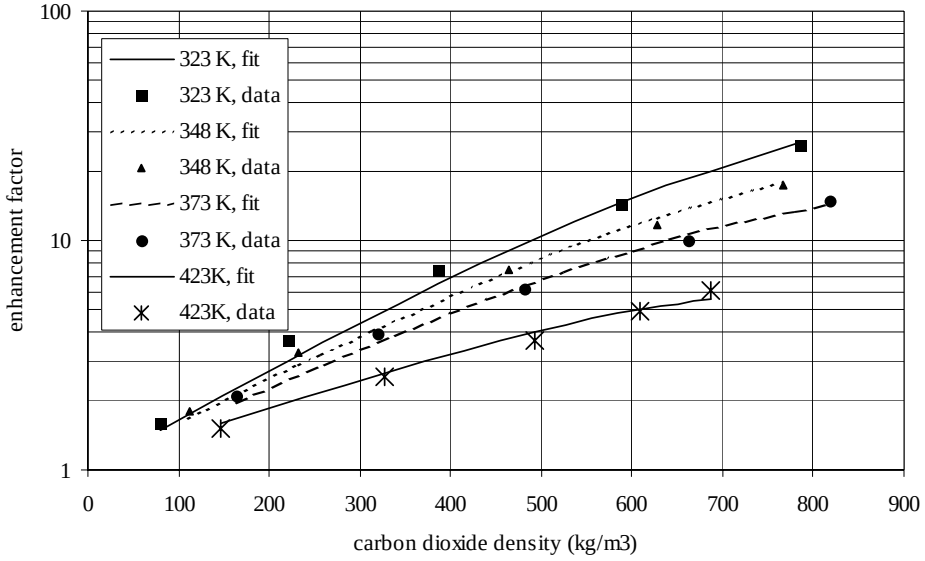

Fig. 3.2. Fitted curves of the enhancement factor $(y^{sat}\rho_{CO2}/\rho_{H2O}^{sat})$ *as a function of pressure for several temperatures*

3.2.4. Application of the model

The aim of the model is to predict how much water has to be added to a supercritical dyeing process (m_{H2O}) to obtain a desired textile humidity (x), at given process conditions (p, T, vessel volume, m_{text} and textile type). The procedure is as follows:

1. From temperature, ρ_{H2O}^{sat} and x_{max} are calculated with Eq. (16) and (8) respectively.
2. From p, T and vessel volume V follow: ρ_{CO2} (IUPAC tables) and Γ (Eq. (19)).
3. From ρ_{CO2}, m_{text}, ρ_{text} and V, the carbon dioxide mass m_{CO2} is calculated (Eq. (7)).
4. The model is now reduced to a system of 6 equations: Eq. (2) to Eq. (6) and Eq. (9). From experience it has to be known at which value of x the coloration of a certain type of textile is maximal. Substituting this x in Eq. (3) and Eq. (4) leaves 6 unknown variables: θ_{H2O}, γ_{H2O}, y,

m_{H2O}^{text}, m_{H2O} and m_{H2O}^{CO2}. The system can be solved and the output m_{H2O} gives the amount of water that has to be added to a dyeing vessel to obtain maximum textile coloration.

To illustrate the application of the model an example is given. 100 kg Mercerized cotton is dyed in $scCO_2$ (30 MPa, 373 K) in a 500-liter vessel. If it is known from experience that the coloration has an optimum at a water content of 0.126 g water/g dry textile, the procedure is:

1. For 373 K, Eq. (16) delivers ρ_{H2O}^{sat} = 0.59 kg water/m^3. Eq. (8) gives x_{max} = 0.15 kg water/kg dry textile.
2. From the IUPAC tables [7] it follows that for p = 30 MPa and T = 373 K the density of $scCO_2$ is ρ_{CO2} = 662 kg/m^3. The enhancement factor calculated with Eq. (19) is Γ = 10.4.
3. From Eq. (7) it follows that m_{CO2} = 288 kg.
4. The desired textile humidity is x = 0.126 kg/kg. Solving Eq. (2) to Eq. (6) and Eq. (9) gives the six unknown variables:

   θ_{H2O} = 0.84 $\quad$ γ_{H2O} = 1.1 $\quad$ y = 0.0084

   m_{H2O}^{CO2} = 2.3 kg $\quad$ m_{H2O}^{text} = 13 kg $\quad$ m_{H2O} = 15 kg

The model predicts that when m_{H2O} = 15 kg of water are added to the dyeing vessel, optimal coloration is obtained. It should be noted that the model assumes that the textile does not contain any water when it is placed in the dyeing vessel. This is only true when the textile is in equilibrium with dry air. When the textile is stored in humid air prior to dyeing, a correction should be made. This is illustrated with the example treated above: if the cotton is stored at 293 K and with a relative air humidity of 65%, according to Bobeth et al. [13], the moisture content is 0.11 kg water / kg dry cotton. This means that for the 100 kg of cotton not 15 kg of water, as was predicted by the model, but only 4 kg of water have to be added to obtain the desired water content of 0.126 g water/g dry cotton during the dyeing process. For other storage temperatures and air humidities, textile humidities are readily available in the tables and graphs from Bobeth et al. [13] and Morton and Hearle [6], for cotton, viscose, silk and wool.

3.3. Conclusions

A model was proposed to calculate the optimal amount of water in a supercritical dyeing process from dyeing temperature, pressure, vessel volume and textile mass. The model can be used for cotton, viscose, silk and wool in supercritical carbon dioxide.

The solubility and the activity coefficient of water in textile were modeled. The resulting equations were fitted between 347 and 377 K with experimental data for air but are also valid under supercritical dyeing conditions.

The solubility of water in $scCO_2$ as a function of density and temperature was modeled with a solubility enhancement factor derived from statistical thermodynamics. At typical textile dyeing conditions (373 K, 30 MPa) the solubilities predicted by this factor are in agreement with experimental data from literature.

Appendix A

From statistical thermodynamics (Hill [15]) it follows that the chemical potential μ_i of a system of n_i particles i at temperature T can be calculated from the canonical ensemble partition function Z:

$$\mu_i = -\frac{1}{\beta}\frac{\partial \ln Z}{\partial n_i} \qquad \text{(a1)}$$

where $\beta = 1/kT$ and k is the Boltzmann constant.

According to Vera and Prausnitz [16] and Reif [17] the partition function for non-ideal fluids can be approximated by the generalized Van der Waals form:

$$Z = \frac{1}{n!}\left(\frac{2\pi m}{h^2\beta}\right)^{\frac{3}{2}n}\left[(V - V_{ex})\exp(-\beta U)\right]^n q_{r,v}^n \qquad \text{(a2)}$$

where m is particle mass, h is Planck's constant, V_{ex} is the volume excluded by the particles and U is the average attractive potential energy between one particle and all others in the fluid. The final term, $q_{r,v}^{n}$, accounts for rotational and vibrational energies of the particles and according to Gasser [18] it is a function of temperature only for small molecules like water or carbon dioxide. To allow the derivation of an analytical solution like Eq. (18), a simplification is needed here: It is assumed that the rotational and vibrational term $q_{r,v}^{n}$ is negligible compared to the other contributions in Eq.(a2). The validity of this assumption is checked in a later stage by fitting the final result of the derivation Eq. (18) to experimental data from literature.

The total potential U is the sum of ½ n pair potentials (u) where the factor ½ is introduced because each potential is shared by 2 particles. For u an average value can be estimated from the attractive term of the Lennard-Jones potential:

$$U = \frac{1}{2} nu = \frac{1}{2} \frac{n}{V} \int_{\sigma}^{\infty} -4\varepsilon \left(\frac{\sigma}{r} \right)^{6} 4\pi r^{2} dr = -8\pi\sigma^{6}\varepsilon \frac{n}{V} \int_{\sigma}^{\infty} \left(\frac{1}{r} \right)^{4} dr = -\frac{8\pi\sigma^{3}\varepsilon n}{3V} \qquad \text{(a3)}$$

where ε and σ are the Lennard-Jones parameters and r is the distance between a pair of particles.

Substituting the right-hand term of Eq. (a3) in Eq. (a2) and taking the natural logarithm gives:

$$\ln Z = -n \ln n + n + \frac{3}{2} n \ln \left(\frac{2\pi m}{h^{2}\beta} \right) + n \ln(V - V_{ex}) + \frac{8\beta\pi\sigma^{3}\varepsilon n^{2}}{3V} \qquad \text{(a4)}$$

because lnn! = nlnn-n for large values of n.
Combining Eq. (a4) with Eq. (a1) yields the pure-compound chemical potential:

$$\mu = -\frac{1}{\beta}\frac{\partial}{\partial n}\left(-n\ln n + n + \frac{3}{2}n\ln\left(\frac{2\pi m}{h^2\beta}\right) + n\ln(V - V_{ex}) + \frac{8\beta\pi\sigma^3\varepsilon n^2}{3V}\right)$$

$$= -\frac{1}{\beta}\left(-\ln n + \frac{3}{2}\ln\left(\frac{2\pi m}{h^2\beta}\right) + \ln(V - V_{ex}) - \frac{V_{ex}}{V - V_{ex}} + \frac{16\beta\pi\sigma^3\varepsilon n}{3V}\right) \qquad \text{(a5)}$$

where the term $V_{ex}/(V\text{-}V_{ex})$ is introduced because of the dependence of V_{ex} on n.

Eq. (a5) can be applied for gases, liquids and supercritical fluids. When Eq. (a5) is substituted in the liquid (L) - gas (G) equilibrium condition $\mu^L = \mu^G$, the term $3/2\ln(2\pi m/h^2\beta)$ cancels because it is the same for a gas and a liquid. The equilibrium condition becomes:

$$\begin{aligned} &-\ln n^L + \ln(V^L - V_{ex}^L) - \frac{V_{ex}^L}{V^L - V_{ex}^L} + \frac{16\beta\pi\sigma^3\varepsilon n^L}{3V^L} = \\ &-\ln n^G + \ln(V^G - V_{ex}^G) - \frac{V_{ex}^G}{V^G - V_{ex}^G} + \frac{16\beta\pi\sigma^3\varepsilon n^G}{3V^G} \end{aligned} \qquad \text{(a6)}$$

or, taking one mole in each phase:

$$\begin{aligned} &-\ln N_A + \ln(V_m^L - b) - \frac{b}{V_m^L - b} + \frac{16\beta\pi\sigma^3\varepsilon N_A}{3V_m^L} = \\ &-\ln N_A + \ln(V_m^G - b) - \frac{b}{V_m^G - b} + \frac{16\beta\pi\sigma^3\varepsilon N_A}{3V_m^G} \end{aligned} \qquad \text{(a7)}$$

if N_A is Avogadro's number, V_m is the molar volume and b is the molar excluded volume. The two-phase system described by Eq. (a7) is at the vapor pressure of the pure compound. Here, water is regarded at temperatures up to 377 K, so that it can be stated that the pressure of the system is so low that the term $b/(V_m^G - b)$ can be neglected. The parameter σ is eliminated by setting the molar excluded volume equal to the Van der Waals volume: $b = 2/3\ \pi N_A\sigma^3$:

$$\ln(V_m^L - b) - \frac{b}{V_m^L - b} + \frac{8\beta b\varepsilon}{V_m^L} = \ln(V_m^G - b) + \frac{8\beta b\varepsilon}{V_m^G} \qquad \text{(a8)}$$

$$\frac{V_m^L - b}{V_m^G - b} = \exp\left(8\beta b\varepsilon\left(\frac{1}{V_m^G} - \frac{1}{V_m^L}\right)\left(\frac{b}{V_m^L - b}\right)\right) = \exp\left(-\frac{8\beta b\varepsilon}{V_m^L} + \frac{b}{V_m^L - b}\right) \qquad \text{(a9)}$$

because the reciprocal of the molar gas volume is negligible compared to that of the liquid. As discussed above, the pressure is low, so that $V_m^G - b$ is approximately V_m^G and Eq. (a9) becomes:

$$\frac{1}{V_m^{ig}} = \frac{1}{V_m^L - b}\exp\left(-\frac{8\beta b\varepsilon}{V_m^L} + \frac{b}{V_m^L - b}\right) \qquad \text{(a10)}$$

where ig denotes “ideal gas”. This equation is used in combination with Eq. (a18) that will now be derived.

When a solution of water (component 1) in supercritical carbon dioxide (2) is regarded, the total partition function is the product of the 2 individual partition functions or $Z = Z_1 Z_2$:

$$Z = \frac{1}{n_1! n_2!}\left(\frac{2\pi m_1}{h^2\beta}\right)^{\frac{3}{2}n_1}\left[(V - V_{ex})\exp\left(\frac{8\beta\pi\sigma_1^3\varepsilon_{11}n_1}{3V} + \frac{8\beta\pi\left(\frac{\sigma_1 + \sigma_2}{2}\right)^3\varepsilon_{12}n_2}{3V}\right)q_{1,r,v}\right]^{n_1} \cdot\cdot\cdot\cdot\cdot$$

$$\cdot\cdot\cdot\cdot\left(\frac{2\pi m_2}{h^2\beta}\right)^{\frac{3}{2}n_2}\left[(V - V_{ex})\exp\left(\frac{8\beta\pi\sigma_2^3\varepsilon_{22}n_2}{3V} + \frac{8\beta\pi\left(\frac{\sigma_1 + \sigma_2}{2}\right)^3\varepsilon_{21}n_1}{3V}\right)q_{2,r,v}\right]^{n_2} \qquad \text{(a1)}$$

where $\varepsilon_{12} = \varepsilon_{21}$ represents the binary interaction energy between a water and a carbon dioxide molecule. The corresponding Lennard-Jones distance is $[(\sigma_1 + \sigma_2)/2]^3$. Substitution of Z in Eq. (a1) and carrying out the differentiation to the

particles 1 gives the chemical potential of water μ_1 dissolved in supercritical carbon dioxide. In the differentiation , it is taken into account that the excluded volume is occupied by both components: $V_{ex} = V_{ex,1} + V_{ex,2}$, or, if v_i is the volume excluded by a single particle of component i: $V_{ex} = n_1 v_1 + n_2 v_2$.

$$\mu_1 = -\frac{1}{\beta}\left(\begin{array}{l} -\ln n_1 + \frac{3}{2}\ln\left(\frac{2\pi m_1}{h^2\beta}\right) + \ln(V - V_{ex}) - \frac{n_1 v_1}{V - V_{ex}} + \frac{16\beta\pi\sigma_1^3\varepsilon_{11}n_1}{3V} + \\ \frac{16\beta\pi\left(\frac{\sigma_1+\sigma_2}{2}\right)^3\varepsilon_{12}n_2}{3V} - \frac{n_2 v_1}{V - V_{ex}} + \ln q_{1,r,v} \end{array}\right) \quad \text{(a12)}$$

Using the molar excluded volume $b_1 = 2/3\ \pi N_A \sigma_1^3$, introducing the combined excluded volume $b_{12} = 2/3\ \pi N_A [(\sigma_1+\sigma_2)/2]^3$ and setting $\mu_1^L = \mu_1^G$:

$$\begin{array}{l} -\ln n_1^L + \ln(V^L - V_{ex}^L) - \frac{n_1^L v_1}{V^L - V_{ex}^L} + \frac{8\beta b_1 \varepsilon_{11} n_1^L}{V^L N_A} + \frac{8\beta b_{12}\varepsilon_{12} n_2^L}{V^L N_A} - \frac{n_2^L v_1}{V^L - V_{ex}^L} = \\ -\ln n_1^G + \ln(V^G - V_{ex}^G) - \frac{n_1^G v_1}{V^G - V_{ex}^G} + \frac{8\beta b_1 \varepsilon_{11} n_1^G}{V^G N_A} + \frac{8\beta b_{12}\varepsilon_{12} n_2^G}{V^G N_A} - \frac{n_2^G v_1}{V^G - V_{ex}^G} \end{array} \quad \text{(a13)}$$

Or, taking one mole of water and neglecting the solubility of CO_2 in the liquid phase:

$$\begin{array}{l} -\ln N_A + \ln(V_m^L - b_1) - \frac{b_1}{V_m^L - b_1} + \frac{8\beta b_1 \varepsilon_{11} n_1^L}{V^L N_A} = \\ -\ln n_1^G + \ln(V^G - V_{ex}^G) - \frac{n_1^G v_1}{V^G - V_{ex}^G} + \frac{8\beta b_1 \varepsilon_{11} n_1^G}{V^G N_A} + \frac{8\beta b_{12}\varepsilon_{12} n_2^G}{V^G N_A} - \frac{n_2^G v_1}{V^G - V_{ex}^G} \end{array} \quad \text{(a14)}$$

Furthermore: $\frac{8\beta b_1 \varepsilon_{11} n_1^L}{V^L N_A} >> \frac{8\beta b_1 \varepsilon_{11} n_1^G}{V^G N_A}$ and $\frac{n_2^G v_1}{V^G - V_{ex}^G} >> \frac{n_1^G v_1}{V^G - V_{ex}^G}$ because the solubility of water in the gas phase is low. Neglecting both small terms and substituting b_1/N_A for v_1:

$$-\ln N_A + \ln(V_m^L - b_1) - \frac{b_1}{V_m^L - b_1} + \frac{8\beta b_1 \varepsilon_{11} n_1^L}{V^L N_A} = -\ln n_1^G + \ln(V^G - V_{ex}^G) + \frac{8\beta b_{12} \varepsilon_{12} n_2^G}{V^G N_A} - \frac{n_2^G v_1}{V^G - V_{ex}^G} \quad \text{(a15)}$$

Introducing the molar concentration of component i in phase α as $N_i^\alpha = \frac{n_i^\alpha}{V^\alpha N_A}$ gives:

$$\ln(V_m^L - b_1) - \frac{b_1}{V_m^L - b_1} + \frac{8\beta b_1 \varepsilon_{11} n_1^L}{V^L N_A} = \ln\left(\frac{1}{N_1^G} - \frac{V_{ex}^G N_A}{n_1^G} \cdot \frac{n_2^G N_A V^G}{n_2^G N_A V^G}\right) + 8\beta b_{12} \varepsilon_{12} N_2^G - \frac{b_1}{1/N_2^G - 1/N_{2,max}} \quad \text{(a16)}$$

$$\Longrightarrow \ln(V_m^L - b_1) - \frac{b_1}{V_m^L - b_1} + \frac{8\beta b_1 \varepsilon_{11} N_A}{V^L N_A} = \ln\left(\frac{1}{N_1^G} - \frac{N_2^G}{N_{2,max} N_1^G}\right) + 8\beta b_{12} \varepsilon_{12} N_2^G - \frac{b_1 N_2^G N_{2,max}}{N_{2,max} - N_2^G} \quad \text{(a17)}$$

$$\Longrightarrow \frac{N_1^G}{1 - N_2^G / N_{2,max}} = \frac{1}{V_m^L - b_1} \exp\left(\frac{b_1}{V_m^L - b_1} - \frac{8\beta b_1 \varepsilon_{11}}{V_m^L} + 8\beta b_{12} \varepsilon_{12} N_2^G - \frac{b_1}{M_{CO2}} \frac{\rho_{CO2}^{max} \rho_{CO2}}{\rho_{CO2}^{max} - \rho_{CO2}}\right) \quad \text{(a18)}$$

Combining Eq. (a10) and Eq. (a18) :

$$\frac{N_1^G}{1 - N_2^G / N_{2,max}} = \frac{1}{V_m^{ig}} \exp\left(\frac{8 b_{12} \varepsilon_{12} N_2^G}{kT} - \frac{b_1}{M_{CO2}} \frac{\rho_{CO2}^{max} \rho_{CO2}}{\rho_{CO2}^{max} - \rho_{CO2}}\right) \quad \text{(a19)}$$

Substituting N_1^{ig} for $1/V_m^{ig}$, 1000 ρ_{CO2}/M_{CO2} for N_2^G :

$$\frac{N_1^G}{N_1^{ig}} = \left(1 - \frac{N_2^G}{N_{2,max}}\right) \exp\left(\frac{8 b_{12} \varepsilon_{12} 1000 \rho_{CO2}}{kTM_{CO2}} - \frac{b_1}{M_{CO2}} \frac{\rho_{CO2}^{max} \rho_{CO2}}{\rho_{CO2}^{max} - \rho_{CO2}}\right) \quad \text{(a20)}$$

Setting $N_1^G/N_1^{ig} = y\rho_{CO2}/\rho_{H2O}^{sat} = \Gamma$ and $N_2^G/N_{2,max} = \rho_{CO2}/\rho_{CO2}^{max}$, where ρ_{CO2}^{max} denotes the maximum density of carbon dioxide and introducing the constant κ:

$$\frac{y^{sat}\rho_{CO2}}{\rho_{H2O}^{sat}} = \left(1 - \frac{\rho_{CO2}}{\rho_{CO2}^{max}}\right)\exp\left(\frac{\kappa\rho_{CO2}}{T} - \frac{b_1}{M_{CO2}}\frac{\rho_{CO2}^{max}\rho_{CO2}}{\rho_{CO2}^{max} - \rho_{CO2}}\right) \qquad \text{(a21)}$$

References

1. E. Bach, E. Cleve and E. Schollmeyer, Past, Present and Future of Supercritical Fluid Dyeing Technology - An Overview, *Rev. Prog. Color*, **32**, 88 (2002).
2. W.J.T. Veugelers, H. Gooijer, J.W. Gerritsen and G.F. Woerlee, European Patent EP 1 126 072 A2, 2001.
3. M. Van der Kraan, M.V. Fernandez Cid, G.F. Woerlee, W.J.T. Veugelers, G.J. Witkamp, Dyeing Natural and Synthetic Textiles in Supercritical Carbon Dioxide with Reactive Dyes, in: A. Bertucco (Ed.), Proceedings of the Fourth International Symposium on High Pressure Technology and Chemical Engineering, vol.1, 2002, p.199.
4. T.P. Nevell, Cellulose: structure, properties and behaviour in the dyeing process, in: J. Shore (Ed.), Cellulosics Dyeing, Society of Dyers and Colourists, Bradford, 1995, 1-80.
5. J.M. Smith and H.C. Van Ness, Introduction to Chemical Engineering Thermodynamics, 4th ed., McGraw-Hill, New York, 1987, 346.
6. W.E. Morton and J.W.S. Hearle, Physical Properties of Textile Fibres, 3rd ed., The Textile Institute, Manchester, 1993, 174.
7. S. Angus, B. Armstrong and K.M. de Reuck, International Thermodynamic Tables of the Fluid State, vol.3, Pergamon Press, Oxford, 1976, table 3.
8. K.A. Evelein, R.G. Moore and R.A. Heidemann, Correlation of the Phase Behavior in the Systems Hydrogen Sulfide–Water and Carbon Dioxide–Water, Ind. Eng. Chem., *Process Des. Dev*. **15** (3), 423 (1976).
9. J.G. Wiegerink, The Moisture Relations of Textile Fibres at Elevated Temperatures, *Text. Res.* **10**, 357 (1940).

10. J.M. Prausnitz, R.N. Lichtenthaler and E. Gomes de Azevedo, Molecular Thermodynamics of Fluid-Phase Equilibria, 3rd ed., Prentice Hall, New Jersey, 1999, 262.
11. B.E. Poling, J.M. Prausnitz and J.P. O'Connel, The Properties of Gases and Liquids, 5th ed., McGraw-Hill, New York, 2001, A-59.
12. R.H. Perry and D.W. Green, Perry's Chemical Engineers' Handbook, 7th ed., McGraw-Hill, New York, 1997, 2-12.
13. D.R. Lide, Handbook of Chemistry and Physics, 75th ed., CRC Press, Boca Raton, 1994, 6-48.
14. W. Bobeth, W. Berger, H. Faulstich, P. Fischer, A. Heger, H.-J. Jacobasch, A Mally and I. Mikut, Textile Faserstoffe, Springer-Verlag, Berlin, 1993, 237.
15. T.L. Hill, An Introduction to Statistical Thermodynamics, Addison-Wesley Publishing Company, Massachusetts, 1960, 19.
16. J.H. Vera and J.M. Prausnitz, Generalized van der Waals Theory for Dense Fluids, *Chem. Eng. J*. **3**, 1 (1972).
17. F. Reif, Fundamentals of Statistical and Thermal Physics, McGraw-Hill, New York, 1965, 426.
18. R.P.H. Gasser and W.G. Richards, An Introduction to Statistical Thermodynamics, World Scientific Publishing Co., Singapore, 1995, 40.

Chapter 4

Equilibrium Study on the Disperse Dyeing of Polyester Textile in Supercritical Carbon Dioxide

Abstract

The dyeing of polyester textile in supercritical carbon dioxide ($scCO_2$) was investigated experimentally. The influence of temperature and density of the $scCO_2$ on the process was studied in the ranges (85-125)ºC and (400-550) kg/m^3. The dye saturation concentration in the polyester increased and the distribution coefficient decreased with temperature, the latter showing a logarithmic dependence on the reciprocal of temperature. Increasing the fluid density gave an increasing saturation concentration and a decreasing distribution coefficient. When the right temperature and solvent density were chosen for the supercritical process, the same dye concentration could be attained as in aqueous dyeing. It was found that the adsorption of the dye on the polyester followed Nernst adsorption, as is the case in aqueous dyeing. The experiments showed that the dyeing was exothermic, with a negative change of entropy accompanying the transfer of dye from the dissolved to the adsorbed state. The thermodynamic characteristics of supercritical and aqueous dyeing were concluded to be roughly the same, with similar saturation concentrations, thermodynamic affinities and heats and entropies of dyeing. The observed shrinking of the polyester during the dyeing process was also similar to what is normal in aqueous dyeing. The exposure to $scCO_2$ had no effect on the strength of the textile.

Contents submitted to the Textile Research Journal

4.1. Introduction

The large-scale water pollution in current industrial dyeing processes poses an environmental problem and an economical burden for the textile industry. In the last few decades, researchers have therefore investigated supercritical fluids (SCF's) as an alternative to water as a dyeing medium.

The best suited SCF for this application is carbon dioxide, because it is inexpensive, non-toxic and non-flammable. Due to its green and safe character, supercritical carbon dioxide ($scCO_2$) is already in use on an industrial scale in the extraction of caffeine from coffee and tea. Typical conditions for textile dyeing in $scCO_2$ are 30 MPa and 120ºC, resulting in a liquid-like CO_2-density of 585 kg/m^3.

The most important advantage of dyeing in $scCO_2$ instead of water is the easier separation of solvent and residual dye: depressurization after the dyeing leads to precipitation of the dye and delivers clean, gaseous CO_2, so that both compounds can be recycled.

An additional advantage of dyeing in $scCO_2$ is caused by the physical properties of the supercritical state: The density is liquid-like, so that low-vapor pressure compounds, such as dyes, can be dissolved. The viscosity is lower and the diffusion coefficient in a SCF is higher than in a liquid, facilitating mass transport. When dyeing non-polar textiles such as polyester, the $scCO_2$ acts as a swelling agent, plasticizing the polymer and increasing the rate of dye diffusion inside the fiber [1]. Since CO_2 is a non-polar solvent, disperse dyes can be dissolved without the need for dispersing agents, i.e. simpler dye formulations can be used than in aqueous dyeing.

The review by Bach et al. [2] mentions that natural and synthetic fibers have been dyed successfully in $scCO_2$. Schmidt et al. [3] have shown that $scCO_2$-dyeing does not damage the fibers, as long as the temperature is kept below 160ºC.

Most publications in the field of supercritical dyeing treat the measurement and modeling of dye solubility in $scCO_2$ [4-21]. The present chapter aims to contribute to a less researched [22-26] subject in polyester dyeing: it describes a quantitative

equilibrium study of saturation colorations, adsorption isotherms and distribution coefficients.

An equilibrium study or, in other words, an investigation of the dyeing thermodynamics, is important because, as will be clear from the above considerations, a supercritical solvent forms a quite different dye bath than a liquid solvent. Furthermore, as is discussed by Kikic e.a. [27], $scCO_2$ dissolves in polyester, changing its properties and possibly also its thermodynamic behavior in a dyeing process. Up to now, it has been reported, e.g. by Chang e.a. [22], that the coloration of polyester in $scCO_2$ increases with pressure and temperature, but a more systematic study on this subject is desirable.

The aim of this work is to investigate the influence of the density and temperature of the $scCO_2$ on the polyester saturation coloration and the distribution coefficient. Also the thermodynamic parameters governing the supercritical dyeing process are determined for two dyes. The coloration and the thermodynamic parameters are compared to those reported for aqueous dyeing. Finally, the adsorption isotherms of two dyes on polyester are determined to assess if Nernst adsorption is the dyeing mechanism, as is the case for dyeing in water.

4.2. Theory of Dyeing

4.2.1. Dye solubility in $scCO_2$

To describe the thermodynamics of the supercritical dyeing system, it is necessary to know how much dye is present in the dyeing vessel. The solubility of compounds in $scCO_2$ can be described by several semi- or purely empirical expressions, fitted to experimental data. In the present work, the purely empirical equation 1 is used, because Jouyban et a. [28] showed that this expression is accurate for 106 low vapor pressure compounds, including dyes:

$$\ln y = M_0 + M_1 p + M_2 p^2 + M_3\, pT + M_4 T/p + M_5 \ln \rho \qquad (1)$$

where y is the solubility in mole fraction, ρ is the density of pure $scCO_2$ (kg/m^3) at the dyeing pressure p (MPa) and dyeing temperature T (K) and M_0 - M_5 are fit parameters. The value of C^{CO2} (g/g) is now:

$$C^{CO2} = y\frac{M_{dye}}{M_{CO2}} \tag{2}$$

where M_{dye} and M_{CO2} are the molar masses (g/mol) of dye and carbon dioxide.

4.2.2. Distribution coefficient

The thermodynamic affinity ($-\Delta\mu^0$, J/mole) of dye for textile is defined as [29]:

$$-\Delta\mu^0 = RT\ln\frac{a^{PET}}{a^{CO2}} \tag{3}$$

where R is the universal gas constant (J/mole/K), T is the dyeing temperature (K) and a^{PET} and a^{CO2} are the activities of the dye in the polyester and the $scCO_2$ phase. The activities are defined as the ratio's of the dye fugacities in the corresponding phase (f^{PET} and f^{CO2}) relative to the standard-state fugacity f^0 , the standard state being solid dye at the dyeing temperature and 1 bar:

$$a^{PET} = \frac{f^{PET}}{f^0} \qquad\qquad a^{PET} = \frac{f^{CO2}}{f^0} \tag{4}$$

The fugacities in the PET and the $scCO_2$ follow from the definitions of the activity coefficients γ^{PET} and γ^{CO2}:

$$f^{PET} = C^{PET}\gamma^{PET}f \qquad\qquad f^{CO2} = C^{CO2}\gamma^{CO2}f \tag{5}$$

where C^{PET} and C^{CO2} are the dye concentrations (g/g) in both phases and f is the fugacity of pure solid dye at the dyeing temperature and at the dyeing pressure. Eliminating f^{PET} and f^{CO2}:

$$a^{PET} = \frac{C^{PET}\gamma^{PET}f}{f^0} \qquad a^{CO2} = \frac{C^{CO2}\gamma^{CO2}f}{f^0} \tag{6}$$

In aqueous dyeing it is common practice [30] to put $f = f^0$, i.e. to assume that the fugacity of the dye is independent of pressure. This is also assumed for the supercritical process. The system regarded here is saturated with dye, so that $\gamma^{PET} = \gamma^{CO2} = 1$. The activities are now equal to the concentrations and equation 3 can be simplified to:

$$-\Delta\mu^0 = RT\ln\frac{C^{PET}}{C^{CO2}} \tag{7}$$

The ratio of C^{PET} (g/g) and C^{CO2} (g/g) is the distribution coefficient K:

$$K \equiv \frac{C^{PET}}{C^{CO2}} \tag{8}$$

In this work, the values for K are determined at several temperatures and $scCO_2$-densities, using equation 8.

The thermodynamic affinity is equal to the standard free energy change of dyeing ΔG^0 (J/mole), and therefore:

$$\Delta\mu^0 = \Delta G^0 = \Delta H^0 - T\Delta S^0 \tag{9}$$

where ΔH^0 and ΔS^0 are the changes in standard enthalpy (J/mole) and entropy (J/mole/K) during the dyeing process. Combining equations 7, 8 and 9 gives:

$$\ln K = -\left(\frac{\Delta H^0}{RT}\right) + \frac{\Delta S^0}{R} \tag{10}$$

for a saturated dye bath. According to equation 10, constructing a Van ‘t Hoff plot, i.e. plotting ln K as a function of 1/T leads to a straight line and gives the values of the standard enthalpy and entropy of dyeing. Equation 10 is known to hold for

aqueous dyeing processes [29] and it is investigated here if it is also valid for supercritical dyeing.

As discussed by Burkinshaw [30], disperse aqueous polyester dyeing is an exothermic process ($\Delta H^0<0$) and the accompanying change in entropy is negative ($\Delta S^0<0$). The enthalpy and entropy changes are those associated with the transfer of dye from the dissolved to the adsorbed state. In the present work, this is investigated for the case of $scCO_2$, for two disperse dyes. Also the standard affinities of the dyes are determined.

The distribution coefficients are determined here at maximum coloration, i.e. for polyester saturated with dye. The values for C^{PET} are measured. The values of C^{CO2} that are to be substituted in equation 8, are the dye solubilities in $scCO_2$, from equation 2.

4.2.3. Adsorption isotherm

In disperse aqueous dyeing, when the equilibrium concentration of dye in polyester is plotted against the concentration in the dye bath, a straight line is obtained, indicating that the dyeing obeys a Nernst or partition mechanism. The linearity is observed below and at the saturation point, i.e. the distribution coefficient is independent of concentration in the fiber or in the water. Up to now, only two publications have appeared on dye adsorption isotherms in $scCO_2$, one reporting a linear adsorption isotherm [25] and the other a Langmuir isotherm [24]. In this work the dye isotherms in $scCO_2$ are investigated further, for two dyes.

4.2.4.Effect of supercritical dyeing on polyester textile

In the aqueous dyeing process, polyester is heated with steam of 150 to 200ºC, prior to dyeing. This is done to relax the polymer molecules in the fiber, to remove the intermolecular stresses that are formed in the fiber spinning process. Without this so-called heat-setting, excessive shrinking of the cloth occurs whenever it is exposed to high temperatures, e.g. in a dye bath. It is investigated in this work what the shrinking behavior of heat-set and non-heat-set polyester is when it is dyed in $scCO_2$. Also the tensile strength before and after dyeing are determined, to check for possible fiber damage.

4.3. Experimental

4.3.1. Materials

The polyester (poly(ethylene terephtalate)) was piqué-knitted, washed to remove the spinning oils and heat-set at 195ºC by the supplier: Ames Europe, Enschede (The Netherlands). The yarn was 167 dtex, the specific weight of the cloth was 120 g/m^2. The CO_2 was purchased from HoekLoos (The Netherlands) and had a purity of 99.97 %. The acetone was technical grade from Chemproha (The Netherlands). The N,N-dimethylformamide was 99.8% from Merck Chemicals (The Netherlands).

The properties of the dyes used in this study are given in table 4.1. Their structures are given in figure 4.1. All dyes were purchased from Sigma Aldrich (The Netherlands) and used without further purification.

Table 4.1. Properties of the dyes used in this study, with molecular weight (M), wavelength of maximum absorption (λ_{max}) and the purity according to the supplier

Dye	M (g/mole)	λ_{max} (nm)	purity (%)
Disperse Orange 13	352	427	90
Disperse Orange 3	242	443	90
Disperse Red 1	314	502	95

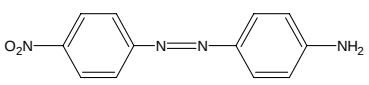

Disperse Orange 3

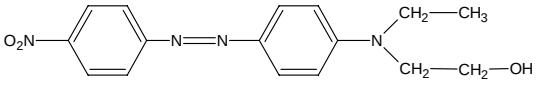

Disperse Red 1

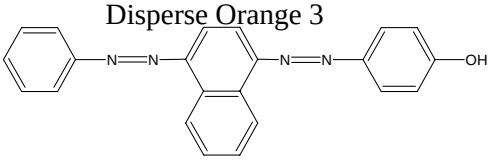

Disperse Orange 13

Figure 4.1. Molecular structures of the dyes used in this study

4.3.2. Dyeing equipment and procedure

The experiments were conducted in a 40-liter stainless steel pressure vessel with a perforated drum inside that contained 100 g textile cloth. The drum rotated at 60 rpm. The dye was put in a 50 ml porous stainless steel cylinder (pore size 10μm) that was fixed inside the drum. A simplified scheme of the equipment is given in figure 4.2. The system was pressurized in 10 minutes, with a air-driven reciprocating pump (Resato International, The Netherlands). The dyeing vessel was heated with a steam jacket. During the heating, the $scCO_2$ reached the desired pressure and temperature in 30 minutes. After that, pressure and temperature remained constant. During the dyeing, the $scCO_2$ was circulated through the vessel by a centrifugal pump (Autoclave Engineers, USA) at a flow rate of 30 liter/min, to intensify mixing inside the vessel.

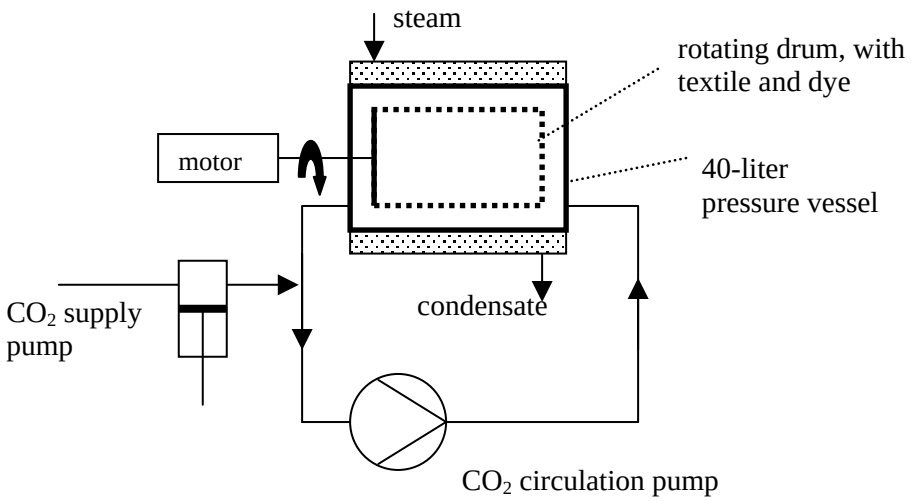

Figure 4.2. Experimental 40-liter dyeing machine

In the experiments in $scCO_2$ where the influence of temperature and density on the saturation coloration was investigated, the PET was dyed for 6 and 8 hours. No difference in coloration was measured. Because of this observation and because, after these experiments, dye powder was left in the porous steel cylinder, it was concluded that the PET had reached saturation. The distribution coefficient was calculated with equation 8, taking C^{PET} from equation 12 (below) and C^{CO2} from equation 2.

Also the experiments in $scCO_2$ for the determination of the sorption isotherms were done for 6 and 8 hours. Again, no color differences were observed but now all dye had disappeared from the steel cylinder, leading to the conclusion that after these dyeing times, the dye distribution between the $scCO_2$ and the PET was at equilibrium but below saturation. The amount of dye in the PET-cloth (C^{PET}) was taken from equation 12, the amount of dye remaining in the solvent (C^{CO2}) was calculated from the dye mass balance:

$$m^{TOTAL} = m^{PET} C^{PET} + m^{CO2} C^{CO2} \tag{11}$$

with m^{TOTAL} denoting the mass of pure dye (g) introduced into the vessel prior to the experiment, m^{PET} the mass of dyed polyester (100g) and m^{CO2} the mass (g) of $scCO_2$ in the dyeing vessel. The latter was calculated as the product of density at 120ºC and 300 bar (585 kg/m^3) and vessel volume (40 liter): m^{CO2} = 23000 g.

To check the shrinkage of the polyester during the dyeing, the weight per unit area cloth was measured before and after the dyeing. This was done for both heat-set and non-heat-set polyester.

4.3.3. Analyses

After each dyeing experiment, the dyed PET-cloth was washed with acetone at room temperature to remove any unfixed dye. The PET was then subjected to a Soxhlet-extraction with boiling N,N-dimethylformamide (DMF) in an oil bath of 180ºC. After all dye had been removed, the dye concentration in the DMF was determined with a UV/VIS spectrophotometer, at the wavelength of maximum absorption given in table 1. The dye concentration in the PET was then calculated with:

$$C^{PET} = \frac{C^{DMF} m^{DMF}}{m^{PET}} \tag{12}$$

where C^{PET} is the concentration (g/g) of dye in the PET, C^{DMF} is the dye concentration (g/g) in the DMF, m^{DMF} is the mass of DMF after extraction (g) and m^{PET} is the mass of PET (g).

4.4. Results and Discussion

4.4.1. Dye solubility in $scCO_2$

The solubility fits are constructed for three dyes: Disperse Orange 3, Disperse Orange 13 and Disperse Red 1. The fit parameters of equation 1 are given in table 4.2. The fits are presented graphically in figures 4.3, 4.4 and 4.5. It can be seen that the solubilities of Disperse Orange 3 and Disperse Red 1 are described well, that of Disperse Orange 13 less accurately, but acceptable for our purpose. For Disperse Orange 3 and Disperse Red1, the fits cover almost the entire dyeing temperature range, for Disperse Orange 13, the fit range does not cover the higher dyeing temperatures.

Table 4.2. Fit parameters for equation 1, describing the solubility of Disperse Orange 3, Disperse Orange 13 and Disperse Red 1 in supercritical carbon dioxide

Dye	Disperse Orange 3	Disperse Orange 13	Disperse Red 1
Reference	[6]	[8]	[14]
M_0	-0.006745	-48.69	0.07694
M_1	-0.2452	0.7175	-0.6607
M_2	-0.003408	-0.01720	$-5.833 \cdot 10^{-4}$
M_3	$1.102 \cdot 10^{-3}$	$9.821 \cdot 10^{-4}$	$1.776 \cdot 10^{-3}$
M_4	-0.2199	0.3863	-0.2913
M_5	0.6311	4.747	1.448

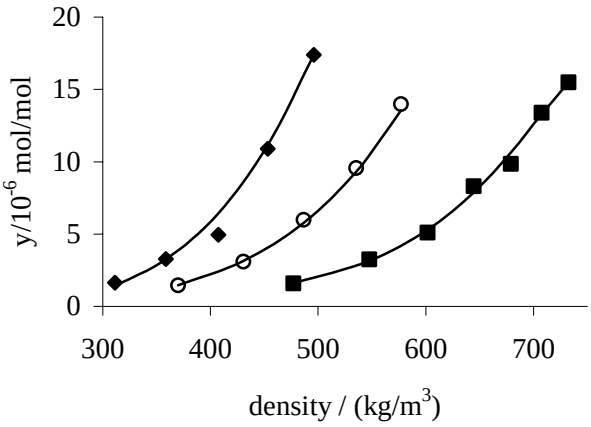

Figure 4.3. Solubility (y) of Disperse Orange 3 as a function of carbon dioxide density, with drawn lines representing the fitted curves of equation 1 and points representing literature data [6]: ■ 353 K, ○ 373 K, ◆ 393 K

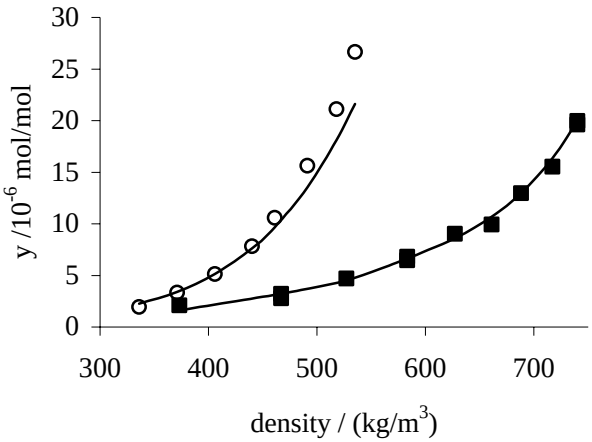

Figure 4.4. Solubility (y) of Disperse Orange 13 as a function of carbon dioxide density, with drawn lines representing the fitted curves of equation 1 and points representing literature data [8]: ■ 330 K, ○ 370 K

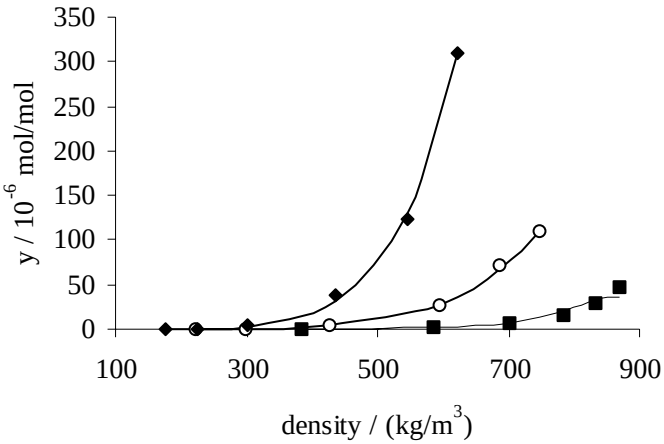

Figure 4.5. Solubility (y) of Disperse Red 1, with drawn lines as the fitted curves and points representing literature data [14]: ■ 323 K, ○ 353 K, ◆ 383 K

4.4.2. Distribution coefficient

For two dyes, Disperse Orange 3 and 13, the saturation coloration and the distribution coefficient was investigated. The measured values of the saturation coloration C^{PET} are shown for Disperse Orange 3 in table 4.3, for two $scCO_2$-

Table 4.3. Saturation concentrations of Disperse Orange 3 in polyester (C^{PET}) and in carbon dioxide (C^{CO2}) and the distribution coefficients K, as a function of temperature T, for two CO_2-densities

density kg/m^3	T (K)	Pressure MPa	C^{PET} / 10^{-2} g/g	C^{CO2} / 10^{-6} g/g	K
400	368	165	1.61	9.88	1630
	378	178	1.79	16.6	1080
	388	192	1.93	27.3	707
	393	199	2.04	34.8	586
550	358	195	1.50	26.0	577
	368	218	1.95	46.6	418
	378	241	2.19	79.8	274
	388	264	2.77	134	207
	393	276	2.94	170	173
	398	287	3.18	217	147

Table 4.4. Saturation concentrations of Disperse Orange 13 in polyester (C^{PET}) and in carbon dioxide (C^{CO2}) and the distribution coefficients K

density kg/m^3	T (K)	pressure MPa	C^{PET} / 10^{-2} g/g	C^{CO2} / 10^{-6} g/g	K
400	368	165	1.50	9.88	4230
	378	178	1.69	16.6	3190
	388	192	1.85	27.3	2280
	393	199	1.90	34.8	1880
550	368	218	1.83	46.6	998
	378	241	2.08	79.8	730
	388	264	2.22	134	532

densities, together with the calculated values for C^{CO2} and the resulting distribution coefficients K. The corresponding values for Disperse Orange 13 are given in table 4.4. To get a clear impression for the dyeing conditions, also the dyeing pressures are given in the tables. The saturation coloration of Disperse Orange 13 in $scCO_2$ at 378 K (105ºC) and 550 kg/m^3 is 2.1 mass percent, close to the value reported in literature for aqueous dyeing at 100ºC (2.0 mass percent) [31].

It can be seen from the tables that coloration increases with the temperature and the density (or pressure) of the $scCO_2$. This was reported earlier for other dyes in $scCO_2$, e.g. by Chang e.a. [22].

The Van ‘t Hoff plots of the distribution coefficient are given in figure 4.6 for Disperse Orange 3. The R-squared values for 400 and 550 kg/m^3 are 0.976 and 0.998, indicating good agreement of the experimental results with equation 10. Also figure 4.7, showing the plots for Disperse Orange 13, shows agreement with equation 10, the R-squared values for 400 and 550 kg/m^3 being 0.994 and 0.999 respectively.

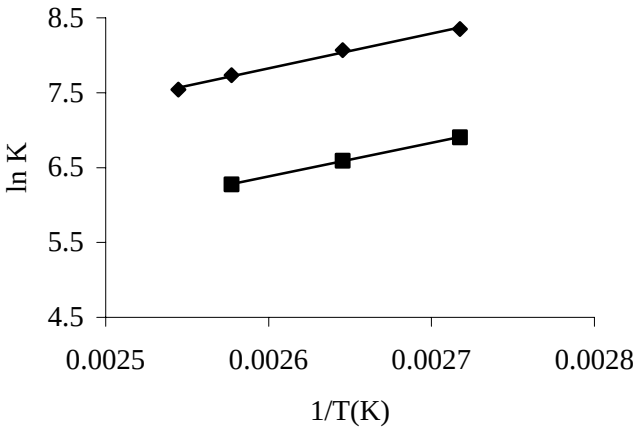

Figure 4.6. Distribution coefficient K of Disperse Orange 3 as a function of dyeing temperature T, for different $scCO_2$-densities: ◆ 400 kg/m^3, ■ 550 kg/m^3

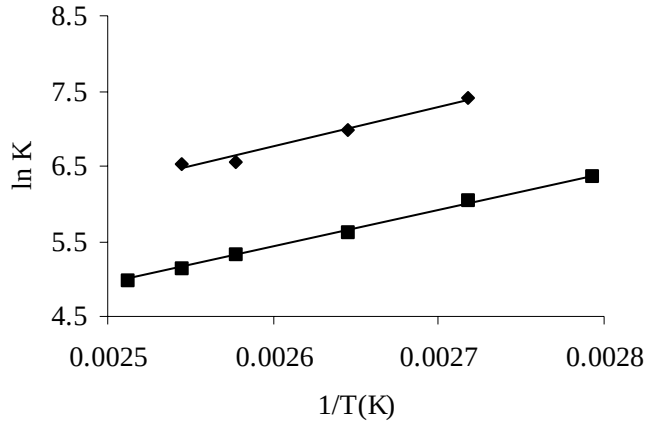

Figure 4.7. Distribution coefficient K of Disperse Orange 13 as a function of dyeing temperature T, for different $scCO_2$-densities: ◆ 400 kg/m^3, ■ 550 kg/m^3.

The fact that equation 10 is valid here, confirms the assumption made between equations 6 and 7, about the negligible influence of pressure on the fugacity f of the pure dye was allowed, even though the pressures in $scCO_2$ are far higher than in aqueous dyeing.

It can be seen in figures 4.6 and 4.7, that the distribution coefficient decreases with temperature. Regarding equation 10 it can then be stated that the enthalpies of

dyeing are negative, i.e. the process is exothermic. This is an apparent contradiction with the observation made earlier in tables 3 and 4, that the coloration C^{PET} increases with temperature. The explanation is that also C^{CO2} increases with temperature and relatively more than C^{PET}, so that the ratio of C^{PET} and C^{CO2}, the distribution coefficient, decreases. In other words, the transfer processes of dye from the standard (solid) state to either the adsorbed state in the PET or to the dissolved state in the $scCO_2$ are both endothermic processes. The transfer of dye from the dissolved to the adsorbed state, the actual dyeing step, is exothermic.

There is also a negative entropy of dyeing, caused by the dye molecules taking on a state of higher order when going from the supercritical to the adsorbed state on the polyester molecules. As was discussed above, negative enthalpy and entropy changes are also reported for aqueous dyeing.

The thermodynamic affinities of dyeing are calculated with equation 9, taking a temperature of 100ºC as example. The affinity becomes less negative as density increases, reflecting that, going from 400 to 550 kg/m^3, the distribution coefficient decreases. This shows that the relative increase of C^{PET} with density is less than the relative increase in C^{CO2}.

Table 4.5 shows values of $\Delta\mu^0$ that are in or near the range that is characteristic of physisorption, which is -20 to 0 kJ/mol [32]. The affinity of Disperse Orange 13 for polyester in water at 100ºC is $\Delta\mu^0$ = -13 kJ/mol.[31], not equal to but in the same order as is calculated here for $scCO_2$. This value was determined for polyester that was heat-set at 195ºC, just as the polyester used in this work. The enthalpies, entropies and affinities mentioned in the table are all similar to those measured in water for other disperse dyes [33].

Table 4.5. Standard enthalpy (ΔH^0), entropy (ΔS^0) and affinity ($\Delta\mu^0$) of dyeing in $scCO_2$ at 400 and 550 kg/m^3, for two disperse dyes

Dye	Density kg/m	ΔH^0 kJ/mole	ΔS^0 Jmole/K	$\Delta\mu^0$ (100ºC) kJ/mol
Disperse	400	-43	-57	-22
Orange 3	550	-41	-61	-18
Disperse	400	-39	-36	-25
Orange 13	550	-37	-44	-21

4.4.3. Adsorption isotherm

In these experiments, Disperse Orange 3 and Disperse red 1 were used to dye polyester. To investigate whether or not the adsorption follows a linear Nernst isotherm, dyeing experiments were done with both the $scCO_2$ and the polyester below saturation. The results are given for two dyes in figure 4.8. The R-squared coefficients for Disperse Orange 3 and Disperse red 1 are both 0.996, showing a linear dependence of C^{PET} on C^{CO2}.

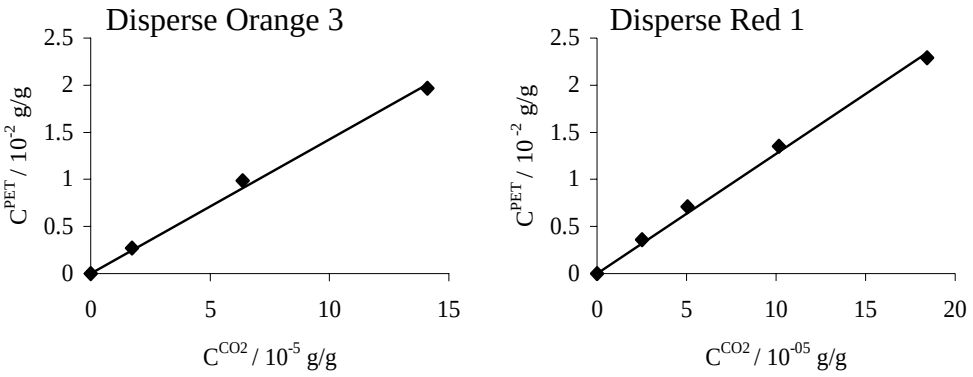

Figure 4.8. Adsorption isotherms for two disperse dyes, in $scCO_2$ at 550 kg/m^3 and 115ºC

4.4.4.Effect of supercritical dyeing on polyester

To investigate the effect of the dyeing process on the polyester cloth, the shrinkage and the tensile strength were determined, at the laboratory of Ames Europe. The results are given in table 4.6. The increase of the mass per unit cloth area of the non-heat-set polyester increases by 70% during supercritical dyeing. For the heat-set polyester, this is only 20%, similar to the percentages normally observed in aqueous dyeing [34]. This indicates that heat-set polyester has to be used for dyeing in $scCO_2$, to avoid excessive shrinkage. In table 4.6 it can be seen that the tensile strength of the polyester cloth is not significantly affected by the exposure to the supercritical dye bath. In the dyeing experiment on which table 4.6 is based, Disperse Red 1 was used as dye, the temperature was 115ºC and the $scCO_2$-density was 550 kg/m^3.

Table 4.6. Specific mass and tensile strength of heat-set and non-heat-set polyester, before and after dyeing in $scCO_2$ of 115ºC and 550 kg/m^3

		specific mass (g/m^2)	tensile strength (N)	
			length	width
heat-set	before dyeing	123	483	457
	after dyeing	147	494	476
non-heat-set	before dyeing	123	335	479
	after dyeing	206	634	529

4.5. Conclusions

When polyester is dyed with disperse dyes in supercritical carbon dioxide, the saturation coloration increases with temperature and density of the $scCO_2$. The same coloration can be achieved in $scCO_2$ as in water, as long as the density is sufficiently high.

The distribution coefficient K decreases with density and temperature, showing a logarithmic dependence on the reciprocal of temperature. This temperature-dependence is similar to that observed in aqueous dyeing. The polyester swelling by the carbon dioxide does not affect the temperature-dependence of the distribution coefficient.

The transfer of dye from the dissolved state to the adsorbed state, i.e. the actual dyeing step of the process, is an exothermic process, although the saturation dye concentration in the polymer increases with temperature. This apparent contradiction is caused by the increase of dye concentration in the CO_2 with temperature being relatively larger than the increase of the dye concentration in the polyester. The dyeing step is accompanied by a negative entropy change. The values of the enthalpies, entropies and thermodynamic affinities in supercritical dyeing are in the same order of magnitude as in aqueous dyeing.

The linearity of the adsorption isotherms that is observed in water, is also found in supercritical carbon dioxide, indicating a Nernst adsorption mechanism.

Dyeing polyester in $scCO_2$ leads to similar shrinkage of the cloth as in aqueous dyeing, provided that heat-set polyester is used. The textile fibers are not damaged by the supercritical dyeing process.

It can be concluded that the disperse dyeing process of polyester behaves thermodynamically much the same in supercritical carbon dioxide as it does in water and, what is more important, the same color depths can be achieved in both dyeing media.

References

1. S. Sicardi, L. Manna and M. Banchero, Comparison of Dye Diffusion in Poly(ethylene terephtalate) Films in the Presence of a Supercritical or Aqueous Solvent, *Ind. Eng. Chem. Res.* **39**, 4707 (2000).
2. E. Bach, E. Cleve and E. Schollmeyer, Past, Present and Future of Supercritical Fluid Dyeing Technology – an Overview, *Rev. Prog. Color.* **32**, 88 (2002).
3. A. Schmidt, E. Bach and E. Schollmeyer, Damage to Natural and Synthetic Fibers Treated in Supercritical Carbon Dioxide at 300 bar and Temperatures up to 160 Degrees C, *Text. Res. J.* **72** (11), 1023 (2002).
4. S.L. Draper, G.A. Montero, B. Smith and K. Beck, Solubility Relationships for Disperse Dyes in Supercritical Carbon Dioxide, *Dyes and Pigments* **45**, 177 (2000).
5. J. Fasihi, Y. Yamini, F. Nourmohammadian and N. Bahramifar, Investigations on the Solubilities of Some Disperse Azo Dyes in Supercritical Carbon Dioxide, *Dyes and Pigments* **63**, 161 (2004).
6. A. Ferri, M. Banchero, L. Manna and S. Sicardi, An Experimental Technique for Measuring High Solubilities of Dyes in Supercritical Carbon Dioxide, *J. Supercrit. Fluids* **30** (1), 41 (2003).
7. B. Guzel and A. Akgerman, Solubility of Disperse and Mordant Dyes in Supercritical CO_2, *J. Chem. Eng. Data* **44**, 83 (1999).

8. U. Haarhaus, P. Swidersky and G.M. Schneider, High-Pressure Investigations of the Solubility of Dispersion Dyestuffs in Supercritical Gases by VIS/NIR Spectroscopy. Part I – 1,4-Bis(octadecylamino)-9,10-anthraquinone and Disperse Orange 13 in CO_2 and N_2O up to 180 MPa, *J. Supercrit. Fluids* **8**, 100 (1995).
9. S.N. Joung and K.-P. Yoo, Solubility of Disperse Anthraquinone and Azo Dyes in Supercritical Carbon Dioxide at 313.15 to 393.15 K and from 10 to 25 MPa, *J. Chem. Eng. Data* **43**, 9 (1998).
10. S.N. Joung, H.Y. Shin, Y.H. Park and K.-P. Yoo, Measurement and Correlation of Solubility of Disperse Anthraquinone and Azo Dyes in Supercritical Carbon Dioxide, *Korean J. Chem. Eng.* **15** (1), 78 (1998).
11. T. Kraska, K.O. Leonhard, D. Tuma and G.M. Schneider, Correlation of the Solubility of Low-volatile Organic Compounds in Near- and Supercritical Fluids Part II. Applications to Disperse Red 60 and Two Disubstituted Anthraquinones, *Fluid Phase Equilibria* **194-197**, 469 (2002).
12. J.W. Lee, J.M. Min and H.K. Bae, Solubility Measurement of Disperse Dyes in Supercritical Carbon Dioxide, *J. Chem. Eng. Data* **44**, 684 (1999).
13. H.-M. Lin, C.-Y. Liu, C.-H. Cheng, Y.-T. Chen and M.-J. Lee, Solubilities of Disperse Dyes of Blue 79, Red 153 and Yellow 119 in Supercritical Carbon Dioxide, *J. Supercrit. Fluids* **21** (1), 1 (2001).
14. T. Shinoda and K. Tamura, Solubilities of C.I. Disperse Red 1 and C.I. Disperse Red 13 in Supercritical Carbon Dioxide, *Fluid Phase Equilibria* **213**, 115 (2003).
15. B. Wagner, C.B. Kautz and G.M. Schneider, Investigations on the Solubility of Anthraquinone Dyes in Supercritical Carbon Dioxide by a Flow Method, *Fluid Phase Equilibria* **158-160**, 707 (1999).
16. D. Tuma, B. Wagner and G.M. Schneider, Comparative Solubility Investigation of Anthraquinone Disperse Dyes in Near- and Supercritical Fluids, *Fluid Phase Equilibria* **182**, 133 (2001).
17. T. Shinoda and K. Tamura, Solubilities of C.I. Disperse Orange 25 and C.I. Disperse Blue 354 in Supercritical Carbon Dioxide, *J. Chem. Eng. Data* **48**, 869 (2003).
18. K. Mishima, K. Matsuyama, H. Ishikawa, K.-I. Hayahi and S. Maeda, Measurement and Correlation of Solubilities of Azo Dyes and

Anthraquinone in Supercritical Carbon Dioxide, *Fluid Phase Equilibria* **194-197**, 895 (2002).
19. A.S. Ozcan, A.A. Clifford and K.D. Bartle, Solubility of Disperse Dyes in Supercritical Carbon Dioxide, *J. Chem. Eng. Data* **42**, 590 (1997).
20. D. Tuma and G.M. Schneider, Determination of the Solubilities of Dyestuffs in Near- and Supercritical Fluids by a Static Method up to 180 MPa, *Fluid Phase Equilibria* **158-160**, 743 (1999).
21. H.-D. Sung and J.-J. Shim, Solubility of C.I. Disperse Red 60 and C.I. Disperse Blue 60 in Supercritical Carbon Dioxide, *J. Chem. Eng. Data* **44**, 985 (1999).
22. K.-H. Chang, H.-K. Bae and J.-J. Shim, Dyeing of PET Textile Fibers and Films in Supercritical Fluids, *Korean J. Chem. Eng.* **13** (3), 310 (1996).
23. M.R. De Giorgi, E. Cadoni, D. Maricca and A. Piras, Dyeing Polyester Fibres with Disperse Dyes in Supercritical CO_2, *Dyes and Pigments* **45**, 75 (2000).
24. A.S. Özcan and A. Özcan, Adsorption Behavior of a Disperse Dye on Polyester in Supercritical Carbon Dioxide, *J. Supercrit. Fluids, **in press***.
25. I. Tabata, J. Lyu, S. Cho, T. Tominaga and T. Hori, Relationship between the Solubility of Disperse Dyes and the Equilibrium Dye Adsorption in Supercritical Fluid Dyeing, *Color. Technol.* **117**, 346 (2001).
26. M.-W. Park and H.-K. Bae, Dye Distribution in Supercritical Dyeing with Carbon Dioxide, *J. Supercrit. Fluids* **22**, 65 (2002).
27. I. Kikic, F. Vecchione, P. Alessii, A. Cortesi, F. Eva and N. Elvassore, Polymer Plasticization Using Supercritical Carbon Dioxide: Experiment and Modeling, *Ind. Eng. Chem. Res.* **42**, 3033 (2003).
28. A. Jouyban, H.-K. Chan and N.R. Foster, Mathematical Representation of Solute Solubility in Supercritical Carbon Dioxide Using Empirical Expressions, *J. Supercrit. Fluids* **24**, 19 (2002).
29. H.H. Sumner, in: A. Johnson (Ed.), The Theory of Coloration of Textiles, 2nd ed., Society of Dyers and Colourists, Bradford (U.K.), 255 (1989).
30. S.M. Burkinshaw, Chemical Principles of Synthetic Fiber Dyeing, Chapman and Hall, London (1995).
31. E. Merian, J. Carbonell, U. Lerch and V. Sanahuja, The Saturation Values, Rates of Dyeing, Rates of Diffusion and Migration of Disperse Dyes on Heat-Set Polyester Fibres, *Am. Dyestuff Rep*. **53**(26), 11 (1964).

32. Y. Yu, Y.-Y. Zhuang and Z.-H. Wang, Adsorption of Water-soluble Dye onto Activated Functionalized Resin, *J. Colloid Interf. Sci.* **242**, 288 (2001).
33. R.H. Peters, Textile Chemistry, Volume III, Elsevier, Amsterdam, 105 (1975).
34. S. Fransman, Ames Europe B.V., Personal communication.

Chapter 5

The Influence of Variable Physical Properties and Buoyancy on Heat Exchanger Design for Near- and Supercritical Conditions

Abstract

Computational fluid dynamics simulations were done on heated supercritical carbon dioxide flowing up or down in a vertical pipe. The impairment or enhancement of heat transfer caused by the temperature-induced variation of physical properties was investigated, as well as the effect of buoyancy. The simulations show, for non-buoyant flow, that for pressures above 120 bar, the effect of variation in physical properties is small and a constant-property Nusselt relation can be used for a heat exchanger design. For pressures below 120 bar, the variation in physical properties has to be taken into account for a correct heat exchanger design. For non-buoyancy conditions the Krasnoshchekov - Protopopov equation can be used to calculate heat transfer coefficients. It was observed that buoyancy can enhance heat transfer coefficients up to a factor 3. When buoyancy is active, the highest heat transfer coefficients are realized when the fluid flows downward. The Jackson and Hall correction factor for the calculation of heat transfer coefficients under buoyancy was confirmed by the simulations.

Contents published in J. Supercrit. Fluids **34**, 99 (2005)

Symbols

a	constant	-
b	constant	-
c	constant	-
c_p	specific heat at constant pressure	$Jkg^{-1}K^{-1}$
d	pipe diameter	m
e	constant	-
g	gravitational acceleration	ms^{-2}
Gr	Grashof number, $Gr = gd^3\rho(\rho_b-\rho_w) /\mu^2$	-
H	enthalpy	Jkg^{-1}
h	heat transfer coefficient	$Wm^{-2}K^{-1}$
k	thermal conductivity	$Wm^{-1}K^{-1}$
Nu	Nusselt number, $Nu = hd/k$	-
p	pressure	bar
Pr	Prandtl number, $Pr = \mu c_p/k$	-
q	heat flow	Js^{-1}
Re	Reynolds number, $Re = \omega d/\mu$	-
T	temperature	K and °C
U_o	overall heat transfer coefficient	$Wm^{-2}K^{-1}$

Greek

ρ	density	kgm^{-3}
μ	dynamic viscosity	Pa·s
ω	mass flux	$kgm^{-2}s^{-1}$
Φ_m	mass flow	kgs^{-1}

subscripts

b	at bulk conditions
cp	at constant properties
i	inside of pipe
o	outside of pipe
pc	at pseudo-critical temperature
vp	at variable properties
w	at wall conditions
c	critical

5. 1. Introduction

In designing heat exchangers for supercritical fluids a complication arises that is not encountered when dealing with liquids or gases. The strong variation of the fluid physical properties with temperature around the critical point influences heat transfer strongly.

This problem has led to a great deal of research and many publications are to be found in which Nusselt relations for the calculation of heat transfer coefficients have been constructed and fitted to experimental work, as is reviewed by Pitla et al. [1]. The present work is an investigation into the phenomena around the critical point and into the buoyancy phenomenon, i.e. free convection caused by temperature-induced density differences. Computational fluid dynamics simulations of heated supercritical carbon dioxide flows through vertical pipes are carried out.

The objective is to study when and how the variable properties and the buoyancy must be taken into account in the Nusselt-relation for heating. For buoyancy conditions in a heated flow, it is investigated what the position of a pipe and the direction of the flow should be.

The importance of having information on tube-side heat transfer coefficients in supercritical fluid heat transfer can be illustrated by regarding the individual heat transfer resistances of shell-side, wall and tube-side. The overall heat transfer coefficient for a steel pipe is calculated with:

$$\frac{1}{U_o} = \frac{1}{h_o} + \frac{d_o \ln(d_o/d_i)}{2k_{steel}} + \frac{d_o}{d_i h_i} \qquad (1)$$

where U_o is the overall heat transfer coefficient corresponding with the outside area of the tube, h_o and h_i are the outside and inside film coefficients, d_o and d_i are the outside and inside tube diameters and k_{steel} is the thermal conductivity of the steel tube wall. As an example is taken here supercritical carbon dioxide (scCO2) being heated with steam in a pipe with d_o=16 mm, d_i=13 mm and k_{steel}=16 $Wm^{-1}K^{-1}$ so that $2k_{steel}/(d_o\ln(d_o/d_i))$=10000 $Wm^{-2}K^{-1}$. The heat transfer coefficient for

condensing steam is h_o=8000 $Wm^{-2}K^{-1}$. It can be seen in several publications [1-7] that, without the influence of variable properties or buoyancy, the tube-side heat transfer coefficient for $scCO_2$ is in the order of h_i=6000 $Wm^{-2}K^{-1}$. All three contributions of Eq. (1) have the same order of magnitude, so it is important to take into account enhancement or impairment of tube-side heat transfer caused by variations in physical properties or buoyancy.

5.2. Nusselt-relations

For fluids with physical properties that can be regarded as temperature-independent, the generally applied Nusselt-relation for the calculation of the tube-side heat transfer coefficient is, according to Jackson and Hall [2,3]:

$$Nu_{cp} = \frac{h_{cp} d_i}{k_b} = 0.0183 Re_b^{0.82} Pr_b^{0.5} \qquad (2)$$

or:

$$h_{cp} = 0.0183 \cdot d_i^{-0.17} \omega^{0.82} k_b^{0.5} \mu_b^{-0.33} c_{p,b}^{0.5} \qquad (3)$$

where Nu_{cp} is the Nusselt number in case of constant properties, evaluated at bulk conditions, h_{cp} is the corresponding tube-side heat transfer coefficient, k_b is the thermal conductivity of the fluid at bulk conditions, Re_b and Pr_b are the Reynolds and Prandtl numbers at bulk conditions, ω is the mass flux and μ_b and $c_{p,b}$ are the dynamic viscosity and the specific heat at constant pressure at bulk conditions. In Eq. (2), the physical properties are assumed constant in radial direction. In the longitudinal direction of a pipe, the bulk temperature and therefore the physical properties do change. Eq. (2) delivers the local heat transfer coefficient.

Around the pseudo-critical point, thermal conductivity, viscosity and specific heat vary strongly. It should be noted here that this temperature is higher than the critical temperature (31°C) when the pressure is above its critical value (74 bar). As is shown in Fig. 5.1 for 80 bar (pseudo-critical temperature T_{pc} = 34°C) , the variation in the factor $c_{p,b}^{0.5}$ is much larger than the change in the factor $k_b^{0.5}\mu_b^{-0.33}$, so that it can be expected that the heat transfer coefficient from Eq. (3) will follow

the trend of the specific heat, i.e. showing peaks at the pseudo-critical temperature. Indeed, these peaks were observed in the experiments of Swenson et al. [4] for water.

Eq. (2) can be used to predict the heat transfer coefficient at supercritical conditions only at low temperature differences between wall and bulk because then the physical properties can be regarded as constant in radial direction.

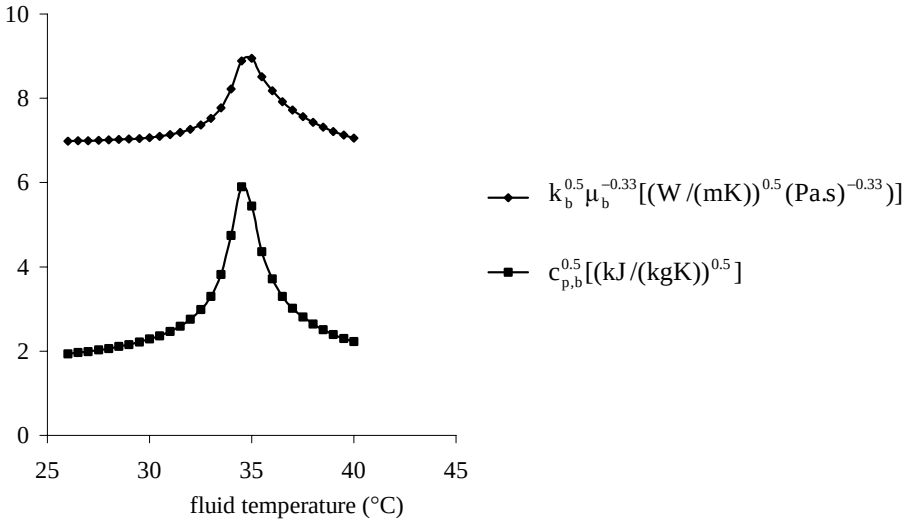

Fig. 5.1. Influence of the variation of carbon dioxide physical properties around the pseudo-critical temperature at 80 bar on the constant-property heat transfer coefficient of Eq. (3)

At higher wall-to-bulk temperature differences, specific heat, viscosity, thermal conductivity and density will show radial gradients and Eq. (2) is no longer valid. Instead, the variable properties have to be taken into account. This is mostly done by introducing correction factors in the form of ratios of wall to bulk properties raised to an empirical power:

$$Nu_{vp} = Nu_{cp}\left(\frac{\overline{c_p}}{c_{p,b}}\right)^a\left(\frac{\rho_w}{\rho_b}\right)^b\left(\frac{\mu_w}{\mu_b}\right)^c\left(\frac{k_w}{k_b}\right)^e \qquad (4)$$

where Nu_{vp} is the variable-property Nusselt number, a, b, c and e are constants, ρ is the fluid density and $\overline{c_p}$ is the average specific heat that can be calculated from the specific enthalpy H and temperature T according to Pitla et al. [1]:

$$\overline{c_p} = \frac{H_w - H_b}{T_w - T_b} \tag{5}$$

In practice, not all corrections in Eq. (4) are necessary. Krasnoshchekov and Protopopov [5] only corrected for specific heat and density and still obtained a relation that could be fitted to experimental data for a heated carbon dioxide flow in a vertical pipe:

$$Nu_{vp} = \frac{h_{vp} d_i}{k_b} = Nu_{cp} \left(\frac{\overline{c_p}}{c_{p,b}} \right)^a \left(\frac{\rho_w}{\rho_b} \right)^b \tag{6}$$

with $a=0.4$ at $T_b<T_w<T_{pc}$ and $1.2T_{pc}<T_b<T_w$,

$a=0.4+0.2[(T_w/T_{pc})-1]$ at $T_b<T_{pc}<T_w$,

$a=0.4+0.2[(T_w/T_{pc})-1][1-5\{(T_b/T_{pc})-1\}]$ at $T_{pc}<T_b<1.2T_{pc}$ and $T_b<T_w$,

and $b=0.35-0.05p/p_c$.

where h_{vp} is the variable-property tube-side heat transfer coefficient, T_b, T_w and T_{pc} are temperatures at bulk, wall and pseudo-critical conditions and p and p_c are pressure and critical pressure respectively.

Other forced convection correlations for heating CO_2 in a vertical pipe have been proposed but according to Jackson and Hall [2], Eq. (6) is the most accurate and is supported by the most experimental data. Although Krasnoshchekov and Protopopov used a more complex constant-property Nusselt number, Jackson and Hall [2] found that substituting Eq. (2) in Eq. (6) gave equally good results so this will also be done in this work.

For a very high wall-to-bulk temperature difference an extra complication is introduced. In this case, temperature-induced density variations cause free convection or buoyancy that disturbs the flow profile and thereby influences the heat transfer. When the fluid is heated while flowing down, buoyancy action leads

to a sharpened velocity profile relative to normal turbulent flow (Fig. 5.2a, b). This leads to a steeper shear stress profile and therefore to more turbulence; the heat transfer is enhanced.

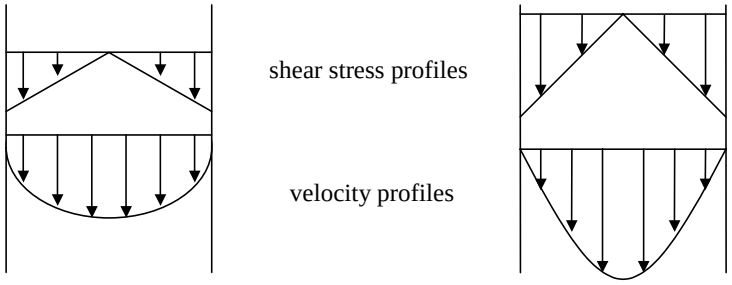

a) normal turbulent flow profiles

b) sharpened velocity profile and increased shear stress

Fig. 5.2. Schematic drawing of buoyancy effect, in downward heated pipe flow, leading to a sharpened velocity profile and a steeper shear stress profile, relative to normal turbulent pipe flow

When the fluid is flowing upwards, buoyancy causes either enhancement or impairment of heat transfer, depending on the magnitude of the buoyancy-effect: Low buoyancy action (Fig. 5.3a) leads to a flattened velocity profile, less shear stress and impairment of heat transfer whereas high buoyancy action (Fig. 5.3b) gives an M-shaped velocity profile, increased shear stress (W-profile) and therefore enhanced heat transfer.

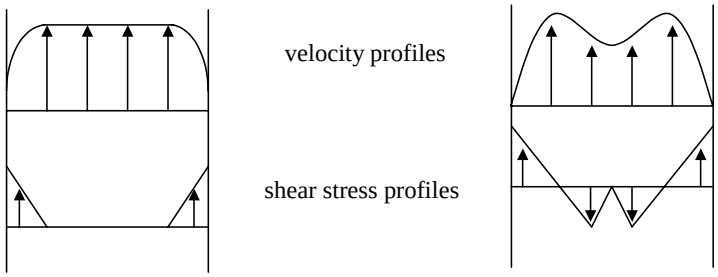

a) flattened velocity profile and less shear stress

b) M-shaped velocity profile and increased shear stress

Fig. 5.3. Schematic drawing of buoyancy effect, in upward pipe flow, leading to either a flattened velocity profile and decreased shear stress or to an M-shaped velocity profile and increased shear stress

It was observed by Walisch et al. [6] that heat transfer coefficients for heated horizontal pipes are below those of vertical pipes with down flow. Since Walisch et al. conducted their experiments both far away and close to the pseudo-critical temperature and for different pressures, it is assumed here that the heat transfer coefficients from the simulations for down flow will be larger than for horizontal flow for the range of conditions treated here. Therefore, simulations for horizontal flow are not carried out in this work.

Hall and Jackson [7] found that, in a vertical pipe with up- or down flow, buoyancy has to be taken into consideration when the bulk Grashof and Reynolds numbers are such that:

$$\mathrm{Gr_b}\,\mathrm{Re_b^{-2.7}} > 5\cdot 10^{-6} \tag{7}$$

where $\mathrm{Gr_b}$ is the Grashof number evaluated at bulk conditions.

No correlation for buoyancy in upward flow exists but buoyancy in a downward heated flow was described by Jackson and Hall [3] with a correction factor so that the Nusselt number for mixed forced and free convection $\mathrm{Nu_{mix}}$ becomes:

$$Nu_{mix} = 0.0183\,Re_b^{0.82}\,Pr_b^{0.5}\left(\frac{\overline{c_p}}{c_{p,b}}\right)^a\left(\frac{\rho_w}{\rho_b}\right)^b\left[1+2750\left(\frac{Gr_b}{Re_b^{-2.7}}\right)^{0.91}\right]^{1/3} \quad (8)$$

The tube-side heat transfer coefficients predicted by Eq. (8) are used here to compare with the results from computational fluid dynamics simulations.

5.3. Computational fluid dynamics simulations

Heated turbulent CO_2-flows in a vertical pipe were simulated using the computational fluid dynamics program FLUENT, version 5.0. Turbulence was modeled with the k-ε model. The flow entering the pipe was hydrodynamically fully developed. Variation of the physical properties of the CO_2 (density, specific heat, thermal conductivity and viscosity) with temperature was approximated by piecewise linear functions (isobars). The deviations between the approximate linear values and values from the NIST database [8] were less than 1% for all physical properties.

In the simulations, the enthalpy H_{in} of the CO_2 flowing into the simulated pipe and the mass flow rate Φ_m were known. The program delivered the enthalpy H_{out} of the CO_2 at the end of the pipe. The heat q that was transported to the CO_2 was calculated with $q = \Phi_m(H_{out}-H_{in})$. The tube-side heat transfer coefficient h_i was then calculated with $q = h_iA(T_w-T_b)$. The length of the simulated pipe was short so that the calculated h_i can be regarded as a local heat transfer coefficient. Only tube-side coefficients were calculated.

5.4. Results and discussion

Simulations were carried out for constant bulk pressure and for constant bulk density. In industrial practice these two cases are encountered in continuous and batch processes respectively. For both cases, the wall temperature was set constant in the simulations. In a continuous process this is realistic, in a batch heating process it is not. In the latter case, therefore, the heat transfer coefficients resulting from the simulations should be regarded as momentary values. It should be noted

here that the conditions “constant pressure” and “constant density” refer to the bulk fluid. On a microscopic level, gradients in pressure and density do exist due to the transport of thermal energy.

The constant bulk-pressure process was simulated for heated down flow in a pipe of internal diameter 13 mm, mass flow 0.3 kg/s, bulk temperature T_b = 30 °C. The tube-side heat transfer coefficients h_i were calculated from the simulation results and plotted as a function of wall temperature in Fig. 5.4. According to Eq. (7), buoyancy was negligible so that only the variation of physical properties in radial direction is expected to influence heat transfer.

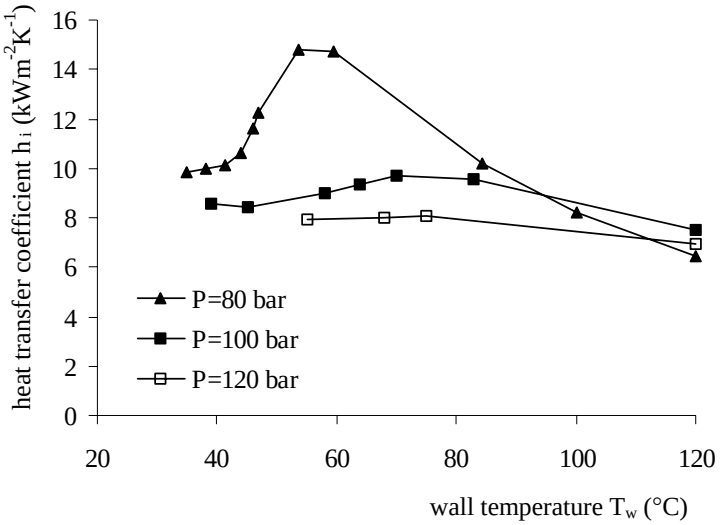

Fig. 5.4. Heat transfer coefficient as a function of wall temperature and pressure, for heated down flow at bulk temperature 30℃. Simulation results showing the effect of the temperature-induced variation of specific heat

It can be seen in Fig. 5.4 that the heat transfer coefficient follows the same trend as the specific heat does at the pseudo-critical temperature: showing peaks that decrease in height and shift to higher temperatures when the pressure increases. This can be understood by realizing that a peak in the specific heat in the thermal boundary layer will give a peak in the heat transfer coefficient. However, this would mean that, at a low wall-to-bulk temperature difference, the peak in transfer coefficients should be observed when the wall has the pseudo-critical temperature. From Liao and Zhao [9] it is known that at 80 and 100 bar, the pseudo-critical

temperatures are 35 and 45°C respectively. The peaks in Fig. 5.4 lie at higher temperatures because even at low wall-to-bulk temperature difference, in reality the wall will have to be somewhat above pseudo-critical to realize a pseudo-critical temperature in the thermal boundary layer.

To illustrate the influence of the variable properties, the values of h_i from Fig. 5.4 were compared to the constant-property heat transfer coefficient h_{cp} calculated from Eq. (2). In Fig. 5.5 the ratio h_i/h_{cp} is plotted as a function of wall temperature. The horizontal dashed line at $h_i/h_{cp} = 1$ represents the constant-property situation. Going from low to high wall temperature, it can be seen that first the simulations agree with the constant-property relation Eq. (2) within 10%, i.e. the ratio h_i/h_{cp} is near unity.

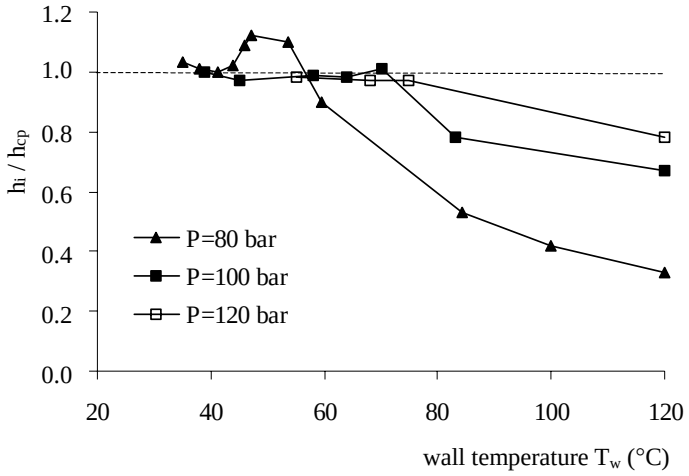

Fig. 5.5. Normalized heat transfer coefficient as a function of wall temperature. Simulation results showing the effect of specific heat and pressure, at bulk temperature 30℃

This corresponds to a wall-to-bulk temperature difference so low, that no radial gradient in specific heat exists, i.e. the condition for using Eq. (2) is met. Going further up in wall temperature, the peaks of Fig. 5.5 indicate that Eq. (2) underestimates the peaks in heat transfer for the case of 80 bar.

On the right-hand side of the peaks in Fig. 5.5, impairment of heat transfer occurs, i.e. the ratio h_i/h_{cp} falls below unity, especially at low pressures. This cannot be caused by buoyancy, according to Eq. (7). It is caused by the variation of density and specific heat in radial direction.

density-effect
At high wall temperatures, the density at the wall is significantly lower than in the bulk and a low-density, gas-like fluid transports heat less effectively. The density variation in radial direction is less prominent at higher pressure and so is the resulting impairment of heat transfer.

heat capacity effect
Due to the choice of bulk temperature (30°C), the specific heat in the bulk is higher than at the wall, especially for high wall temperatures. This leads to an overestimation of the heat transfer coefficient by Eq. (2). The specific heat effect is less significant for higher pressures.

The impairment by density variation is a general phenomenon; whether or not the effect of specific heat occurs depends on the choice of bulk temperature. From Fig. 5.5 it also follows that for 120 bar and higher, the constant-property relation Eq. (2) can be used for design purposes for wall temperatures up to 120°C.

A comparison between heat transfer coefficients from the simulations and from the variable-property relation Eq. (6) is made in Fig. 5.6 for the same conditions as in the 80 bar case of Fig. 5.5. It can be seen that Eq. (6) has an accuracy of ± 30 %.

The above cases are examples of constant bulk-pressure heat transfer, corresponding with industrial continuous processes. For heat transfer at constant bulk-density, corresponding with industrial batch processes, the simulation results are shown in Fig. 5.7. During the simulations, the fluid was heated from 80 bar and 33°C to 300 bar and 112 °C at a wall temperature of 120°C. Buoyancy-effects were not important according to Eq. (7). It can be seen that the heat transfer coefficient deviates significantly from the constant-property case at low pressure. This is the same observation that was made earlier because the left-hand side of the heating curve corresponds with a large temperature difference between wall and bulk, i.e.

an overestimation of heat transfer by Eq. (2) because of specific heat and density variation in radial direction.

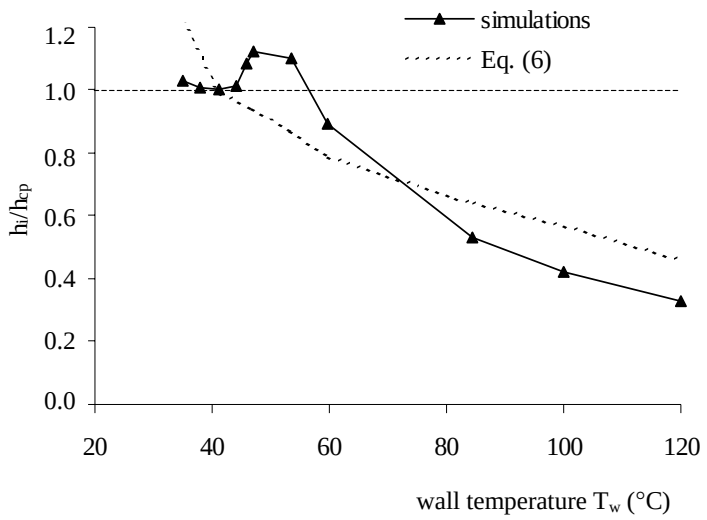

Fig. 5.6. Normalized heat transfer coefficient as a function of wall temperature, for 80 bar and a bulk temperature of 30°C. Comparison of simulation results with Eq. (6)

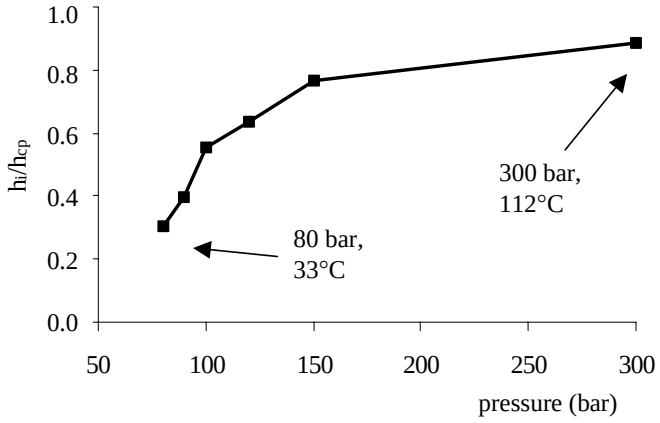

Fig. 5.7. Simulation results showing the change in normalized heat transfer coefficient during isochoric heating of carbon dioxide of 615 kg/m^3, flowing at 0.3 kg/s in a 13 mm pipe

It should be noted here that Eq. (2), containing the specific heat at constant pressure c_p, is used for a process occurring at constant bulk density, where the heating leads to a pressure increase. This is allowed because Eq. (2) is not used to calculate the whole heating process from 33 to 112 °C, in which case the specific heat at constant volume would be expected, but only the momentary heat transfer coefficient. For a short piece of pipe, such as is simulated here, the bulk-pressure can be regarded as constant and therefore the use of c_p and of Eq. (2) is permitted.

The importance of taking into account the variation of physical properties is illustrated by Fig. 5.5 and Fig. 5.7. For conditions where $h_i/h_{cp} = 0.5$, for example, Eq. (1) indicates that the overall heat transfer coefficient U_o is 30% lower than predicted by Eq. (2).

Because in Fig. 5.4 to Fig. 5.7 no buoyancy is active, the influence of varying physical properties could be investigated. Simulations were also carried out at 120 bar and large Grashof numbers so that not only forced but also free convection is significant. It was observed earlier that the variation of physical properties has a limited influence at 120 bar, so that in this case any significant deviation from the constant-property situation will be caused by buoyancy. In the simulations wall and bulk temperatures were 134 and 104°C respectively. Fig. 5.8 shows the resulting heat transfer coefficients as a function of Reynolds number for a heated vertical flow of CO_2 in a 13 mm pipe, both for upward and downward flow.

It follows from Fig. 5.8 that, at large Reynolds number, there is no difference between up- and down flow. At these conditions, buoyancy is negligible and the constant-property equation is satisfactory for design purposes. At intermediate Re values (from the dashed line down to Re = 40000), the heat transfer coefficient for upward flow is lower than predicted by the constant-property relation Eq. (2) ($h_i/h_{cp} <1$) while the down flow coefficient stays approximately constant. This is the effect of the flattening of the velocity profile in the upward flow (Fig. 5.3a). Going from Re = 40000 further down in Reynolds number, the heat transfer coefficients for both up- and down flow become larger than predicted by Eq. (2), i.e. the ratio h_i/h_{cp} is larger than unity. The enhancement is caused by the steeper shear stress profile in the down flow (Fig. 5.2b) and by the W-shaped shear stress profile in the up flow (Fig. 5.3b). In the buoyancy regime, to the left of the dashed line, the heat

transfer for the down flow is larger than for the up flow for the whole range of Re. At very low flow rates (very low Re), as the regime of pure free convection is approached, the difference between up- and down flow vanishes, which was also reported by Jackson and Hall [3]. The limit for the onset of buoyancy from Eq. (7) ($GrRe^{-2.7} = 5 \cdot 10^{-6}$) corresponds with the dashed line; the simulation results confirm the validity of the buoyancy criterion.

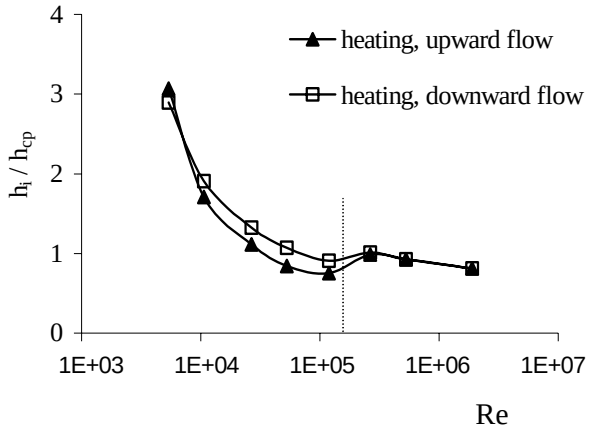

Fig. 5.8. Influence of buoyancy on the normalized heat transfer coefficient for carbon dioxide flowing in a vertical pipe at 120 bar. Comparison of simulation results for up- and downward flow. The dashed line indicates the onset of buoyancy (Eq. (7)).

In Fig. 5.9, the above discussed simulation results for the heated down flow are plotted together with the heat transfer coefficients that are predicted by Eq. (8). The figure shows that the agreement is good, confirming the validity of Eq. (8).

The results from the mixed convection simulations (Figs. 5.8 and 5.9) show that buoyancy can increase heat transfer significantly relative to the constant-property situation. For example, if a value of $h_i/h_{cp} = 2$ can be realized, Eq. (1) then predicts an increase in the overall heat transfer coefficient U_o of 25%.

All simulations and model calculations were carried out for CO_2 in 13 mm pipes. However, the results presented here are also applicable for other systems (other

fluids and pipe diameters), as long as the relevant dimensionless numbers (Re, Pr and Gr) of a regarded system are the same as the ones in this work.

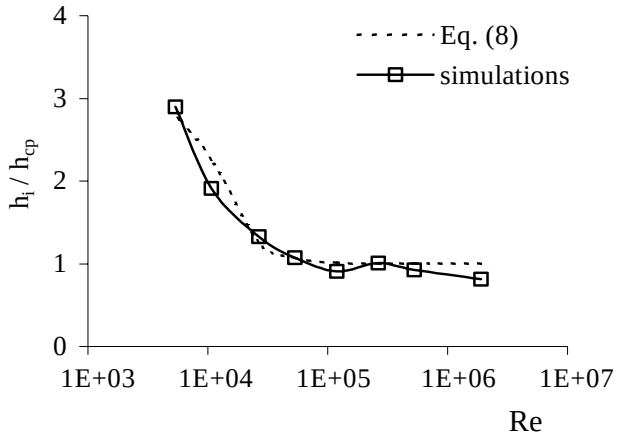

Fig. 5.9. Influence of buoyancy on the normalized heat transfer coefficient for carbon dioxide flowing down in a heated vertical pipe at 120 bar. Comparison of simulations with Eq. (8)

5.5. Conclusions

For a heated vertical flow of CO_2 without buoyancy, the constant-property Nusselt relation is not suitable for pressures below 120 bar as it can introduce an overestimation of the overall heat transfer coefficient by 30 %. For such conditions, the variable-property relation of Krasnoshchekov and Protopopov is acceptable for design purposes.

The criterion that Jackson and Hall developed, to determine when buoyancy is important, was confirmed by the CFD-results.

In the mixed convection regime in downward heated flow, the CFD simulations gave results that agreed with the Jackson and Hall buoyancy correction factor combined with the Krasnoshchekov-Protopopov relation. The action of buoyancy can lead to an increase in heat transfer coefficient as large as 25 %.

A heat exchanger for heating should be placed in a vertical position with the fluid flowing downwards when buoyancy is active. A vertical up flow or a horizontal flow will always result in a smaller heat transfer coefficient.

References

13. S.S. Pitla, D.M. Robinson, E.A. Groll, S. Ramadhyani, Heat Transfer from Supercritical Carbon Dioxide in Tube Flow: A Critical Review, *HVAC&R Research* **4** (3), 281 (1998).
14. J.D. Jackson, W.B. Hall, Forced Convection Heat Transfer, in: S. Kakaç, D.B. Spalding (Eds.), Turbulent Forced Convection in Channels and Bundles, vol.2, 1979, 563.
15. J.D. Jackson, W.B. Hall, Influences of Buoyancy on Heat Transfer to Fluids Flowing in Vertical Tubes under Turbulent Conditions, in: S. Kakaç, D.B. Spalding (Eds.), Turbulent Forced Convection in Channels and Bundles, vol.2, 1979, 640.
16. H.S. Swenson, J.R. Carver, C.R. Kakarala, Heat Transfer to Supercritical Water in Smooth-Bore Tubes, *ASME Journal of Heat Transfer* nov. 1965.
17. A. Krasnoshchekov, V.S. Protopopov, Heat Exchange in the Supercritical Region During the Flow of Carbon Dioxide and Water, *Teploenergetika* **6** (12), 26130 (1972).
18. T. Walisch, W. Dörfler, Ch. Trepp, Heat Transfer to Supercritical Carbon Dioxide in Tubes with Mixed Convection, HTD-Vol. 350, vol. 12, ASME 1997, National Heat Transfer Conference, 79.
19. W.B. Hall, J.D. Jackson, Laminarization of Turbulent Pipe Flow by Buoyancy Forces, ASME Paper no. 69-HT-55 (1969).
20. National Institute for Standards and Technology (NIST) Chemistry Webbook, http://webbook.nist.gov/chemistry.
21. S.M. Liao and T.S. Zhao, Measurements of Heat Transfer Coefficients from Supercritical Carbon Dioxide Flowing in Horizontal Mini/Micro Channels, *J. Heat Transfer* **124**, 413(2002).

)

Chapter 6

Process and Equipment Design for a 100-Liter Polyester Beam Dyeing Machine

Abstract

A technical-scale, 100-litre machine was designed and built to test polyester beam dyeing in scCO2, with respect to the performance of the equipment and the process.

The design aims at introducing 1 mass percent of dye into 13 kg polyester cloth in a 2-hour process. Per batch, 95% of the CO2 is recovered and stored for reuse. The dyeing conditions are 300 bar and 120ºC.

A new pressure vessel was designed, consisting of a steel liner with carbon fibers wound around it to take up the radial forces. The axial pressure forces are taken up by an external steel yoke keeping both lids of the vessel in place.

To circulate the CO_2 with the dissolved dye through the textile roll, a low-pressure centrifugal pump was placed inside the dyeing vessel.

Although the equipment designed in this chapter is smaller, the process is the same as in the industrial-scale 1000-litre machine discussed in chapter 7. This gives the opportunity to test and optimize the performance of the process. The two most costly items of an industrial-scale machine, the dyeing vessel and the circulation pump, were both especially designed for the technical-scale machine in a cheaper form, thereby facilitating the scale-up of the supercritical dyeing process.

6.1. Introduction

In the previous chapters, different machine configurations were used in the experiments. In the present chapter, a polyester beam-dyeing machine is discussed. In such a machine, also used in current aqueous dyeing, the knitted or woven polyester cloth is wound around a perforated pipe. The pipe is closed at one end and the water or, in this case, the $scCO_2$, is pumped into the other end of the pipe. The flow is then forced through the PET-layers; the dye molecules simultaneously diffuse into the fibers. Figure 6.1 gives a schematic impression of the dyeing principle.

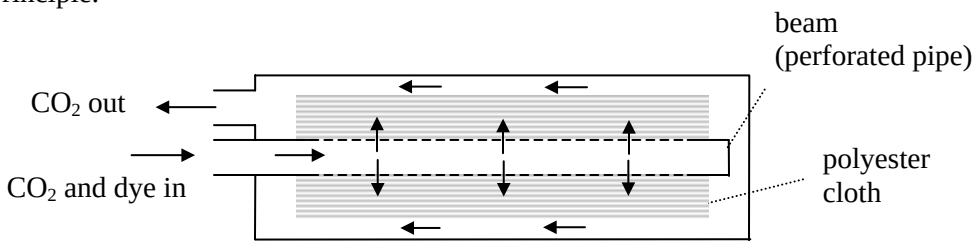

Figure 6.1. Schematic representation of a beam dyeing process

The dyeing machine developed in this chapter is large compared to the dyeing machines described in literature [1] and in chapters 2 and 4 but is still an order of magnitude smaller, in volume, than the industrial-size (1000-liter) machine discussed in chapter 7. The aim of the currently discussed 100-liter dyeing machine is testing the process with respect to:

1. Effect of heating and cooling rate. It is known from aqueous dyeing that too fast a temperature rise or drop results in uneven dyeings of the PET. It is to be tested if this phenomenon also puts a restriction on the heating and cooling rate in $scCO_2$.
2. Evenness of dyeing as a function of dyeing time, CO_2-flow rate, beam diameter and the diameter of the holes in the beam.
3. Dye dosing. An appropriate way of introducing and dissolving the dye powder into the $scCO_2$ is to be developed.
4. The leveling time. After all dye has diffused into the PET, the inside of the textile roll is darker than the outside. When the CO_2-flow is now continued, the color will be equilibrated. It should be determined how long this leveling takes.

5. The required time and temperature of rinsing. After dyeing, the CO_2 contains residual dye that is to be flushed out of the vessel to avoid contamination of the machinery and the cloth. The optimal rinsing time and temperature must be determined.
6. Problems with deposition of cyclic trimers. It has been observed by Montero et al. [2], that PET-dyeing in $scCO_2$ can lead to deposition of ethylene terephtalate trimers inside the dyeing machinery. This problem is to be investigated with the 100-liter machine.

It should be noted that the machinery was designed and built, but no experimental results are available at this moment. Both the process and the equipment were designed in close cooperation with FeyeCon D&I B.V. (The Netherlands).

6.2. Boundary conditions for the 100-litre beam-dyeing machine

The machine is designed for one set of boundary conditions (table 6.1). The aim of the process is to introduce 1 mass% of dye into 13 kg of polyester. The textile, as rolled up on the beam, has a density of 500 kg/m^3. Since chapter 4 showed sufficient coloration at 120ºC and 300 bar, these values are taken as the working temperature and pressure in the design.

Table 6.1. Boundary conditions for the 100-liter beam-dyeing machine

Mass of PET roll (kg)	13
Length x diameter (m)	0.45 x 0.28
Beam diameter (m)	0.06
Dyeing temperature (ºC)	120
Design temperature (ºC)	150
Dyeing Pressure (bar)	300
Design pressure (bar)	350
Desired dye concentration (g/(gPET)	0.01

6.3. Process steps

The consecutive steps of the process are given in table 6.2, together with the times for which the corresponding equipment items are designed. The aim is a total process time of 2 hours. Figure 6.2 gives a simplified process flow diagram.

Table 6.2. Process steps and times

Process step	Time (min)
Loading textile and dye	3
Pressurization	15
Dyeing at 120ºC and 300 bar	45
Leveling	15
Rinsing at 80ºC and 300 bar	20
Depressurization	20
Unloading textile	2
Total batch time	120

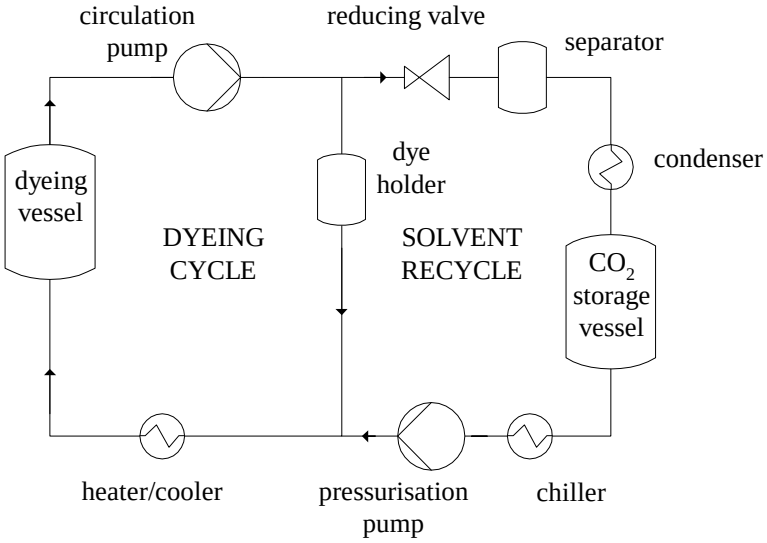

Figure 6.2. Simplified process flow diagram for the supercritical beam dyeing process

After the textile and the dye powder are loaded, the dyeing vessel is pressurized with CO_2. In the last part of the pressurization step, the circulation pump and the heat exchanger are started. The CO_2 is heated at the same time as new CO_2 is pumped into the machine until the desired temperature (120ºC) and pressure (300 bar) are reached.

During the dyeing step, the CO_2 is circulated from the dyeing vessel, over the dye holder, the heat exchanger and back into the dyeing vessel. In this way, dye dissolution and PET dyeing take place simultaneously.

After 45 minutes, the dye dosing stops. In the leveling time that follows, the flow rate, temperature and pressure are kept constant. After this step, the dye is distributed over the PET and the scCO_2. Depressurization would lead to precipitation of dye on both the textile and the inner parts of the dyeing machine and therefore the vessel is rinsed with fresh CO_2. During the rinsing, clean CO_2 from the storage vessel is pumped into the machine while CO_2 containing residual dye is removed through the reducing valve. The circulation pump and the heater are still running at this time.

The reducing valve keeps the pressure in the dyeing vessel at 300 bar during the rinsing step. The CO_2 exiting the valve enters the separator, where it is gasified to precipitate the dye in order to obtain a flow of clean CO_2 in the direction of the condenser.

The gaseous CO_2 is condensed and stored in liquid form. During the rinsing, the pressure in the CO_2-recycling part is kept constant by keeping the temperature in the storage vessel at the saturation temperature at 60 bar (22ºC), using the coolant flowing through the condenser.

The aim of the rinsing step is to lower the dye concentration in the vessel, so that depressurization does not lead to precipitation of dye onto the cloth and the machinery. In the rinsing step, dye will be extracted from the fibers. This negative effect is minimized by lowering the temperature from 120 to 80ºC while the pressure is kept constant by the pressurization pump. However, as is illustrated for 5 dyes in appendix 6.1, this leads to a decrease in dye solubility of maximally a factor 2. When the coloration of the polyester is to be above one half of the

maximum coloration, the CO_2 at the beginning of the rinsing step contains dye concentrations above one half of the solubility, following from the linearity of the absorption isotherms in chapter 4. Cooling then results in precipitation of dye in the machine and on the cloth. To avoid this, the first part of the rinsing time can be carried out at 120ºC and only then the temperature is lowered to 80ºC.

When the dyeing machine is regarded as ideally mixed, the time t (s) required to decrease the concentration from c_0 to c in the vessel volume V (0.10 m^3) by rinsing with volume flow rate Φ_V (pump flow $1.2 \cdot 10^{-4}$ m^3/s) is given by integrating the mass balance:

$$V \frac{dc}{dt} = -\Phi_V c \tag{6.1}$$

from $t = 0$; $c = c_0$ to $t = t$; $c = c$, leading to:

$$c = c_0 \exp\left(-\frac{t\Phi_V}{V} \right) \tag{6.2}$$

From equation 6.2 it follows that the first 5 minutes of the rinsing have to be carried out at 120ºC, the concentration is then $c = 0.7\ c_0$. The next 5 minutes, rinsing and cooling occur simultaneously. In this way, the temperature of 80ºC is reached at the moment that the dye concentration $c = 1/2\ c_0$, i.e. after 10 minutes of rinsing. It is also calculated that a total of 20 minutes of rinsing leads to a decrease in dye concentration of the $scCO_2$ by 75%, i.e. $c = 1/4\ c_0$. It is assumed that the remaining 25% does not significantly affect the coloration of the next batch.

The process and equipment design allows changes in the times of heating, cooling, dyeing, leveling and rinsing as well as changes in CO_2 flow rate, beam dimensions and in the dye dosing device, so that all six issues mentioned in section 6.1 can be investigated.

6.4. Solvent cycle

The process is drawn in a temperature-entropy diagram in figure 6.3. Point A represents the storage vessel conditions (saturated liquid at 22ºC, 60 bar). From point A to B, the CO_2 from the storage vessel is sub cooled isobaric to 20ºC, a temperature with boiling pressure 57 bar, to prevent cavitation of the pressurization

pump. From B to C, the CO_2 is pumped into the dyeing vessel. This is assumed to be an isentropic process. Energy dissipation in the pump will bend the top of line BC to the right. On the other hand, the CO_2 in the dyeing vessel will lose part of its heat to the steel and the polyester, bending the top of line BC to the left.

From point C on, the circulation and heating of the CO_2 are started while the pressurization pump still runs. The effect is a simultaneous pressure, temperature and density increase, leading to point D that represents the dyeing conditions (120ºC, 300 bar). From D to E, the CO_2 is cooled isobaric from 120 to 80ºC; the pressurization pump is used to simultaneously increase the density in the dyeing vessel from 585 to 745 kg/m^3.

During the rinsing period, the conditions inside the dyeing vessel remain those of point E (80ºC, 300 bar). The CO_2 that is used for the rinsing, follows the route E→F→G→A→B→E (line BE is not drawn in the diagram). From E to F, the CO_2

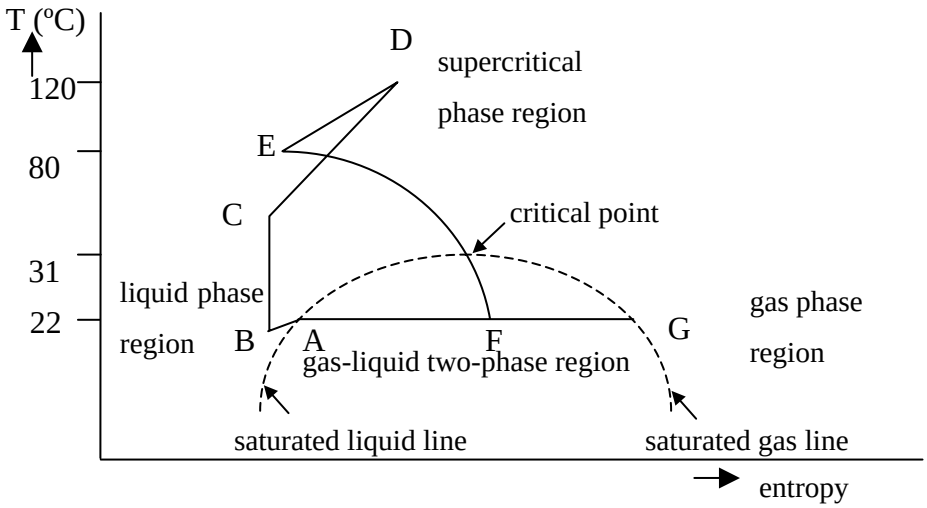

Figure 6.3. Temperature-entropy diagram for CO_2, showing the solvent cycle during the supercritical dyeing process

passes through the regulating valve, undergoing an isenthalpic expansion into the two-phase region, ending at the 60 bar isobar (line AG). The liquid mass fraction in point F, being 0.4, represents the amount of CO_2 that is to be evaporated in the separator. During evaporation, the CO_2 goes to the saturated gas line (point G). In

the condenser it crosses from G to A through the two-phase region. As liquid CO_2 reenters the storage vessel, the cycle is closed.

After the rinsing, the pressure in the dyeing vessel is lowered through the regulating valve until it is equal to the pressure in the storage vessel (60 bar). The pressure in the dyeing vessel is then further reduced to 10 bar with the gas booster. The final temperature in the dyeing vessel is estimated to be between –20 and 20ºC. This corresponds with a density of (21±2) kg/m^3, giving a total amount of 95% of CO_2 that is recycled per batch.

6.5. Equipment design

6.5.1. Dyeing vessel

The vessel was designed by Solico B.V. (The Netherlands). The internal length and diameter are 1350 and 350 mm. The volume available in the vessel for the scCO_2 is 100 liters. The working and design pressures are 300 and 350 bar, respectively, the working and design temperatures are 120 and 150ºC.

Configuration of the vessel.

As discussed in chapter 7, a thin-walled steel liner with composite fibers wound around it tangentially to take up the pressure forces in radial direction [3], is economically favorable to use, instead of a completely steel dyeing vessel. Two lids are used, not connected to the vessel, to distribute the axial forces over 6 steel plates that are placed around the vessel as a yoke. The yoke is moved up and down by two spindles, both driven by the same motor to ensure equal movement of both sides of the yoke. During movement, the yoke is guided by 4 positioners, as is shown in figure 6.4. The outer length, width and thickness of the plates are 2250, 800 and 30 mm.

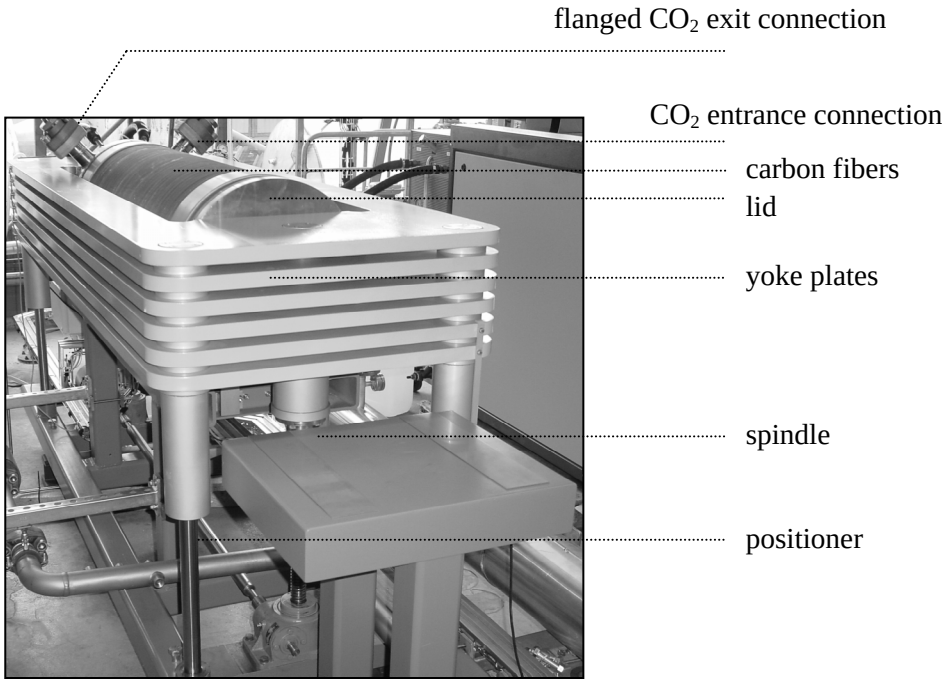

Figure 6.4. Photograph of the closed 100-litre dyeing vessel

To load and unload polyester rolls, the yoke is lowered so that one of the lids can be moved away from the vessel by means of a pneumatic linear drive underneath the vessel. Attached to the lid, a cart on wheels, supporting the beam with textile, is then also pushed out. Inside the vessel, the cartwheels are guided by rails, welded onto a stainless steel shell that covers the lower 115º of the liner. Figures 6.5 A, B give a schematic impression of the opened vessel and a cross-section of the cart loaded with textile, respectively.

Because of economical reasons, as discussed in chapter 7, the circulation pump is placed inside the dyeing vessel. The lid on the pump-side of the vessel can be pulled out manually, to perform maintenance on the pump. The CO_2 entrance and exit are on top of the lid, as is shown in figure 6.6. Figure 6.7 gives a complete impression of the vessel and its contents, together with the flow path of the CO_2.

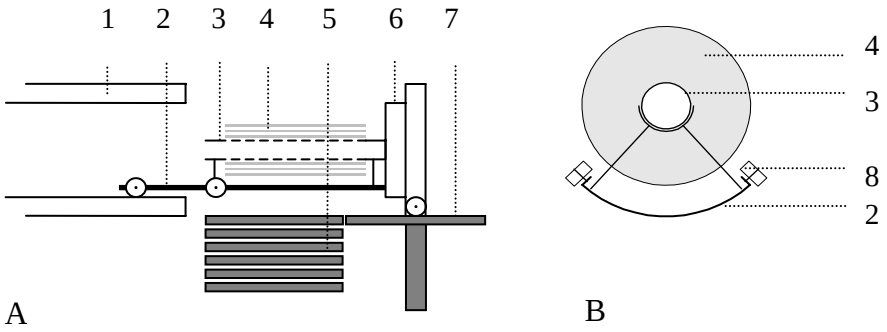

1.	vessel wall	5.	yoke plates
2.	cart bottom	6.	lid
3.	beam	7.	support table
4.	polyester roll	8.	cart wheel

Figure 6.5. Schematic representation of the dyeing vessel in open position, with a longitudinal section (A) and a cross-section of the loaded cart (B)

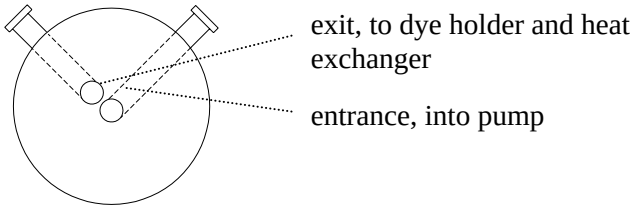

Figure 6.6. Schematic presentation of the pump-side lid, showing the CO_2 entrance and exit.

When the yoke is lowered or raised, contact with the lids is to be avoided. A distance of 3 mm is realized by pressing the lids against the vessel with:

- the pneumatic linear drive, on the beam-side and
- springs attached to the lid on the pump-side.

When the vessel is pressurized, the lids move 3 mm outwards until there is contact with the yoke. On the lids, lip seals are placed, designed to slide along the internal surface of the liner. Regarding the internals of the dyeing vessel, the movement of

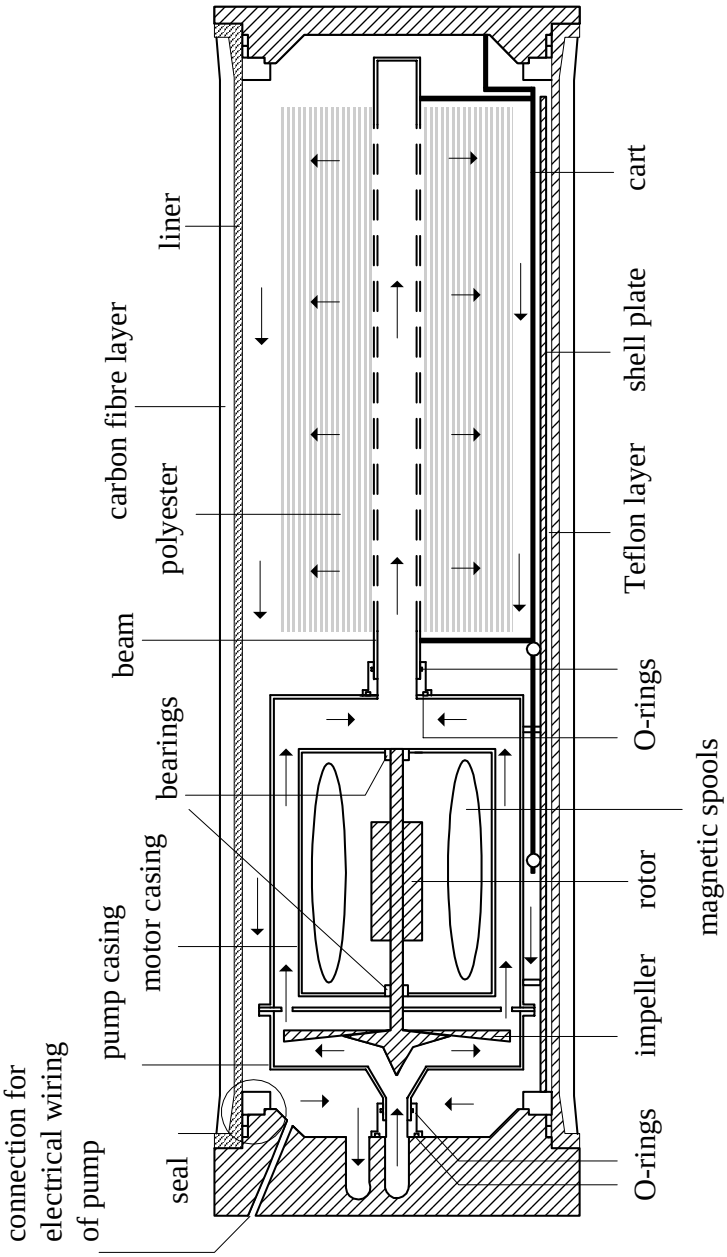

Figure 6.7. Detailed drawing of the 100-litre dyeing vessel

the lids is compensated by allowing the O-rings in figure 6.7 to slide 6 mm. Because of the 3 mm movement of the pump-side lid, the CO_2 entrance and exit of the vessel are connected to the rest of the machine by flexible stainless steel hoses.

Materials of construction.

All parts of the vessel and the internals are made of stainless steel (AISI 316), with the exception of:

- the lip seals, made from Rulon®, with PEEK back-up rings,
- the 4 O-rings in figure 6.7, made of a Viton® core with Teflon® jacket and
- the axes of the cartwheels are made of brass because this material is dry-running. The use of steel is avoided here because the required grease on the bearings would dissolve into the scCO_2.

In the choice of the material for the liner and the composite, care is taken that the strain of the liner is higher so that the pressure-induced deformation of the liner will follow that of the composite. For the liner, duplex (stainless steel 1.4462) is chosen since it has a large tensile strength, relative to other stainless steel types. For the composite material, the standard carbon fiber type T 700 is taken because it is cheaper and has a higher stiffness and tensile strength than other composite materials, like aramid or glass fiber [4]. The matrix to keep the carbon fibers together is a high-temperature epoxy resin, because it binds well with carbon fibers and it can be applied at the design temperature of the dyeing vessel (150ºC).

The physical properties of the liner and the fiber material are given in table 6.3. Calculations [4] show that at the working pressure of 300 bar, the stress in the liner in tangential direction is 430 MPa, below the creep limit. At this pressure, the liner is pressed outwards against the composite layer. At a pressure of 2070 bar inside the vessel, the composite layer is at its tensile strength of 2450 MPa.

Cyclic fatigue tests on composite samples at 150ºC have shown a 50 % failure probability for $2 \cdot 10^6$ cycles at a stress of 510 MPa, well above the stress of 430 MPa at the working pressure. For the liner this fatigue limit was calculated to be 565 MPa. This suffices since the vessel is designed for only 25000 dyeing batches. The diameter increase at the dyeing pressure of 300 bar is 1.5 mm. The seals are designed to compensate for this enlargement.

Table 6.3. Mechanical properties of the liner and the composite layer for the 100-litre dyeing vessel [4]

Liner	Material	Duplex stainless steel	
	Thickness	10	mm
	Creep limit	460	MPa
	Fatigue limit ($2 \cdot 10^6$ cycles)	565	MPa
Composite layer	Material	Carbon fiber in epoxy resin	
	Thickness	40	mm
	Tensile strength	2450	MPa
	Fatigue limit ($2 \cdot 10^6$ cycles)	510	MPa

6.5.2. Circulation pump

Pump capacity

At 120ºC and 300 bar, dye solubilities lie between 10^{-4} and 10^{-5} g dye / g CO_2 [5-8]. It is assumed here that:

- the CO_2 is saturated, containing 10^{-5} g dye / g CO_2, when leaving the dye holder and
- the CO_2 contains a negligible amount of dye when exiting the textile roll.

To introduce 1 mass% of dye into 13 kg PET, a total amount of 13000 kg CO_2 needs to be circulated in the 45 minutes mentioned in table 6.2. Since the density of $scCO_2$ at 120ºC and 300 bar is 585 kg/m^3, this means that a pump capacity of 30 m^3/hour is needed. The resulting CO_2 velocity in the 2" SCH 160 pipes is 5.7 m/s.

Pressure drop

The required head of the circulation pump is determined by several pressure drop contributions. The calculations are given in appendix 6.2. It is concluded that the total pressure drop over the machine, to be delivered by the circulation pump, is 2 bar.

The combination of capacity and head have led to the choice of a 3000 rpm centrifugal pump with a maximum capacity of 30 m^3/hour at 3 bar head, designed in cooperation with and supplied by Packo Inox N.V. (The Netherlands). The electric motor for the pump has a capacity of 7.5 kW, is controlled with a frequency drive and was delivered by Electromotorenfabriek Nijmegen (The Netherlands).

Materials of construction

All parts of the motor and pump are made of stainless steel (AISI 316 and 304), with the exception of:

- The electrical copper spools of the motor.
- The resin in which the spools are fixed is a product from Electromotorenfabriek Nijmegen (The Netherlands). This product was tested at the Delft University of Technology and found to be not soluble in $scCO_2$ and not damaged by repeated depressurizations.
- The bearings. Since grease dissolves in $scCO_2$, dry-running bearing are used. The balls are made of silicium nitride and run in steel cages with a dry-lubrication coating. The bearings are a product from SKF Nederland.
- The electrical wiring to the motor is copper, coated with Teflon®.
- The rotor is made from soft iron.

6.5.3. Pressurization pump

Because an air-driven piston-cylinder pump was found to be suitable for liquid CO_2 in the 40-litre machine discussed in chapter 4, such a device was also chosen here. The pump has to fill the vessel in 15 minutes (table 6.2) and rinse the vessel sufficiently in 20 minutes. The latter duty determines the required flow rate, following from equation 6.2 as $1.2 \cdot 10^{-4}$ m^3/s at 300 bar. This leads to the choice of a type P200-65-2 from Resato Int. B.V. (The Netherlands). The pump has two heads; both suction pipes are chilled in 1.5 meter double-pipe exchangers by water from the cooling machine.

6.5.4. Dye holder

To prevent dye powder from reaching the dyeing vessel, which would lead to staining of the textile, the dye has to be molecularly dissolved in the $scCO_2$. A device is used consisting of a combination of a filter housing and a powder dosing device, as shown in figure 6.8.

After the dye has been dosed, it is kept from entrainment by a stainless steel candle filter, with pore size 10 μm. The $scCO_2$ flows past the dissolving particles and through the filter material towards the dyeing vessel. The volume of the filter housing is 3 liters. The dosing device has yet to be developed; the possibility of dosing powder into a pressurized machine has been proven by Eggers et al. [9].

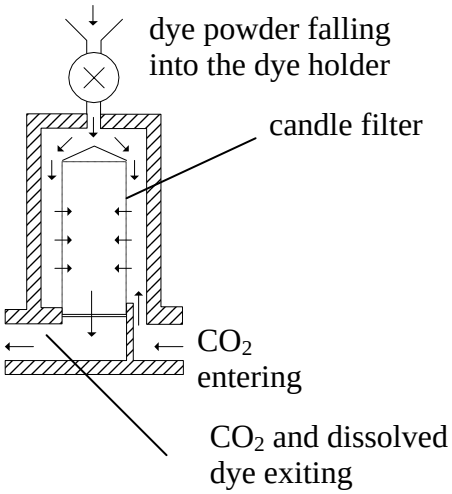

Figure 6.8. Dye dissolution unit with dosing and candle filter

6.5.5. Heat exchanger

As discussed above, each dyeing cycle involves heating and cooling of the CO_2, polyester and steel. To save on equipment cost, this is both done in one heat exchanger. Because in a dyeing process the ease of cleaning of the tubes is important, a single-pass exchanger is used. Two configurations are possible for this equipment item. Firstly, the steam and cooling water compartments on the shell-side can be separated, as shown in figure 6.8. Secondly, it is possible to send both the steam and the cooling water through the same compartment, as is shown in figure 6.9.

In the case of figure 6.9, care should be taken to avoid flow of steam into the cooling water system and vice versa, because cooling water systems are designed for lower pressures than steam systems and because the presence of water in steam pipes leads to water hammer. Therefore, figure 6.9 contains six more valves than figure 6.8. Four valves separate the cooling water from the steam system and two valves are needed to squeeze water out of the shell and into the drain, using pressurized air, when the duty from the exchanger switches from cooling to heating. The advantage of the configuration in figure 6.8 is an easier control; it is therefore used in current industrial aqueous dyeing processes. The advantage of the configuration shown in figure 6.9 is a smaller, cheaper heat exchanger and it is therefore chosen for the 100-litre dyeing machine.

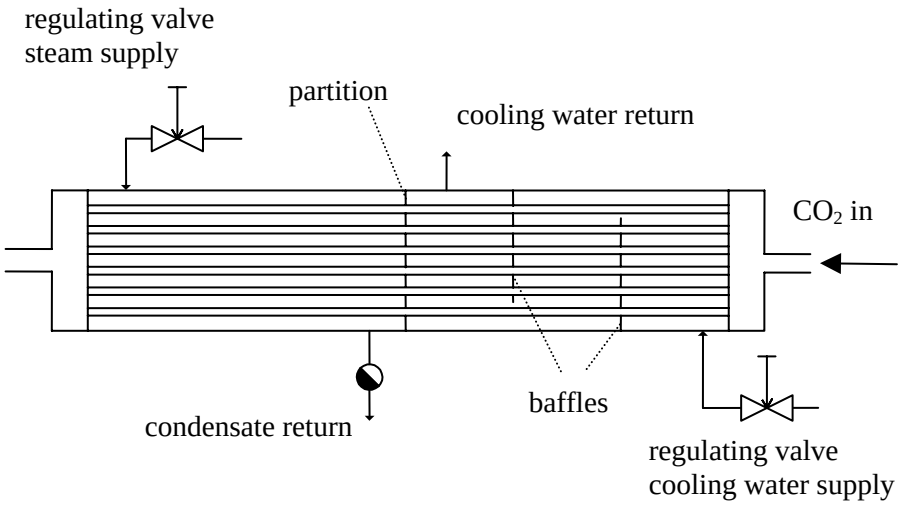

Figure 6.8. Possible configuration for alternate heating and cooling, with separate compartments for steam and cooling water

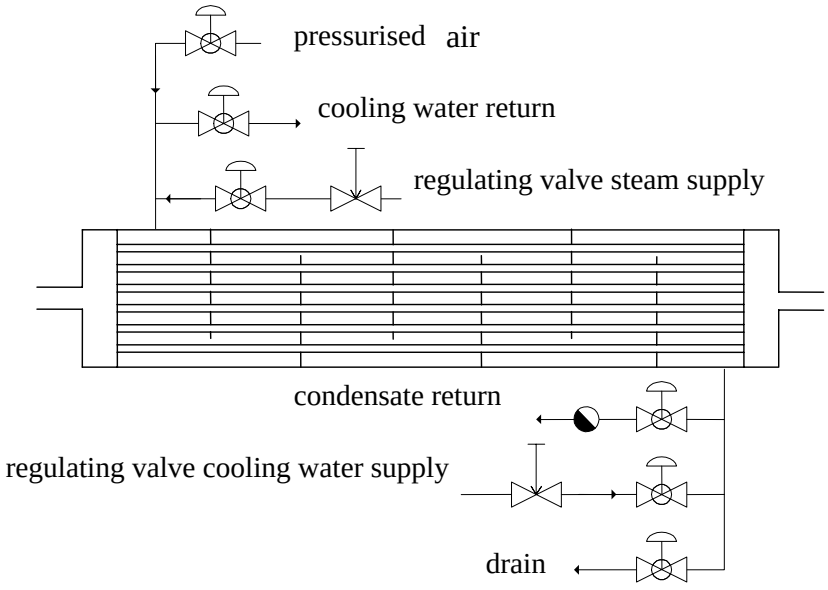

Figure 6.9. Heat exchanger configuration for the 100-litre dyeing machine, with a single shell-side compartment for both steam and cooling water

The temperature of the $scCO_2$ in the dyeing vessel is measured and determines the flow rate of the steam or cooling water into the heat exchanger via the corresponding regulating valves. Since the heating and cooling times are yet to be investigated, the heat exchanger is designed for relatively short, minimum heating and cooling periods, in both cases 5 minutes.

Heating

The circulation pump, and thus the heating, starts when a pressure of 150-200 bar is reached. It was concluded in chapter 5 that, for these conditions, the influence of temperature-induced variations of physical properties in radial direction of a heat exchanger pipe can be neglected, i.e. a constant-property relation for calculation of the heat transfer can be used. Also buoyancy can be neglected according to chapter 5.

Walish et al. [10] measured that for Reynolds number larger than 10^5, upward, downward and horizontal flows of $scCO_2$ all have the same heat transfer coefficients (±20%). Since the Reynolds number in the dyeing process is $6 \cdot 10^5$, a horizontal heat exchanger for the 100-litre dyeing machine is designed, using the constant-property equation 5.2. A heating time of 5 minutes is calculated when 23 pipes of 1/4" SCH 40 (external diameter 13.72 mm, wall thickness 2.24 mm, length 1950 mm) are used. A steam temperature of 150ºC is taken, the tube-side heat transfer coefficient is 8000 $Wm^{-2}K^{-1}$, making the overall coefficient 2000 $Wm^{-2}K^{-1}$, according to equation 5.1.

Cooling

The tube-side coefficient is 8000 $Wm^{-2}K^{-1}$. The water, from a cooling tower, has a temperature of 20ºC. The shell-side coefficient is calculated with Kern's method [11ª] to be 9000 $Wm^{-2}K^{-1}$. This value is an order of magnitude larger than what is normal for a shell-side liquid. The reason is the small flow area between the pipes, leading to large Reynolds numbers and fast heat transfer. The overall heat transfer coefficient from equation 5.1 is now 2000 $Wm^{-2}K^{-1}$. The time needed to cool the $scCO_2$, polyester and steel from 120 to 80ºC is 5 minutes.

The resulting heat exchanger (figure 6.9) was designed in cooperation with and supplied by GTI Siersema Procestechnologie (The Netherlands). It is built at an

incline of 1º to allow the condensate and cooling water to flow out. For the same purpose, a space of 5 mm is left open between the baffles and the shell wall. To allow thermal expansion of the exchanger, a bellow is implemented in the shell wall. All parts of the machine are made of stainless steel (AISI 304), with the exception of the Teflon® O-rings in the heads.

6.5.6. Regulating valve

In the regulating valve, the pressure of the CO_2 changes from 300 bar to 60 bar. Since this process is fast and the piping is insulated, the expansion is isenthalpic, so that the temperature-entropy diagram of carbon dioxide gives the temperature (22ºC) and the mass fraction of liquid (0.4) in the CO_2 downstream of the reducing valve, flowing into the separator vessel.

The valve selection is based on the required flow coefficient K_V, generally defined as:

$$K_V = Q\sqrt{G/\Delta p} \tag{6.3}$$

where Q is the volume flow (m^3/hour), G is the specific gravity or the CO_2-density relative to the density of water at 20ºC and Δp is the pressure drop over the valve (bar).

It is calculated that a flow coefficient $K_V = 0.03$ is needed to realize the throughput (0.4 m^3/hour) needed to rinse the vessel sufficiently in 20 minutes, according to equation 6.2. To depressurize the machine from 300 to 100 bar, the regulating valve is used; the required flow coefficient for this step is $K_V = 0.11$. The further pressure drop from 100 to 60 bar is realized by opening a by-pass valve over the regulating valve. The chosen valve, supplied by Samson Regeltechniek B.V. (The Netherlands), has characteristics $K_V = 0.16$ and regulating ratio 50:1.

6.5.7. Separator

The maximum amount of liquid that is to be boiled off by the steam jacket of the separator is 0.05 kg/s. A conservative estimation of the inside film coefficient of 800 $W/m^2/K$ [11[b]] gives an overall heat transfer coefficient of 400 $W/m^2/K$. With a steam temperature of 150ºC and internal and external vessel diameters of 0.183 and 0.220 m, it follows that the height of the steam jacket should be 0.2 m. To compensate for fouling by dye powder, a height of 0.3 m is taken. The content of the separator is 20 liters.

Figure 6.10. Separator vessel for the 100-litre dyeing machine

To minimize entrainment of precipitated dye particles, the CO_2 is introduced into the bottom of the vessel tangentially. For the same reason, the CO_2 leaving the separator passes through a filter, mounted inside the vessel, above the liquid level. To avoid flooding of the separator, which would lead to pollution of the storage vessel with dye, the temperature of the CO_2 is measured below and above the liquid level. The valve regulating the CO_2-flow into the separator shuts when the liquid rises too much.

All parts of the separator are made of stainless steel (AISI 316), with the exception of the screw lid (stainless steel 1.6582) and its Teflon® O-ring. The working pressure being 60 bar, the design pressure of the separator is taken as 100 bar.

6.5.8. Gas booster

An air-driven piston-cylinder gas booster is used from Maximator Gmbh (Germany). It was calculated that a type DLE5-2-NN-C has sufficient capacity to lower the pressure from 60 to 10 bar in the 20 minutes mentioned in table 6.2.

6.5.9. Cooling machine

As cooling medium, water with 10% ethylene glycol is used. Since the required cooling capacity for the suction pipes of the pressurization pump is small, the capacity of the cooling machine is determined by the heat flow through the condenser, amounting 12 kW. A CH380 chiller from Piovan (Italy) is chosen, with a capacity of 50 kW.

6.5.10. Condenser

The flow through the condenser during the rinsing is 0.084 kg/s, requiring a condenser of minimally 12 kW. The outside film coefficient, following from the Nusselt relation for condensation outside horizontal tubes [11[c]], is 2200 $W/m^2/K$. The overall coefficient becomes 1000 $W/m^2/K$, so that the required pipe length is 20 m, when the cooling medium is 10ºC and flowing through a pipe of 16 mm outside diameter and 2 mm wall thickness. Inside the condenser, two pipe spirals of each 16 m are placed concentrically, as shown in figure 6.11.

6.5.11. Storage vessel

To save on equipment cost, the condenser and the storage vessel are combined into one structure. The storage vessel has a volume of 250 liters, and working and design pressures of 60 and 100 bar, respectively. The liquid level in the storage vessel is detected with a differential pressure transmitter.

All parts of the condenser and the storage vessel are made of stainless steel (AISI 316), with the exception of the Teflon®/steel flange seal.

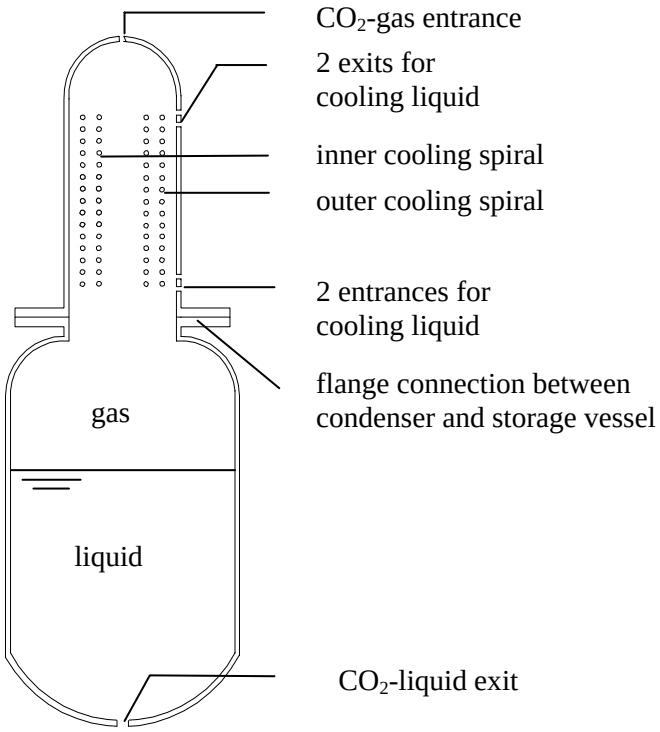

Figure 6.11. Integrated condenser-storage vessel unit for the 100-litre dyeing machine

Appendix 6.1. Comparison of dye solubilities at 80 and 120º at 300 bar.

Table 6.4. Solubilities (g/m^3) of several dyes in supercritical carbon dioxide at 300 bar, for different temperatures (T)

Dye	T (ºC)		Reference
	80	120	
Solvent Brown 1	62	73	[12]
Disperse Blue 79	260	425	[13]
Disperse Red 324	36	45	[13]
Disperse Red 153	21	21	[14]
Disperse Yellow 119	12	26	[14]

Appendix 6.2 Pressure drop calculation for the 100-litre beam-dyeing machine.

All pressure drop contributions are calculated for rinsing conditions: 300 bar, 80ºC.

1. Pressure drop over the textile

The fiber diameter was determined to be 200 μm by taking SEM pictures of the polyester cloth (figure 6.12). The Reynolds numbers at the inside and outside of the textile roll follow from the velocity (0.1 and 0.02 m/s respectively), density during rinsing (745 kg/m^3), fiber diameter and viscosity ($6.4 \cdot 10^{-5}$ Pa·s) and amount 230 and 45 respectively. The flow through the textile roll is laminar and the corresponding pressure loss can thus be calculated with the Darcy equation for radial flow through a porous cylinder [15]:

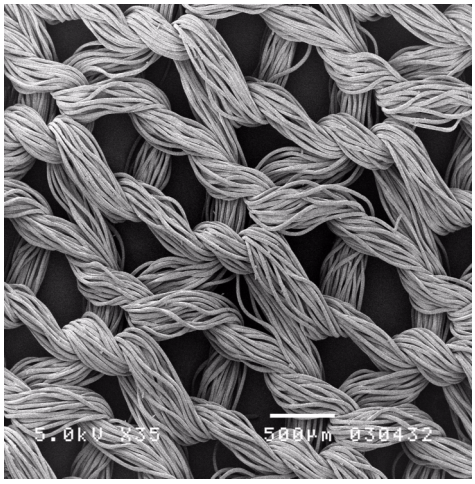

Figure 6.12. Scanning Electron Microscope (SEM) picture of the knitted polyester

$$\frac{dp}{dr} = \frac{\mu \Phi_V}{2\pi\alpha L} \tag{6.4}$$

with p = pressure (Pa), r = radius (m), μ = viscosity, Φ_V = volume flow rate ($8.3 \cdot 10^{-3}$ m^3/s), L = cylinder length (0.45 m) and α is the medium-specific flow resistance coefficient is assumed to be similar to that in [15]: $1.0 \cdot 10^{-11}$ m^{-2}.

Integrating equation 6.4 from the inside (radius r) to the outside (radius R) of the textile roll gives the pressure drop Δp:

$$\Delta p = \frac{\mu \Phi_V}{2\pi\alpha L} \ln\left(\frac{R}{r}\right) \tag{6.5}$$

With r = 0.03 m and R = 0.14 m, it follows that the pressure drop contribution from the textile roll is 0.29 bar.

2. Pressure drop over the piping

The machine has a total of L = 4 m 2" SCH 160 pipes, with internal diameter D = 43 mm. The pipe velocity is 5.7 m/s, Re = $3 \cdot 10^6$. The Fanning friction factor now being f = 0.0025 [17[a]], the pressure drop is $\Delta p = 2f\rho v^2 L/D$ = 0.1 bar. The flexible hoses, both 1.5 m in length, have an internal diameter of only 35 mm and therefore give a pressure loss of 0.2 bar. There are ten 90º bends in the machine, each with a friction factor K_W = 0.8 [17[b]], giving a joint pressure drop of $\Delta p = 10\ K_W\ 0.5\rho v^2$ = 0.8 bar. The total pressure drop contribution of the piping is thus 1.1 bar.

3. Pressure drop over the dye holder

As discussed below, the CO_2 passes through a stainless steel filter candle in the vessel into which the dye is dosed. The pressure drop follows from the equation (6.6) which, together with the properties of the *SIKA-FIL 10* filter material is given by the manufacturer: GKN Sinter Metals (Germany) .

$$\Delta p = \frac{\Phi_V s \mu}{A \alpha} \tag{6.6}$$

with s = filter layer thickness (0.0008 m), A = filter surface (0.04 m) and α is the permeability coefficient of the filter material ($9 \cdot 10^{-12}$ m^2). The contribution to the pressure drop is relatively small: 0.04 bar. The joint pressure loss in the entrance and exit of the dye holder (total K_W = 0.5 [17[b]]) and in the sharp 90º bend inside (K_W = 1.5) is 0.2 bar. The total pressure drop over the dye holder is 0.24 bar.

4. Pressure drop over the heat exchanger

As explained below, the heat exchanger has 23 pipes of internal diameter 9.24 mm. The resulting pipe velocity is 5.4 m/s, so that Re = $6 \cdot 10^5$, the Fanning friction factor is 0.004 and the pressure drop 0.3 bar. The entrance from the 2" pipe into the head and the exit of the 9.24 mm pipes into the other head both give negligible pressure loss due to the large flow area in the heads. The entrance from the head into the 9.24 mm pipes is characterized by K_W = 1 [17[b]]. The entrance from the head into the 2" pipe has a factor K_W = 0.5. The resulting pressure drop from

entrance and exit effects is 0.05 bar, giving a total pressure drop over the heat exchanger of 0.35 bar.

The total pressure drop in the 100-litre dyeing machine is concluded to be 2 bar.

References

1. E. Bach, E. Cleve, E. Schollmeyer, M. Bork, P. Koerner, Experience with the Uhde CO_2-Dyeing Plant on Technical Scale. Part 1: Optimization Steps of the Pilot Plant and the First Dyeing Results, *Melliand International* **3**, 192 (1998).
2. G. Montero, D. Hinks and J. Hooker, Reducing Problems with Cyclic Trimer Deposition in Supercritical Carbon Dioxide Polyester Dyeing Machinery, *J. Supercrit. Fluids* **26**(1), 47 (2003).
3. L.J.M.M. Van Schepdael and Stork Prints B.V., Device and Method for the Piece-wise or Batch-wise Refining of Pieces of Substrate, in Particular a Textile Substrate, Under High Pressure, Patent WO 2004/009897A1, 2004.
4. L.J.M.M. Van Schepdael, Composietvat voor gebruik bij superkritisch verven, Feasibility Study Report d.d. 22-03-02, Solico B.V. (The Netherlands).
5. H.-D. Sung and J.-J. Shim, Solubility of C.I. Disperse Red 60 and C.I. Disperse Blue 60 in Supercritical Carbon Dioxide, *J. Chem. Eng. Data* **44**, 985 (1999).
6. T. Shinoda and K. Tamura, Solubilities of C.I. Disperse Red 1 and C.I. Disperse Red 13 in Supercritical Carbon Dioxide, *Fluid Phase Equilibria* **213**, 115 (2003).
7. J.W. Lee, J.M. Min and H.K. Bae, Solubility Measurements of Disperse Dyes in Supercritical Carbon Dioxide, *J. Chem. Eng. Data* **44**, 684 (1999).
8. S.L. Draper, G.A. Montero, B. Smith and K. Beck, Solubility Relationships for Disperse Dyes in Supercritical Carbon Dioxide, *Dyes and Pigments* **45**,177 (2000).
9. R. Eggers, J. von Schnitzler and T. Kempe, Continuous dosing of solids in high pressure systems, 9th Meeting on Supercritical Fluids, 7th Italian Conference on Supercritical Fluids and Their Applications, June 2004, Trieste, Italy.

10. T. Walish, W. Doerfler and Ch. Trepp, Heat Transfer to Supercritical Carbon Dioxide in Tubes With Mixed Convection, HTD volume 350, ASME National Heat Transfer Conference 12 (1997) 79.
11. J.M. Coulson, J.F. Richardson and R.K. Sinnot, Chemical Engineering vol.6: Design, 2nd ed., Pergamon Press, Oxford, 1993, [a]600, [b]569, [c]636.
12. A. Ferri, M. Banchero, L. Manna and S. Sicardi, A new Correlation for the Solubilities of Azoic and Anthraquinone Derivatives in Supercritical Carbon Dioxide, *J. Supercrit. Fluids* **32**(1-3), 27 (2004).
13. A. Ferri, M. Banchero, L. Manna and S. Sicardi, An Experimental Technique for Measuring High Solubilities of Dyes in Supercritical Carbon Dioxide, *J. Supercrit. Fluids* **30** (1), 41 (2003).
14. H.-M. Lin, C.-Y Liu, C.-H Cheng, Y.-T. Chen and M.-J. Lee, Solubilities of Disperse Dyes of Blue 79, Red 153 and Yellow 119 in Supercritical Carbon Dioxide, *J. Supercrit. Fluids* **21**(1), 1 (2001).
15. W.A. Rapp, Y. Yang, G. O'Neal, H. Boyter and G. Hughey, Evaluating Liquor Flow Profiles in Fabric Beam Dyeing, *AATCC Review* **2**, 42 (2002).
16. J.M. Smith, E. Stammers and L.P.B.M. Janssen, Fysische Transportverschijnselen I, Delftse Uitgeversmaatschappij, 6th ed., Delft, 1989, [a]42, [b]47.

Chapter 7

Economic Evaluation of Polyester Beam Dyeing in Supercritical Carbon Dioxide

7.1. Introduction

In the previous chapters, it has been shown that textile dyeing in supercritical carbon dioxide is technically possible. Whether or not it is also economically attractive is investigated in this chapter by comparing the cost of a polyester beam dyeing process in supercritical CO_2 with the cost of the same process in water.

Dyeing methods other than beam dyeing are possible (e.g. jet-dyeing, drum dyeing) but with beam dyeing, the ratio of textile volume and bath volume is the largest. A small bath volume per unit textile volume means smaller equipment and less CO_2 to recycle over the storage vessel. In other words, for a supercritical process to have low investment- and operating-costs, a beam dyeing process is the best option.

7.2. Boundary conditions

The raw material of a polyester finishing plant is usually PET fibers contaminated with spinning oil, an additive that functions as a lubricant during spinning, weaving and knitting. After the PET is woven or knitted, the spinning oil has to be removed from the cloth by passing it through a washing machine. This step is the same for aqueous and supercritical dyeing and therefore these washing costs are left out of consideration in the comparison of both processes. Before supercritical or aqueous dyeing, the polyester has to be heat-set to avoid excessive shrinking of the textile in the dye bath, due to thermal effects. Also this step is identical for the aqueous and the supercritical process and is left out of consideration.

It is assumed that pressurised air, steam and cooling water from a tower are present at the site. The use of these utilities is incorporated in the evaluation, but the required compressor, steam boiler and cooling tower are left out of consideration.

The comparison between both processes is done for dyeing batches of 300 kg PET, an amount that is in the same order as in current industrial practice. The density of solid polyester is 1380 kg/m^3; rolled upon a beam in woven or knitted form it is 250-750 kg/m^3; in this work it is taken to be 500 kg/m^3 in the roll. The perforated pipe (beam) onto which the PET is rolled is assumed to be 0.1 m in diameter for the supercritical and 0.3 m for the aqueous process. Table 7.1 gives an overview of the boundary conditions for both processes.

Table 7.1. Boundary conditions for the supercritical and aqueous dyeing process

	$scCO_2$-dyeing	aqueous dyeing
Mass of PET roll (kg)	300	300
Length x diameter of textile roll (m)	2 x 0.63	2 x 0.69
Beam diameter (m)	0.1	0.3
Dyeing temperature (ºC)	130	130
Pressure (bar)	300	3
Desired dye concentration (g/(gPET)	0.02	0.02
Annual process time (hr/yr)	3500	3500

7.3. Process design for polyester beam dyeing in $scCO_2$

For the industrial supercritical dyeing process, the same process steps and times are used as in chapter 5, leading to a total batch time of 2 hours. Table 7.2 gives an overview. The same process flow diagram applies as was used in chapter 6.

Table 7.2. Process steps and times for polyester dyeing in supercritical carbon dioxide

Process step	time (min)
Loading textile and dye	3
Pressurisation	15
Dyeing	45
Levelling	15
Rinsing	20
Depressurisation	20
Unloading textile	2
Total batch time	120

A dye is chosen with a solubility of 10^{-4} g/(g CO_2). As in chapter 6, it is assumed that the $scCO_2$ can be saturated with dye in the dye holder and that the dye concentration in the $scCO_2$ exiting the PET roll is negligible. The density of the $scCO_2$ is 550 kg/m^3. The transport of 6 kg dye (2 mass % of the textile) to the PET in the dyeing time of 45 minutes requires a flow of 145 m^3/hour. Assuming a flow rate of 6 m/s, this requires standard 4" schedule 160 piping, with inner diameter 87 mm and wall thickness 13.5 mm.

The pressure drop calculations are done in the same manner as in chapter 6, leading to a drop of maximally 0.3 bar over the PET roll and 0.6 bar over the piping. The pressure drop over the heat exchanger is 0.2 bar and also over the dye holder 0.2 bar. The total pressure drop, to be overcome by the circulation pump, is 1.3 bar.

7.4. Equipment for supercritical dyeing

Since no industrial-scale supercritical dyeing machine exists at this moment, the capital cost is calculated by designing such a machine and estimating the purchase costs of all components. Below, the main plant items are discussed.

Dyeing vessel

A dyeing vessel is used with a stainless steel liner reinforced by carbon fibres wound around the circumference, thereby taking up the radial pressure forces. The two lids are kept in place by a steel yoke that takes up the axial pressure forces.

The length of the vessel is 3 m: 2 for the PET roll and 1 m for the pump and motor discussed below. As the textile roll is 0.63 m, the inner diameter of the dyeing vessel is taken as 0.7 m.

The advantage of using a carbon fibre vessel instead of an entirely steel vessel is twofold. Firstly, a steel vessel of inner diameter 0.7 m and a design pressure of 350 bar would have a wall thickness of 0.11 m, making the vessel mass 7000 kg, without yoke or closure. For heating and cooling the CO_2, PET and steel, there is now twice the amount of steam and cooling water per batch needed. The second disadvantage of a steel pressure vessel is that it requires a heat exchange area twice as large as the carbon fibre vessel, if the heating and cooling times are to be equal to the carbon fibre case. The extra costs for cooling water and steam and for the larger heat exchanger lead to an increase of 6 % in the process cost relative to the carbon fibre case.

Circulation pump

The choice and price of the circulation pump is determined by the combination of flow (145 m^3/hour) and pressure drop (1.3 bar) and by the working pressure of 300 bar. The high flow means that a centrifugal pump is required. The high working pressure demands that a magnetic coupling be used between the pump and its motor. Such a pump would cost approximately 100 k€ [2] and weighs heavily on the investment cost. An alternative is to use a standard low-pressure centrifugal pump and place it inside the pressure vessel, together with the motor. The cost of pump and motor is now reduced to 20 k€ [3]. It can be calculated from the tables below that the total process cost is then reduced with 5%. Dry-running bearings are used and a special resin for the electrical spools of the motor, as was discussed in chapter 6.

Pressurisation pump unit

To pump liquid CO_2 from 60 to 300 bar, either a membrane pump or an air-driven piston-cylinder pump can be used. The latter type is chosen here, since it has a 3 to 4 times lower purchase cost. The pressurisation unit contains 6 pumps, with a total flow of 70 liter/min.

Dye holder

The pressure vessel where the dye powder is dissolved in the $scCO_2$ is a stainless steel filter housing of 200 mm internal diameter and height 600 mm. The dye is put into the vessel, upstream of the filter, so that the $scCO_2$ flows past the dye particles and then through the filter.

Heat exchanger

As was discussed in chapter 6, there are 2 possible configurations for the heat exchanger: one in which the steam and cooling water flow through the same shell-side space and one in which the steam- and cooling water parts are segregated. The latter configuration requires less valves,is easier to use in an industrial environment and is therefore chosen here.

The heat exchange area for heating and cooling the $scCO_2$, steel and PET is calculated in the same manner as in chapter 6. As is shown in chapter 5, the heat transfer coefficients for heating and cooling can be calculated with constant-property Nusselt relations. Both the steam- and the cooling water part of the shell have a heat exchange area of 3.4 m^2. Heating and cooling can be accomplished in 10 minutes if 50 stainless steel pipes of type ½" shedule 40 are used. Both the heating and the cooling part should be 1 m in length, the shell diameter is 250 mm.

Separator

The precipitation and collection of residual dye is done in a separator vessel. By means of a steam jacket, the liquid fraction of the CO_2 that results from the expansion from 300 to 60 bar is boiled off and flows to the storage vessel. The separator is designed in the same way as in chapter 6, resulting in a vessel with an internal diameter of 0.3 m and a height of 1 m.

Gas booster unit

The gas boosters are of the air-driven piston-cylinder type. The unit is used to pump the gaseous CO_2 out of the dyeing vessel, after the pressures in the dyeing vessel and the storage vessel are equalised. The unit consists of 2 gas boosters, with a total flow of 50 liters/minute and is able to lower the pressure in the dyeing vessel from 60 to 10 bar in 20 minutes. The remaining CO_2 (20 kg) is vented to the atmosphere, which means that 96% of the CO_2 is recycled per batch.

Condenser

The condenser is designed to liquify the flow of CO_2 leaving the separator during the rinsing step: 0.83 kg/s. The same condenser configuration is taken as in chapter 6: CO_2 flowing on the shell-side and the cooling water on the tube-side. With a cooling water temperature of 0ºC, the required area of heat exchange is 6.4 m^2. The calculation procedure is similar to the one in chapter 6.

Cooling machine

The cooling water needed for the condenser is brought to 0ºC with an electrical cooling machine. The required capacity is estimated to be 140 kW.

Storage vessel

The CO_2 is stored at 22ºC and 60 bar, in liquid form. The required pressure vessel has a volume of 1200 liters.

7.5. Capital costs for supercritical and aqueous dyeing

The capital cost of the main plant items discussed above are listed in table 7.3.

Table 7.3. Investment cost for the main plant items of an supercritical dyeing machine

Main plant item	Capacity		Purchase cost (k€)
Dyeing vessel	1150	liter	90[a]
Circulation pump	150	m^3/hr	20[b,c]
Pressurisation pump unit	70	liter/min	20[d]
Dye holder	20	liter	20[e]
Heat exchanger	2 x 3.4	m^2	30[e]
Separator	70	liter	20[e]
Gas booster unit	50	liter/min	14[f]
Condenser	6.4	m^2	20[e]
Cooling machine	140	kW	55[g]
Storage vessel	1200	liter	20[h]
	Total main plant items:		309 k€

Price estimations from: [a]Solico B.V., [b]Packo Inox N.V., [c]DACE Price booklet, [d]Resato Int. B.V., [e]Estimations based on costs of the 100 liter pilot machine from chapter 6, [f]Maximator GmbH, [g]Piovan S.p.A., [h]Van Steen Apparatenbouw.

The secondary capital costs are presented in table 7.4.

Table 7.4. Overview of the secondary equipment costs for a supercritical dyeing machine

	Cost (k€)
Instrumentation and control	25[a]
Piping	10[b]
Valves	20[a]
Frame and isolation	20[a]
Working hours	14[c]
Total secondary costs:	89 k€

[a]Estimations based on costs of the 100 liter pilot machine from chapter 6, [b]Noxon Stainless B.V., [c]10 weeks à €35/hr.

From tables 7.3 and 7.4 it follows that the cost of producing the supercritical dyeing machine is 398 k€. If an overhead of 25 % is assumed, the purchase cost for a textile dyer would be 500 k€ for a beam dyeing machine for 300 kg polyester batches. This is to be compared with the purchase cost of a machine for aqueous beam dyeing: 100 k€ [4].

For both the supercritical and the aqueous process, the annual capital charge a is calculated with the annuity equation:

$$a = \frac{i}{1-(1+i)^{-N}} \qquad (7.1)$$

With an interest rate i of 6 % and a depreciation time N of 10 years, the annual capital charge is 14 %. Table 7.5 gives an overview of the resulting capital charges for both processes.

Table. 7.5. Capital costs for polyester beam dyeing in scCO$_2$ and water

		CO_2	Water
Investment	k€	500	100
Annual capital charge	k€ / year	70	14
Batch time	hour	2	3.5[a]
Production capacity	ton / year	525	300
Capital charge	€ / batch	40	14
	€ / (kg PET)	0.13	0.047

[a] Data from Ames Europe B.V. and Stork Prints B.V.

7.6 Operating costs for supercritical and aqueous dyeing

The prices of the different utilities and compounds that are needed to operate a dyeing machine are listed in table 7.6.

Table 7.6. Prices of utilities, relevant compounds and operator labour

	Unit	Cost (€ / unit)
Pressurised air (7 bar)	Nm^3	$7 \cdot 10^{-3}$ [a]
Steam	ton	26[b]
Electricity	kWh	0.10[a]
Cooling water (tower)	m^3	0.05[a]
Water	m^3	2.27[c]
CO_2	kg	0.11[d]
Operator labour	hour	28

[a]DACE price booklet, [b]Data from Stork Prints B.V., [c]Price of purchasing, purification and disposal of water, data from Stork Prints B.V., [d]HoekLoos B.V.

The use of utilities and compounds is calculated from the specifications of the equipment and the demands of the process. The heat balance is made with the data from table 7.7.

Table 7.7. Data for the heat balances of the dyeing processes

Material	Specific heat (J/kg/ºC)	Heat of vaporisation (kJ/kg)	Amount in dyeing machine (kg)	
			CO_2-process	Aqueous process
Steel	460		1700	1000[b]
PET	1300		300	300
CO_2	2200[a]	140	560	0
Water	4200	2200[c]	0	1000[b]

[a]Average value, taken between 20 and 130ºC. [b]Data from Stork Prints B.V. [c]At 150ºC

Supercritical process

In table 7.8 the calculated operational costs are shown for the supercritical process.

Table 7.8. Operational costs per batch for polyester beam dyeing in scCO_2

Item	Amount per batch	Price (€)
Pressurised air	1110 Nm^3	7.55
Steam	137 kg	3.55
Electricity	105 kWh	10.50
Cooling water	16 m^3	0.80
CO_2	20 kg	2.20
Dyes	6 kg	60
Maintenance[a]		1.2
Labour cost[b]	0.67 hour	18.67
Total operating cost:		104.47 € / batch 0.35 € / (kg PET)

[a] Maintenance is 3 % of the capital cost. [b] 1 operator for 3 machines

The steam consumption in the table is the sum of the amount of steam needed to heat all steel, PET and CO_2 and the amount that is needed to vaporise the liquid fraction of CO_2 that enters the separator during the rinsing step of the process.

The electricity use of the process is calculated by adding the use of the motor of the centrifugal pump and the use of the cooling machine.

The cost of the dye powder in table 7.8 is based on the current price of dye for aqueous dyeing: 15 €/kg. This includes dispersing agents and since these are not

needed in supercritical dyeing, the dye will be cheaper. It is therefore roughly estimated to be 10 €/kg. It follows from the distribution coefficients given in chapter 4 that the amount of dye remaining in the $scCO_2$ after the dyeing process is small compared to the amount in the PET; it is therefore neglected.

Aqueous process

The dye for the aqueous process contains around 50 % actual dye molecules, the rest is mainly dispersing agents. Therefore, to obtain 2 mass% of dye into the 300 kg of PET, 12 kg dye is needed. Also in the aqueous process, the dye concentration in the machine after the process is neglected.

After the dyeing step, the PET is washed in 1000 liter water with surfactants at 90ºC and subsequently rinsed 3 times with 100 liter water at 60ºC. The time required for dyeing, washing and rinsing together is 3.5 hours [4]. Finally, the PET is dried, using steam. The resulting operating costs are given in table 7.9.

Table 7.9. Operating costs per batch for aqueous polyester beam dyeing

Process step	Item	Amount per batch	Price (€)
	Maintenance		3
Dyeing	Steam	253 kg	6.58
	Electricity	50 kWh[a]	5
	Water	1000 liter[a]	2.27
	Dyes	12 kg	180
	Chemicals[b]	3 kg[a]	9
	Labour cost		32.67[c]
Washing and rinsing	Steam	319 kg	8.30
	Water	4000 liter[a]	9.08
	Chemicals		12.3[a]
	Electricity	50 kWh[a]	5
Drying	Steam	910 kg	23.66
Total operating costs:			297 €/batch
			0.99 € / (kg PET)

[a] Information from Stork Prints B.V. [b]Levelling agents and pH modifiers. [c] Labour cost for dyeing, washing and rinsing together, 1 operator for 3 machines.

7.7. Total process costs

The costs for supercritical and aqueous dyeing are summarised in table 7.10. It is clear that the capital costs are higher and the operating costs are lower for the supercritical process. Because the process costs are largely determined by the operating costs, the process costs are lower when polyester is dyed in $scCO_2$.

Table 7.10. Comparison of costs (€ / (kg PET) for supercritical and aqueous polyester dyeing

	CO_2	Water
Capital cost	0.13	0.047
Operating cost	0.35	0.99
Process cost	0.48	1.04

7.8. Discussion on the proess cost

For the process time, 2 hours was taken in the above calculations. It is possible that, in industrial practice, the time will be longer. It will, however, always be shorter than for the aqueous process. To illustrate the influence of the time on the costs of the supercritical process, the calculations were performed also for a time of 3 hours. The capital and operating costs now become 0.20 and 0.42 €/(kg PET) respectively. The total process cost increases from 0.48 to 0.64 when the time changes from 2 to 3 hours.

In the calculation of the operating costs for supercritical dyeing, the price of dye was estimated roughly to be 10 €/kg, since there is no dye commercially available for dyeing in $scCO_2$. The value must lie between the price of the press cake, the unpurified product of dye synthesis (4 €/kg) and the price of dye for aqueous dyeing, containing dispersing agents (15 €/kg). This means that the process costs for the supercritical process lie between 0.36 and 0.58 € per kg polyester.

In the supercritical process evaluated above, the dye remaining in the CO_2 after dyeing, is separated from the CO_2 by vaporisation of the latter. This separation technique requires continuous vaporisation, condensation and pressurisation of the CO_2 during the rinsing step. An energetically prefferable method is to remove the

dye from the CO_2 by adsorption onto a medium like activated carbon. This separation technique was investigated for dye and $scCO_2$ on a laboratory scale by Von Schnitzler [5], with bleaching earth as adsorptive material. It is unknown how this would affect the process time and it is also unknown what the price of regeneration or disposal of the adsorptive medium is. Therefore, at this moment, the costs of a supercritical process with this alternative separation cannot be estimated.

7.8. Environmental considerations

Closely related to the economical evaluation are the environmental implications of the dyeing process. The dye solvent (water or $scCO_2$) , the chemicals (mainly dyes and dispersing agents) and the different types of energy consumed during the dyeing process are all quantified in this chapter in terms of costs but their use also has environmental consequences.

An quantitative environmental comparison between supercritical and aqueous dyeing can only be made by making life cycle analyses of all compounds and utilities involved. This is beyond the scope of this thesis, but the economical comparison between the supercritical and aqueous processes can also be used as a rough environmental comparison, since the prices of compounds and utilities are a measure for the resources required to produce them. It is possible however, to get a clearer picture of this issue by regarding the solvents, chemicals and energy types qualitatively.

It will be clear that the main environmental advantage of supercritical dyeing is the reuse of 95 % of the solvent. Because the CO_2 is obtained as a waste product from industrial processes like combustion or ammonia synthesis, the venting of the 5 % CO_2 is not a pollution on the account of textile dyeing. As discussed in chapter 1, in polyester dyeing 5-10 % of the dye is not used and ends up in the wastewater. In $scCO_2$-dyeing, all dye can be reused, which forms a second environmental advantage of the supercritical process. In short, the supercritical process is environmentally superior to the aqueous process when the use of compounds is regarded. Table 7.11 gives an overview of the use of compounds and energy in both the supercritical and the aqueous process. The disperse dyes that are used in

supercritical dyeing are the same as in aqueous dyeing, so that the human and ecological toxicity of these compounds does not play a role in the comparison of the processes.

It can be seen in table 7.11 that different types of energy are used in both dyeing processes. The use of cooling water is neglected here. For a comparison with respect to energy consumption, it is calculated how much carbon dioxide is formed in the production of the pressurized air, steam and electricity. The generation of 1 Nm^3 pressurised air of 7 bar requires 0.125 kWh [6], the CO_2-production for 1 kWh electricity is 0.61 kg [7] and the CO_2-production for steam formation is 118 kg CO_2 / ton steam [7]. The resulting amounts of carbon dioxide associated with the energy use in the dyeing processes are given in table 7.12. Supercritical dyeing requires less energy and is therefore associated with a 26% lower CO_2-emission.

Table 7.11. Environmental comparison between the supercritical and the aqueous polyester dyeing process, regarding the uses of compound and utilities

compound/ utility		unit	CO_2	water
water		kg	0	5000[a]
CO_2		kg	20	0
dye	pure dye	kg	6	6
	dispering agent	kg	0	6
chemicals		kg	0	3
pressurized air		Nm^3	1110	0
steam		kg	137	1380[c]
electricity		kWh	105	100
cooling water		m^3	16	0

[a] For dyeing, washing and rinsing. [b] 5% of the amount of CO_2 that is used per batch (560 kg). [c] For dyeing, washing, rinsing and drying.

Table 7.12. Carbon dioxide emission associated with the energy used in supercritical and aqueous dyeing, per 300 kg polyester batch

energy	equivalent CO_2-emission (kg CO_2)	
	supercritical dyeing	aqueous dyeing
steam	16	163
electricity	64	61
pressurised air	85	0
total	165	224

7.9. Conclusions

From the process and equipment design for beam dyeing of 300 kg batches of poyester in $scCO_2$, it follows that the purchase cost for the machine is 500 k€. The equivalent machine for dyeing in water costs 100 k€. The large difference in investment cost is caused by the high pressure of the supercritical process and by the fact that 96 % of the CO_2 is recycled.

The operating costs for the supercritical process are lower than for the aqueous process: 0.35 and 0.99 € per kg of polyester, respectively. This is mainly caused by the higher rate of dyeing and the lower price of dye for the supercritical process.

The overall effect is that it is more than twice as cheap to dye polyester in $scCO_2$ than it is in water. The process costs are 0.48 and 1.04 € per kg of polyester, respectively.

The economic evaluation was based on a supercritical process where the residual dye is separated from the CO_2 by gasifying the latter. When, instead, the dye is removed by adsorption, the supercritical process could be made cheaper. At this moment, no estimation can be made as to how much cheaper.

As the supercritical process requires less compounds and energy, it is concluded to be environmentally benign compared to the aqueous process.

The overall conclusion is that dyeing polyester in $scCO_2$ instead of water, is environmentally superior and reduces the costs with 50 %.

References

1. J. v. Zuidam, Ames Europe B.V., Enschede, The Netherlands, personal communication, 2003-2004.
2. G.F. Woerlee, FeyeCon D&I B.V., internal report, april 1999.
3. DACE price booklet, Dutch Association of Cost Engineers, 22nd ed., Elsevier, 2002.
4. P. Leerkamp, Stork Prints B.V., internal report, february 2003.
5. J. Von Schnitzler, Der Stofftransport in Faerbeprozessen von Polymeren mit Ueberkritischem CO_2, Dissertation Technische Universitaet Hamburg-Harburg, 2001.
6. H. van Heyster, GrassAir, personal communication.
7. Tufts Institute for the Environment, Method for Conducting a Greenhouse Gas Emission Inventory for Colleges and Universities, april 2002.

Epilogue

Suggestions for further research

As was concluded in this thesis, one of the main reasons that the supercritical process is economically superior to the aqueous process, is the higher rate of dyeing. It is therefore recommendable to investigate the kinetics of both disperse and reactive dyeing. Knowledge on the kinetics and the identification of the rate-determining step in non-reactive and reactive dyeing open the possibility of further reducing the process times.

For disperse polyester dyeing, a large number of dyes is commercially available. With respect to reactive dyeing however, more dyes should be synthesized and tested in $scCO_2$, so that the whole color spectrum can be covered.

Regarding the equipment, both the rotating drum machine (chapter 4) and the beam dyeing machine (chapter 6) are to be tested for their applicability in reactive dyeing. The process time and the evenness of the beam have to be measured and optimized in the 100-liter dyeing machine described in chapter 6, both for disperse and reactive dyeing. Finally, an equipment item should be designed, built and tested to introduce the dye powder into the pressurized dyeing machine.

Future of supercritical textile dyeing

It is clear that a large driving force exists for the development and implementation of textile dyeing in $scCO_2$. Water pollution is becoming an ever greater environmental concern and it is likely that the regulations on the quality of treated wastewater will become more stringent in the future. Therefore, the end-of-pipe treatments will require more effort and cost, so that the economical advantage of $scCO_2$ will become even greater. Both the environmental and the economical incentive will increase the demand for a clean dyeing process.

For the implementation of a new dyeing process in industry, the environmental and economical implications, the product quality (color depth, fastness) and the

robustness of the process in practice have to be ascertained. Regarding polyester dyeing, the environmental advantage is clear. The second two issues were investigated satisfactorily in this thesis. The development of the 100-liter polyester beam dyeing machine, described in chapter 6, creates the possibility of carrying out large-scale experiments to test the robustness of the process. Only then can a full-scale 1000-liter pilot machine be designed, built and tested in an industrial environment.

Also for reactive dyeing, the environmental advantage is straightforward. Insufficient information is available, e.g. on kinetics, to evaluate the process economically. The product quality was found to be good in this work: dark colors were obtained and a good fastness. To assess the robustness of the process of reactive dyeing, there is not enough information regarding large-scale experiments. Another issue in implementation concerns the dyes: disperse dyes are commercially available but new reactive dyes have to be designed and synthesized first on a small scale, their performance is to be tested in $scCO_2$ on a small and then on a large scale, investigated with respect to toxicity and finally synthesized on an industrial scale.

In view of the above, disperse dyeing of polyeste will probably be implemented in industry first and reactive dyeing will follow. This thesis treats several of the issues that need to be solved before implementation in industry is possible. A machine is designed and built with which the robustness of disperse dyeing can be tested and the performance of reactive dyes in $scCO_2$ is investigated. Therefore, this thesis is an important step towards the implementation of disperse and reactive textile dyeing in supercritical carbon dioxide.

Dankwoord

Tijdens de vier jaren van mijn promotieonderzoek op API heb ik met veel mensen samengewerkt. De mede- “API-bewoners” zorden ervoor dat het niet alleen een leerzame en productieve tijd was, maar ook een vrolijke.

Allereerst wil ik mijn promotor, Geert-Jan Witkamp, bedanken voor het vertrouwen en de kans aan een interessant en veelzijdig onderzoek te werken. Ook Geert Woerlee bedank ik hiervoor. En, Geert: Bedankt voor de hulp op momenten dat ik vast kwam te zitten. Cor Peters wil ik hierbij bedanken voor de vriendelijke hulp met hoofdstuk 3.

Met Wim Veugelers heb ik het genoegen gehad veel samen te werken. Een genoegen vanwege je efficiënte manier van werken en je praktijkervaring, Wim, maar ook omdat je een bijzonder prettige collega bent, altijd bereid tijd vrij te maken om anderen te helpen.

Jan, Martijn, Carel, Stefan, André, Jos en Gerard: Hartelijk dank voor de inzet bij het tekenen en construeren van de opstellingen en jullie praktische adviezen. Bovendien wil ik jullie bedanken voor de vele keren dat er reparaties en veranderingen aan de apparatuur moesten worden uitgevoerd.

Een grote hulp bij het onderzoek waren Marjan, Özcan, Frans, Elmehdi en Zinaida. Hun werk, in de vorm van experimenten en CFD-simulaties, is overal in dit proefschrift terug te vinden.

Bij de analyses van de geverfde lappen is meermalen de kennis van Michel en Paul van grote waarde gebleken. Hen wil ik bedanken voor de hulp bij zaken als chemicaliën en analytische apparatuur.

Tijdens mijn gehele promotie heb ik veel geleerd van de mensen die vanuit Stork Prints B.V. op het project werkten. Vooral Jan-Willem Gerritsen en Peter Leerkamp bedank ik hiervoor. Ook de medewerkers van Ames Europe en Triade wil ik hierbij bedanken voor hun bijdragen. Ludo en Hans van Solico zijn we dankbaar voor het prachtige ontwerp van het koolstofvezelversterkte verfvat.

Vanaf het begin van mijn API-tijd heb ik veel steun en ideën gekregen van de medewerkers van FeyeCon D&I B.V. Behalve Geert en Wim zijn Ernst, Frank, Gerard en Hubert met hun ervaring op superkritisch gebied behulpzaam geweest. Bedankt!

Vanesa, bedankt voor de aangename samenwerking en de gezellige tijd, in de kamer maar ook op de verschillende congressen en cursussen. Christof, jou wil ik bedanken voor het feit dat je mij, als afstudeerder, op het superkritische pad hebt gebracht. Daar heb ik tijdens mijn promotie geen spijt van gehad. Maaike, bedankt voor de collegialiteit en de gezellige vrijdagavonden met Sietse en jou. Aris en Marcel, gelukkig heb ik met jullie verschillende keren wat stoom kunnen afblazen op momenten dat overdruk dreigde. Jaap, Yohana, Christiana, Frans, Perize, Maaike, Helma, Andreanne, Paolo, Abilash, Stephen, Peter, Mark, Elif, Robert, Brenda, Dima, Marcos, Daniela, Joop en de andere stafleden wil ik bedanken voor de vriendschap en voor de goede sfeer op API. Jelan, bedankt voor je hulp met de omslag.

Uschi, jouw steun is heel belangrijk geweest de afgelopen jaren. Ook voor je geduld wil ik je bedanken, er ging nogal wat tijd en energie in deze klus zitten. Nu hebben we gelukkig weer meer tijd voor elkaar.

Tot slot wil ik opmerken dat ik zonder de goede zorgen van mijn ouders nooit tot een promotie gekomen zou zijn. Bedankt voor alles!

Martijn.

Curriculum Vitae

Martijn van der Kraan

Born: June 5th 1971, Nieuwkoop, The Netherlands

1983 - 1989	Atheneum, Rijksscholengemeenschap Bergen op Zoom
1989 – 2001	Chemical Engineering, Delft University of Technology
2001 – 2005	Ph.D. at the Laboratory for Process Equipment Delft University of Technology
2005	Post-doc at the Laboratory for Process Equipment Delft University of Technology Project Manager, FeyeCon Development and Implementation B.V.

Publications

M. van der Kraan, M.M.W. Peeters, M.V. Fernandez Cid, G.F. Woerlee, W.J.T. Veugelers and G.J. Witkamp The Influence of Variable Physical Properties and Buoyancy on Heat Exchanger Design for Near- and Supercritical Fluids, J. Supercrit. Fluids **34**, 99 (2005).

M. van der Kraan, M.V. Fernandez Cid, G.F. Woerlee, W.J.T. Veugelers and G.J. Witkamp, Equilibrium Study on the Disperse Dyeing of Polyester in Supercritical Carbon dioxide, submitted to The Textile Research Journal.

M. van der Kraan, M.V. Fernandez Cid, G.F. Woerlee, W.J.T. Veugelers and G.J. Witkamp, Dyeing of Natural and Synthetic Textiles in Supercritical Carbon Dioxide with Disperse Reactive Dyes, submitted to The Journal of Supercritical Fluids.

M. van der Kraan, M.V. Fernandez Cid, G.F. Woerlee, W.J.T. Veugelers, C.J. Peters and G.J. Witkamp, Equilibrium Distribution of Water in the Two-phase System Supercritical Carbon Dioxide – Textile, submitted to the Journal of Supercritical Fluids.

M. van der Kraan, O. Bayrak, M.V. Fernandez Cid, G.F. Woerlee, W.J.T. Veugelers and G.J. Witkamp, Textile Dyeing in Supercritical Carbon Dioxide, Proceedings of the 6th International Symposium on Supercritical Fluids, Versailles, France, 2003, 2119.

M. van der Kraan, M.M.W. Peeters, M.V. Fernandez Cid, G.F. Woerlee, W.J.T. Veugelers and G.J. Witkamp, Heat Transfer in High-pressure Carbon Dioxide, Proceedings of the 6th International Symposium on Supercritical Fluids, Versailles, France, 2003, 517.

M. van der Kraan, M.V. Fernandez Cid, G.F. Woerlee, W.J.T. Veugelers and G.J. Witkamp, Dyeing Natural and Synthetic Textiles in Supercritical Carbon Dioxide

with Reactive Dyes, Proceedings of the 4th International Symposium on High Pressure Technology and Chemical engineering, Venice, Italy, 2002, 199.

M. van der Kraan, E. Abdaou, M.V. Fernandez Cid, W.J.T. Veugelers, G.F. Woerlee, G.J. Witkamp, Maximum attainable Colouration of Polyester in Supercritical Carbon Dioxide, Proceedings of the 7th Italian Conference on Supercritical Fluids and their Applications, Trieste, Italy, 2004.